GM/DOT Project F.3(b)
Volume 1: The Bulkhead

Computational Fluid Dynamics Modeling of Post-Crash Vehicle Fires

Submitted by:
Nathan B. Wittasek, Principal Author
Richard D. Pehrson, Contributing Author
Dr. J.R. Barnett, Principal Investigator

Worcester Polytechnic Institute
Center for Firesafety Studies
Worcester, Massachusetts

May 1997

Abstract

Fires originating in the engine compartment of an idealized automobile are being modeled with the intent of developing tools that can be used to examine post-crash vehicle fires. Of particular interest is the radiative, convective, and conductive heat transfer and transport of toxic species and soot from the engine compartment through the windshield and bulkhead. It is the intent of this research to develop the ability to predict the conditions inside the passenger compartment for several hypothetical fire scenarios. Accordingly, the development of a parameterized, turbulent, reacting, multicomponent fluid flow and heat transfer model was undertaken. The commercial software package *TASCflow* has been chosen as the means to accomplish the task outlined above.

Boundary conditions required to obtain the solution have been applied in conjunction with thermally-dependent material properties to arrive at the temperature response of two- and three-layer bulkheads (via Conjugate Heat Transfer). Fire scenarios that will support future modeling efforts have been characterized in the context of the post-crash vehicle fire. The application of TASCflow has proven to be successful and has demonstrated the sensitivity of solution to thermal properties, modeling parameters, as well as environmental conditions.

Executive Summary

The engine and passenger compartments of an idealized automobile are being modeled with the intent of developing tools that can be used to examine post-crash vehicle fires. This process was carried out in an iterative manner such that the phenomena associated with non-reacting bulkhead heat transfer were explored first. Of further interest in the general modeling problem are the phenomena of heat transfer and toxic species transport from the engine compartment through the windshield and bulkhead to the passenger compartment. It is the intent of this research to develop the ability to predict the conditions in the passenger compartment for several hypothetical fire scenarios for a number of automobile geometries. Accordingly, the development of a parameterized, turbulent, reacting, multi-component fluid flow and heat transfer model was undertaken. The heat transfer and fluid flow solver TASCflow has been chosen as the vehicle to accomplish the formidable task outlined above.

The intent of the first deliverable is to (1) Determine the suitability of TASCflow to solve the bulkhead and post-crash vehicle fire modeling problem, (2) Identify appropriate boundary conditions for modeling the bulkhead with a specific focus on constructing plausible hypothetical fire scenarios, (3) Determine appropriate heat transfer properties, (4) Apply TASCflow to various transient bulkhead modeling scenarios, and (5) Compare results from the current modeling effort with those previously performed using the finite element code TASEF-2.

After extensive research into the capabilities of TASCflow as well as the exact nature of the post-crash vehicle fire, it has been conclusively determined that TASCflow provides an excellent basis for current and future modeling efforts. Examination of the car fire modeling challenge revealed that the computational fluid dynamics approach offered by TASCflow was the best option for modeling the complicated geometries, fire scenarios (involving combustion, plastics melting, and toxic species production), transport mechanisms (including turbulent fluid flow and heat transfer), and associated boundary conditions. The principal design fire scenarios that are under development include a variety of engine compartment fires and fuel spill fires. The interaction of these fires with the vehicle and occupants is being researched in Project F.3(a). Generic thermally dependent heat transfer properties for common materials associated with automobiles have been investigated and are currently implemented in the existing heat transfer model. More detailed

analysis of the properties of common vehicle materials are being performed at this time and will be incorporated as the testing is completed.

The application of TASCflow has provided insight into the behavior of insulations and structural materials. The efforts to perform a conjugate heat transfer analysis have proven to be highly rewarding, and compare favorably with the existing modeling efforts as well as empirical data. Two and three layer bulkheads have been analyzed, with special attention given to the effects of environmental conditions (gas velocity, absorptivity, surface emissivity, and turbulent intensity) as well as thermal properties (density, conductivity, and specific heat). The importance of thermal property input parameters has been clearly demonstrated in the context of bulkhead modeling.

The groundwork for the development of an intricate model for car fires has been laid out and efforts have been made to ensure the suitability of TASCflow to achieve the goal of predicting conditions in a post-crash vehicle fire scenario. Preliminary modeling efforts show great promise and have already offered considerable insight into the behavior of materials similar to those used in modern automobiles.

The success of this Computational Fluid Dynamics modeling effort will depend largely upon the development of realistic fire data as well as proper representation and use of thermal properties. Whereas the work to date has shown that the the model predictions are sensitive to the input parameters for the thermal response properties of automotive insulations, lining materials, etc. up to 1300K. Currently, most data scarcely applies past 600K, though work is presently under way to help remedy this problem. The use of small scale material data obtained from such sources as the cone calorimeter may prove to be highly useful with respect to gathering information on the driving potentials for the post-crash scenario.

Contents

List of Figures

List of Tables

Nomenclature

A_p	exposed surface area of plastic (m^2)
C_1	viscosity constant, Planck constant ($W\mu m^4/m^2$)
C_2	viscosity constant, Planck constant (μmK)
C_k	eddy viscosity constant
C_μ	turbulent intensity constant
D	total derivative operator
E	energy (W/m^2)
E_{ab}	absorbed energy in surface a from surface b (W/m^2)
E_b	total emissive power (W/m^2)
F	force (N)
H	total enthalpy of the fluid (kJ/kmol)
H_λ	monochromatric incident radiation per unit time ($W/\mu m$)
H_n	normalized heat load
I	intensity, general ($W/\mu m$)
J	Fick's Law of Diffusion
$J_{\lambda,v}$	volumetric emission coefficient
K	diffusion constant (m^2/s)
K_a	fluid absorption coefficient
K_s	gas phase scattering coefficient
K'_p	particle cross-section per unit volume
L	positional coordinate (m), path length (m)
L_ϵ	length scale for turbulent eddie (m)
MW	molecular weight (μ)
P	pressure (Pa)
Pr	Prandtl Number
R	ideal gas law constant (J/kgK)
$\dot{R}$	net rate of radiation absorption
Re	Reynold's number
S	source term (production, degradation) (kW)
T	temperature (K, ^oC)
T_u	turbulent intensity
Q	Heat energy (kW/m^2)
V	velocity, bulk (m/s), volume (m^3)
$\dot{V}$	volumetric flow rate of fire plume (kg/s)
Y	species concentration (ppm, kg/m^3)
X_i	indexed form of body force (N)

a	empirical coefficient, absorptivity
c	specific heat (pressure constant) (J/kgK)
c_o	speed of light (2.998×10^8 m/sec)
c_p	constant pressure specific heat (J/kgK)
c_v	volumetric specific heat (J/kgK)
$\tilde{c}$	wave or photon speed (m/sec)
d	differential operator
dw	differential solid angle (rad)
ds	differential path length (m)
e	internal energy, exponential function (kW)
e_b	black body energy (W/m^2)
f	body force (N)
f_{sc}	scattering parameter
f_v	volumetric soot concentration
g	acceleration due to gravity (9.81 m/s^2)
h	static enthalpy (kJ/kmol), heat transfer coefficient (W/m^2K)
h_p	Planck's constant (6.625×10^{-23} kW)
h, c	heat of combustion (J/kg)
h, v	heat of vaporization (J/kg)
i	intensity (kW)
k	thermal conductivity, viscosity constant (W/mK)
$\bar{k}$	turbulent kinetic energy (m^2)
k_b	Boltzmann constant (J/K)
k_o	soot concentration (kg/kg)
l	mixing length (m), soot path length (m)
ℓ_u	length of radiation beam passing through differential V (m)
m	mass (kg)
$\dot{m}$	mass production rate of smoke (kg/s)
$\dot{m}_p$	mass loss rate (kg/sec)
n	arbitrary counter
p	pressure (Pa)
q	rate of heat conduction (kW)
r	reflectivity
rad	radiation energy (kW)
t	time (sec)
u	velocity in x-direction (m/sec)
u_i	indexed velocity (m/sec)
v	velocity in y-direction (m/sec)
$\tilde{v}$	frequency of radiation wave (μm^{-1})
w	velocity in z-direction (m/sec)
x	directional variable (m)
x_i	indexed length term (m)
y	directional variable (m)
z	directional variable (m)

Greek Letters

α	absorptivity, diffusivity (m^2/sec)
α_p	generalized power term
β_λ	monochromatic extinction coefficient
∂	partial derivative operator
γ_λ	monochromatic scattering coefficient
γ	Newtonian viscosity term (kg/m sec)
δ	Kronecker delta
δ_t	thermal inertia (kW $\sec^{\frac{1}{2}}/m^2K$)
ϵ	turbulence constant (m^2), emissivity
κ	coefficient of bulk viscosity (kg/m sec)
κ_λ	monochromatic absorption coefficient
λ	wavelength (μm)
μ	kinematic viscosity (kg/m sec)
μ'	second coefficient of viscosity (kg/m sec)
μ_{eff}	effective viscosity (kg/m sec)
ν	dynamic viscosity (m^2/kg)
π	geometric constant
ρ	density (kg/m^3)
ρ_λ	reflected energy at a given wavelength (kW)
σ	normal stress (N/m^2)
σ	Stefan-Boltzmann constant (W/m^2K^4)
σ_f	specific extinction area (m^2/kg)
σ_s	scattering coefficient
τ	shear stress (N/m^2), duration (sec)
ϕ	general variable of interest, rotational angle (rad)
∞	infinity, ambient
∇	del operator
ω	solid angle (rad)
Γ	Schmidt number
Φ	convective simplification variable
Φ_e	hemispherical surface energy flux (kW/m^2)
Ω	thermal resistance (m^2K/W)

Subscripts and Superscripts

E	energy
b	black surface, black body
bi	boundary element
c	compartment
con	convective
e	exposed
f	fluid
g	gas
i	indexed notation
j	indexed notation, dummy variable
k	indexed notation, dummy variable
o	initial
p	particle
r	radiant, to the radiant phase (superscript)
s	surface
sc	scattered
t	turbulent
tot	total
v	vapor
w	water
x	denoting the x-direction
y	denoting the y-direction
z	denoting the z-direction
α	species alpha
λ	specific wavelength
$-$	time average superscript
$'$	fluctuating term superscript
∞	ambient, infinity

Note: Depending on the application, units may vary. Units for constants are a function of the relationships in which they are utilized.

Part I
Background

1 Introduction

Over one third of all post-collision vehicle fire deaths and over one half of the injuries can be attributed to fires originating in the engine compartment, where over two-thirds of these post-collision fires begin [11].

In an effort to find ways to mitigate the consequences of the post-crash vehicle fire scenario, research has been initiated into the realm of car fire modeling using the computational fluid dynamics code TASCflow. At this time, approximately 50 transient runs have been completed in the first phase of the overall deliverable. While earlier runs were performed to help establish proper boundary conditions and model sensitivities to various input parameters, later runs were conducted in a systematic fashion to assist in the study of the effects of environmental and material variations. Conductive heat transfer through a multi-layer boundary has been studied with the intent of determining the relative importance of having an intact bulkhead after an automobile collision. Excellent progress has been made with respect to determining the suitability of TASCflow to model the bulkhead heat transfer problem, as well as more advanced phenomena that will surely influence the simulation of post-crash fires.

The first step towards completing an engineering model of this nature is to properly define the problem so that the simulation reflects reality (as defined by qualitative information and experimental data). The post-crash automobile fire may be characterized by the following entities:

- Readily available ignition sources including hot surfaces in the engine, electrical sparks in the engine or passenger compartment, and mechanically produced sparks resulting from the actual impact or subsequent movement of the vehicle.

- Small spaces in and around the engine compartment with fuel and geometries conducive to rapid heat accumulation and flame spread.

- The presence of a fuel tank which may or may not be ruptured. Dangers associated with a ruptured or leaking fuel tank include pool fires. In the event that the fuel tank is not compromised, the presence of rapid heating may induce high pressures leading to blow-back of fuel and/or spray fires. The likelihood of this particular situation was not quantified in this study.

- The presence of combustible lining materials in the passenger compartment and engine compartment. This includes combustible foams used in seats and ancillary cushions or interior linings.
- Ample ventilation resulting from ruptures or cracks in structural or body elements allowing for combustion as well as additional paths for flame to spread from the exterior or engine compartment to the interior of the passenger compartment.
- Presence of occupants who may be unconscious, trapped, or unable to leave the vehicle for other reasons.
- Significant delays from the time of fire initiation to the time of fire suppression as a result of remoteness and lack of extinguishing agents or the ability to bring the agents to the fire.

An overview of the Computational Fluid Dynamics (CFD) modeling efforts required to address these issues will now be provided.

1.1 General Modeling Tasks

One important objective of a model developed to study the post-crash fire scenario is to evaluate the conditions inside the passenger compartment of the vehicle in question. The modeling effort here includes:

1. **Fire Scenarios** - The initial location and mode of combustion are important to how the fire will spread and grow in intensity. Fires originating in the engine compartment and under the vehicle in the vicinity of the fuel tank were studied in this research. The effects of openings in either the engine compartment bulkhead or the passenger compartment were examined in this context.
2. **Heat and Toxic Gas Production** - The generation of energy and toxic species from the combustion of various fuels inside the engine compartment, passenger compartment, and under the vehicle were the basis for the modeling problem.
3. **Transport mechanisms** - Heat transfer from the initial ignition source through solids (including insulations, structural steels, and other barriers such as windshields) to the passenger compartment were addressed. Radiation, convection, and conduction were simultaneously considered.

4. **Boundary conditions and material properties** - The nature of the materials and surrounding environment is important when trying to accurately predict heat transfer and fluid flow phenomena. Thermally dependent properties and state behavior are required to assess flow-dependant heat conduction as well as kinematic reactions.

Detailed discussion of the fire scenarios used in this study is presented in Section 3.5.

1.2 Discussion of Deliverable

Because of the complicated nature of this problem, it has been necessary to break it down into various subtasks which were completed. The following research has been completed as part of the first deliverable of this project:

1. The suitability of TASCflow for the bulkhead heat transfer problem has been confirmed.

2. Appropriate boundary conditions for modeling the bulkhead have been identified with emphasis on a first estimate appropriate design fire for the engine compartment.

3. Appropriate thermally dependent heat transfer properties for typical insulative materials used in vehicle bulkhead construction have been identified.

4. TASCflow (assuming it is appropriate based on task 1) has been applied to a simple case of a bulkhead consisting of an insulative and a steel layer.

5. The results of task 4 have been compared with the finite element model previously developed for the U.S. Coast Guard.

6. The model of task 4 has been extended to include a third layer. This model is for a bulkhead consisting of a layer of insulation, a steel core and another layer of insulation.

First and foremost, confirmation of the suitability of TASCflow has been accomplished. Because of the unique solver features and grid capabilities inherent in this code, application of this modeling tool to the bulkhead heat

transfer problem has demonstrated the capability to model the major phenomena associated with bulkhead heat transfer *and* the more specific phenomena associated with automobile fires. Furthermore, the adaptive structure within TASCflow enables the user to alter the code to more accurately predict those aspects of fluid flow and heat transfer that are most important. With respect to car fire simulations, this capability is absolutely necessary due to the state of the art of modeling fire spread and fire growth in small spaces with complicated features. TASCflow possesses the necessary features that not only enable, but facilitate the solution of the equations needed to describe the problem at hand.

Modeling of a vertical bulkhead, as specified in this deliverable, was accomplished for two- and three-layer structures. While the bulkheads that were modeled are not intended to represent those bulkheads found in automobiles, they are similar in form. This modeling effort was undertaken in order to validate the conjugate heat transfer code in TASCflow as well as to learn how the boundary conditions and thermal properties affect the response of materials being modeled as conjugate heat transfer objects. Conjugate Heat Transfer (CHT) may be used where heat transfer from fluids and gases to solids and through the solid is of interest. The boundary conditions used to describe the generic bulkhead heat transfer simulation have been fully established and are presented in this report. Those boundary conditions for future efforts have been researched and are presented in Part 3.

Two major design fire scenarios were identified: An engine compartment fire and a pool fire under the engine compartment. Critical combustion parameters (heats of combustion, mass loss rates, etc.) have been determined and material compositions for the development of the boundary conditions for the engine compartment. Likely routes for flame spread have further been identified, and may be utilized in the future development of the engine fire scenario with the TASCflow package.

The complex nature of the heat transfer properties was revealed, and the importance of using the most representative properties was discovered as a result of this modeling effort. Recommendations and methodologies for dealing with a lack of good data have been briefly described, and should prove to be useful for all future efforts. It is important that accurate and *useful* data be obtained if the model is ultimately intended to produce reliable results.

The application of TASCflow to two- and three-layer bulkheads has helped to identify various issues that will pose a challenge to the modeler. Compar-

isons of the results from TASCflow and a finite element model, TASEF-2, have been made with data obtained from tests performed by the United States Coast Guard. Based on a selection of sample runs, it is apparent that TASCflow is capable of modeling conductive/convection heat transfer. It is further evident that the accuracy of these results is not only dependent on turbulence parameters, velocities, surface thermal properties (emissivity), gas properties (absorptivity), and geometry of the enginer compartment model, but also largely upon the conductivity, specific heat, and density of the materials in question. The comparison with the finite element model (which has been extensively validated in past modeling efforts for the United States Coast Guard) has demonstrated that TASCflow is quite capable and is just as dependent on thermal properties as is TASEF-2.

At this time, the suitability of TASCflow has been confirmed for the bulkhead heat transfer as well as the general modeling problem. Appropriate boundary conditions required to obtain the solution have been applied in conjunction with thermally-dependent material properties to arrive at the temperature response of two- and three-layer bulkheads (via Conjugate Heat Transfer). Fire scenarios that will support future modeling efforts have been characterized in the context of the post-crash vehicle fire. The application of TASCflow has proven to be successful and has demonstrated the sensitivity of solution to thermal properties, modeling parameters, as well as environmental conditions.

Part II
Suitability of TASCflow

2 Discussion of the Suitability of TASCflow

The suitability of TASCflow to model (1) bulkhead heat transfer and (2) some aspects of post-crash vehicle fires may be assessed by comparing the **available tools** with the **modeling challenges**. In Section 2.1, an overview of the capabilities found in TASCflow is presented in general terms. Section 2.2 summarizes the major phenomena associated with the post-crash vehicle fire with respect to the available tools in TASCflow (as presented in Section 2.1). Section 2.3 presents an overview of the governing relationships that Advanced Scientific Computing's (ASC) CFD code uses. Because certain aspects of the code are more relevant to the problems associated with the immediate work, special attention will be given to those areas in Sections 2.4, 2.5, 2.6, and 2.7. An overview of the Conjugate Heat Transfer relationships, radiation modeling techniques, combustion modeling, and grid development will be respectively discussed. It is through this careful examination that the suitability of TASCflow to deal with bulkhead heat transfer and the more advanced issues surrounding post-crash vehicle fire research will become evident.

2.1 Brief Overview of TASCflow - Available Tools

The TASCflow software package is designed to solve multidimensional complex fluid flow problems where the presence of non-combustible solids influences the heat transfer and flow predictions. The ability to approximate fluid flow and heat transfer for combustible, or ablative, lining materials also exists in some capacity, and may play a role in further development. TASCflow is being developed via a collaboration between the academic and industrial communities in an effort to provide the most technically sound theory and state-of-the-art discretization methods possible. Although TASCflow contains many useful modeling tools, a few stand out as being particularly important to the problem of modeling post-crash vehicle fires:

- **Basic capability code** required for all predictions includes transient and steady incompressible flow prediction, laminar flow and turbulence modeling, as well as multi-component fluid modeling.
- **Complex grid generation features** allow for more accurate representation of the post-crash vehicle geometries. The use of a robust

pre-processor allows for seamless grid attachment, block-off specification, and detailed specification of boundary conditions.

- **The Source Code Interface** (SCI) allows for modification of existing program parameters and boundary conditions via an array of FORTRAN subroutines. Because of the complex nature of the computational problem, the SCI is an invaluable tool for the engineer wishing to customize the code.

- **The graphically-oriented post-processor** allows for visual manipulation of the data produced in the runs. The various scalar and vector quantities at any point can be colorfully represented, thus allowing visual interpretation of results.

- **Material databases** built into the code allow for easier but more robust combustion calculations important to determining the conditions in a post-crash vehicle fire. Tested models for liquid droplet burning and plastics combustion exist within the TASCflow package.

- **The Conjugate Heat Transfer** (CHT) capability is required to solve heat conduction problems in the solid region of the control volume. Because heat transfer through materials *as well as* flow prediction are important, the CHT capability is indispensable.

- **Reacting and combusting species modeling** via the Eddy Dissipation Model (EDM) allows for simulations of combustion and corresponding species production.

In addition to the features highlighted above, the coupled solver available in TASCflow allows for a more robust solution of the governing equations associated with reaction kinematics. Because it may be necessary to develop complicated chemical reaction models, the code should have the ability to quickly solve numerous steps in the reaction. Furthermore, the coupled solver utilized in TASCflow allows for a *quicker* and *more robust* solution of combustion and radiation equations, which are highly non-linear by nature. The use of temperature-dependent properties where substantial gradients exist also poses problems for typical solvers, but is dealt with appropriately in TASCflow.

2.2 Major Phenomena Associated With the Modeling Problem

This modeling problem presents several unique challenges to the modeler arising from the highly diverse selection of materials as well as the wide latitude of configurations and environmental factors associated with modern automobiles and the post-crash environment. The following is a listing of defining characteristics that lend themselves to the rigors of CFD modeling:

- Complex fluid flow
- Turbulent heat transfer
- Combustion (and species production)
- Detailed geometries

A brief description now follows.

Complex fluid flow - Flows through bulkhead openings, around engine components, through openings in the windshield and into the passenger compartment from the exterior of the vehicle all present very challenging modeling problems. Because of the fundamental importance of these flows to the calculation of heat transfer and combustion in the post-crash vehicle fire, it is critical that these flows be accurately resolved.

The use of the Navier-Stokes equations (to solve momentum) as well as continuity are required in three dimensions. Mass transport is described in part by continuity, but may involve other relationships depending on the nature of the mass being transported (i.e. solid particles vs. fluids). The application of the $K - \epsilon$ turbulence model is appropriate as well. When these equations are solved in conjunction with the energy equations and a prescribed set of closure relationships, it is possible to determine the velocity vectors and thus other scalar quantities at the nodal coordinates.

Turbulent heat transfer - Heat transfer is strongly coupled with the fluid flow equations in fire problems (i.e. flow is buoyancy driven). Consequently, it is virtually impossible to solve for temperature scalars or heat flux values at various points without intimate knowledge of the velocity vector at that point. As for fluid flow, the use of the $K - \epsilon$ turbulence model allows

the user to take turbulent fluctuations into account which influence the heat transfer from the fluid to the surroundings.

Convection (gaseous diffusion), conduction (solid diffusion), and radiation are the three modes of heat transfer that are modeled. While convection predictions will arise from the solution to the momentum and continuity expressions, conduction (in CHT solids) and radiation (currently using either surface-to-surface or diffusion models) are solved independently. The heat transfer is further affected by species/soot production and other phenomena associated with combustion. The interaction between these modes of heat transfer will have a significant impact in the closed environments of the engine and passenger compartment. The nature and quantity of the fuel will further influence which mode of heat transfer is dominant.

Combustion - During the combustion reaction, soot and gaseous species are created. These elements may then have a direct impact on the tenability of the passenger compartment because of the production of toxic species. Multi-step kinetic models specific to the major fuels associated with car fires will be employed, drawing from established combustion theory. The implementation of specialized models, such as the plastics combustion model, allows for further refinement in modeling.

Detailed Geometries - The design of the computational grids and the degree to which these grids represent the geometry of post-crash vehicles is important to modeling effort. Not only does the geometry have to be detailed enough to capture small scale phenomena which influence the conditions inside the passenger compartment, but it must also be "solver friendly" to the CFD code so that properly converged solutions can be obtained in a timely manner.

The ability of TASCflow to create structured or unstructured grids facilitates both the solution and setup of the post-crash scenario. Structured schemes involve coupling the physical geometry with the computational geometry. The principle advantage of such a scheme is that the solutions may be converged more easily and with greater accuracy (spatial derivatives are better defined). The main disadvantage is that problems with extremely irregular geometries cannot be easily defined. The availability of such tools as grid attachment and embedding helps to alleviate the effects of this problem.

Unstructured schemes can be used to easily represent complex geometries

because the grids are not defined according to the computational coordinate system. Typically, a numerical algorithm which defines a control volume relative to its neighbors is used in the unstructured approach. The disadvantages of this approach include extensive computer memory requirements due to the complex data structures as well as reduced accuracy in the solution of the spatial derivatives (resulting from poorly defined mesh lines).

2.3 Governing Equations

The determination of conditions in the passenger compartment of an automobile subjected to post-crash conditions requires an accurate solution of the fundamental conservation equations. These expressions describe the kinetic and energy state of the control volumes in the CFD model with respect to known physical laws. Solution of the continuity, momentum, energy, and species equations set the stage for determining other dependent variables. The following section highlights these fundamental expressions in the context of CFD modeling. Literature relative to the derivation of these conservation laws is available in countless sources including White's *Viscous Fluid Flow* [40], Schlichting's *Boundary Layer Theory* [35], as well as the TASCflow3d *User Documentation - Theory* [1]. Unless noted, all indexed and Cartesian forms of the conservation and state equations have been derived from these sources.

2.3.1 The Eulerian Frame of Reference

The *Eulerian* approach to modeling fluid flow (tracking a fixed control volume over time) has been implemented in TASCflow. A general description of any control volume may be defined according to equation 1.

$$\frac{\mathrm{D}\phi}{\mathrm{D}t} = \frac{\partial \phi}{\partial t} + V \cdot \nabla \phi \tag{1}$$

where ϕ is the independent variable of interest. On the left-hand-side, the convective derivative describes the time rate of change from a Lagrangian perspective in terms of a fixed Eulerian point. The local change in the control volume is described by the first term on the right-hand-side. The dot product of the velocity vector and the divergence of ϕ represents the change due to convection at time t [31].

2.3.2 Conservation of Mass

The conservation of mass describes the mass flux through an infinitesimally small control volume. The sum of the time rate of change in density and the mass flux through the surfaces of a control volume must be equal to zero. Applying the definition of the total derivative, the simplified expression given in equation 2 is obtained.

$$\frac{D\rho}{Dt} + \rho \cdot \nabla \mathbf{V} = 0 \tag{2}$$

For an incompressible fluid (constant ρ), the gradient of the velocity vector must be zero:

$$\nabla \cdot \mathbf{V} = 0 \tag{3}$$

This form is achieved after considerable simplification (by way of implementing the chain rule for differentiation). In simple indexed notation, the conservation of mass is given according to equation 4 [31].

$$\frac{\partial u_i}{\partial x_i} = \nabla \cdot \mathbf{V} = 0 \tag{4}$$

2.3.3 Conservation of Momentum

The dynamic equation for fluid motion is derived by applying Newton's Second Law to a particulate control volume with differential mass dm:

$$dF = dm \frac{D\mathbf{V}}{Dt} \tag{5}$$

Equation 5 is written in vector form for convenience. The term on the left-hand-side, dF has been the subject of considerable mathematical and scientific study in the past century and serves as the basis of the fluid solution found in TASCflow. After summing forces on a fluid particle for the three principle axes of an orthogonal control volume and substituting in the viscous shear stresses, the simplified relationships given in equations 6, 7, and 8 are obtained.

$$\rho \frac{Du}{Dt} = \rho g_x - \frac{\partial p}{\partial x} + \frac{\partial}{\partial x}\left[\mu\left(2\frac{\partial u}{\partial x} - \frac{2}{3}\nabla \cdot \mathbf{V}\right)\right] + \frac{\partial}{\partial y}\left[\mu\left(\frac{\partial u}{\partial y} + \frac{\partial v}{\partial x}\right)\right] + \frac{\partial}{\partial z}\left[\mu\left(\frac{\partial w}{\partial x} + \frac{\partial u}{\partial z}\right)\right] \tag{6}$$

$$\rho \frac{Dv}{Dt} = \rho g_y - \frac{\partial p}{\partial y} + \frac{\partial}{\partial x}\left[\mu\left(2\frac{\partial u}{\partial y} + \frac{\partial v}{\partial x}\right)\right] + \frac{\partial}{\partial y}\left[\mu\left(2\frac{\partial v}{\partial y} - \frac{2}{3}\nabla \cdot \mathbf{V}\right)\right] + \frac{\partial}{\partial z}\left[\mu\left(\frac{\partial v}{\partial z} + \frac{\partial w}{\partial y}\right)\right] \tag{7}$$

$$\rho \frac{Dw}{Dt} = \rho g_z - \frac{\partial p}{\partial z} + \frac{\partial}{\partial x}\left[\mu\left(\frac{\partial w}{\partial x} + \frac{\partial u}{\partial z}\right)\right] + \frac{\partial}{\partial y}\left[\mu\left(\frac{\partial v}{\partial z} + \frac{\partial w}{\partial y}\right)\right] + \frac{\partial}{\partial z}\left[\mu\left(2\frac{\partial w}{\partial z} - \frac{2}{3}\nabla \cdot \mathbf{V}\right)\right] \tag{8}$$

In basic indexed notation, Newton's Second Law may be given in conservation form according to equation 9.

$$\frac{\partial}{\partial t}(\rho \mathbf{V}) + \nabla \cdot \rho \mathbf{V}\mathbf{V} = \rho \mathbf{f} + \nabla \cdot \sigma_{ij} \tag{9}$$

The first term on the left side is the rate of change (increase) of momentum with time in the control volume. The second term represents the convective loss per unit volume through the control surface of the control volume. On the right side, the first term is the body force that acts through the entire control volume. Gravity is assumed to be the only body force. The last term accounts for the surface forces on a per unit volume basis and includes the normal and shear stresses in the stress tensor, σ_{ij}. The $\nabla \cdot \rho \mathbf{V}\mathbf{V}$ term is the divergence of a tensor. After substituting in the viscous stress terms and simplifying, the conservative form of the indexed continuity expression is obtained:

$$\frac{\partial(\rho u_i)}{\partial t} + \frac{\partial}{\partial x_j}(\rho u_i u_j) = X_i - \frac{\partial p}{\partial x_j} + \frac{\partial}{\partial x_j}\left[\mu\left(\frac{\partial u_i}{\partial x_j}\right)\right] \tag{10}$$

2.3.4 Conservation of Energy

The following presentation of the energy equation is taken from Schlichting's *Boundary Layer Theory* [35]. Applying the first law of thermodynamics to a fixed infinitesimally small element serves as the basis for the development of the energy equation.

$$\rho \frac{De}{Dt} + \rho \frac{D(\frac{V^2}{2})}{Dt} = \frac{\partial Q}{\partial t} - \nabla \cdot \mathbf{q} + \rho \mathbf{f} \cdot \mathbf{V} + \nabla \cdot (\sigma \cdot \mathbf{V}) \tag{11}$$

The first term on the right-hand-side represents volumetric heating that can include radiation and combustion effects. Transfer of energy across the surface of the control volume via conduction is represented in the next term. The third and fourth terms account for the work done per unit volume on the control volume by body and surface forces respectively. After considerable mathematical manipulation with the momentum equation, the final form of the energy equation can be expressed as

$$\rho \frac{De}{Dt} = \frac{\partial Q}{\partial t} - \nabla \cdot \mathbf{q} + \Phi \tag{12}$$

As with the continuity and momentum equations, for Cartesian coordinates the energy equation can be expressed using index notation and taking advantage of Fourier's law for conduction,

$$\rho\left(\frac{\partial e}{\partial t}+u_j\frac{\partial e}{\partial x_j}\right)=\frac{\partial Q}{\partial t}-\frac{\partial}{\partial x_j}\left(k\frac{\partial T}{\partial x_j}\right)+\Phi \tag{13}$$

where Φ is a dissipation function reflecting dissipation of energy due to Newtonian stresses (usually with turbulence effects added) and is given according to equation 14. It should be noted that for typical fire modeling scenarios, most of the terms in the function presented in equation 14 are negligible.

$$\Phi=\mu\left[2\left(\frac{\partial u}{\partial x}\right)^2+2\left(\frac{\partial u}{\partial y}\right)^2+2\left(\frac{\partial w}{\partial z}\right)^2+\left(\frac{\partial v}{\partial x}+\frac{\partial u}{\partial y}\right)^2+\left(\frac{\partial w}{\partial y}+\frac{\partial v}{\partial z}\right)^2+\left(\frac{\partial u}{\partial z}+\frac{\partial w}{\partial x}\right)^2\right] \tag{14}$$

Using the relation between internal energy and temperature for an incompressible fluid, $\partial d = c_v \partial T$, allows equation 13 to be expressed in terms of temperature and other flow field variables only

$$c_v\left(\frac{\partial T}{\partial t}+\frac{\partial}{\partial x_j}\left(\rho T u_j\right)\right)=\frac{\partial Q}{\partial t}-\frac{\partial}{\partial x_j}\left(k\frac{\partial T}{\partial x_j}\right)+\Phi \tag{15}$$

2.3.5 Equation of State

The following presentation has been adapted from R.D. Pehrson [31]. Using the three available momentum expressions, continuity, as well as the energy equation provides five equations. However, there are six unknowns (u,v,w,ρ,p, and e) and so another equation is needed to provide closure. By assuming ideal gas behavior, the *ideal gas law* equation of state can be utilized,

$$p=\rho RT \tag{16}$$

It should be noted that the use of equation 16 is at the expense of introducing a seventh variable, the temperature, T.

Additional state relationships are available to relate the thermodynamic variables to the transport constants such as thermal conductivity and viscosity. Sutherland's relation for viscosity as a function of temperature has been used for the combustion gases in the bulkhead model presented in Part 5.

$$\mu=C_1\frac{T^{\frac{3}{2}}}{T+C_2} \tag{17}$$

where C_1 and C_2 are fluid specific constants is just such a relationship. With the specific heat and viscosity known, the Prandtl number relates viscosity to thermal conductivity according to equation 18.

$$Pr = \frac{c_p \mu}{k} \tag{18}$$

2.3.6 Conservation of Species

Derived from mass continuity, the conservation of chemical species represents a specialized form of mass conservation, given according to equation 19.

$$\rho \frac{DY_\alpha}{Dt} = -\nabla \cdot \mathbf{J}_\alpha + S_\alpha \tag{19}$$

The term $\mathbf{J}_\alpha$ is from Fick's Law of diffusion, given in equation 20.

$$\mathbf{J}_\alpha = -\Gamma_\alpha \nabla Y_\alpha \tag{20}$$

Fick's Law for molecular diffusion, derived from the kinetic theory of gases, states that gases in two different parcels of fluid with different concentrations will undergo mixing until there is only one concentration in a constant pressure environment. In conservation form, Fick's Law is written as

$$\frac{\partial(\rho Y_\alpha)}{\partial t} + \nabla \cdot (\rho Y_\alpha \mathbf{V}) = -\nabla \cdot \mathbf{J}_\alpha + S_\alpha \tag{21}$$

Substituting equation 21 into 19, we arrive at the expression for conservation of species with Fick's Law:

$$\frac{\partial(\rho Y_\alpha)}{\partial t} + \frac{\partial}{\partial x_j}(\rho Y_\alpha u_j) = -\frac{\partial}{\partial x_j}\left(-\Gamma_\alpha \frac{\partial Y_\alpha}{\partial x_j}\right) + S_\alpha \tag{22}$$

where Γ_α is the diffusion coefficient.

2.3.7 Turbulence Modeling

Flows associated with combustion or compartment fire scenarios generally exhibit turbulent behavior, characterized by swirling eddies and random mixing. It is necessary to model the effects of turbulence because of the impact that it has on the dissipation of energy, production of species, combustion, and radiation heat transfer. Although the basic relationships developed in

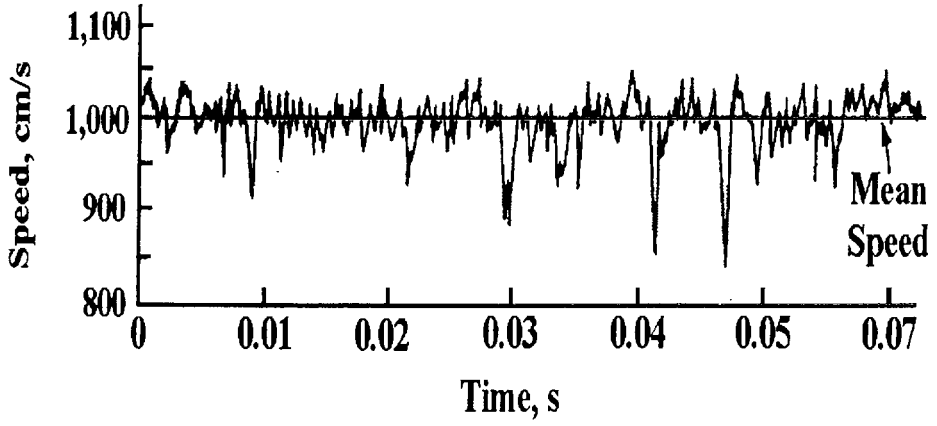

Figure 1: Mean and Fluctuating Turbulence Terms

Sections 2.3.2, 2.3.3, 2.3.4, and 2.3.6 can still be used to describe turbulent gas behavior, some modification is required. As a consequence of the turbulent behavior there are no unified (linear) approaches to modeling the viscous shear stresses, further complicating the efforts of the modeler. Typically, multi-equation models must be employed to adequately represent the phenomena associated with random fluctuations in the flow field.

Most research over the past three decades has focused on the concept of time averaged turbulent flows [27]. The basic premise involves allowing the velocity, temperature, and pressure terms to be broken into two components: a mean value and a fluctuating term. By taking this approach, a set of equations commonly referred to as *Reynolds Equations* are obtained. At this point, the modeling challenge involves properly representing the fluctuating terms with respect to the type of flow that is thought to exist. Figure 1 [40] shows the nature of the mean and fluctuating terms for a simple flow. Figure 2 [40] depicts a series of typical turbulent eddies in a planar flow.

Arising from the time-averaged form of the continuity, momentum, energy, and species equations, the concept of the eddy viscosity has become the standard method to represent the additional effects of turbulence. The turbulent, or eddy viscosity, is a property of the flow, and not the fluid as is the case for the fluid or laminar viscosity, μ. By defining the turbulent

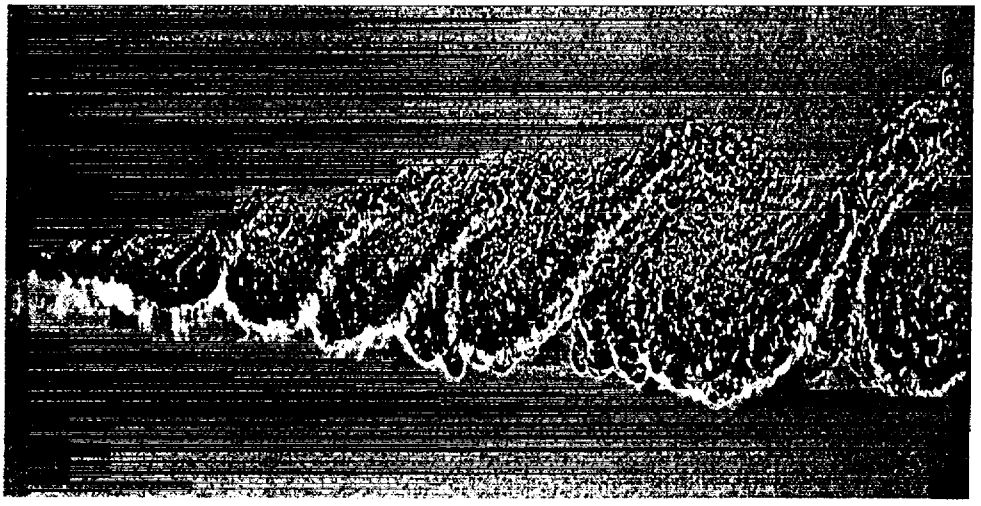

Figure 2: Turbulent Eddie

kinetic energy, $\bar{k} = \frac{1}{2}\bar{u_i'}\bar{u_i'}$, the eddy viscosity was modeled as

$$\mu_T = \bar{\rho} u_T l = C_k \bar{\rho} l \sqrt{\bar{k}} \tag{23}$$

The eddy viscosity, μ_t, has been modeled using the standard two-equation $K - \epsilon$ model [41]. This model has been widely used by fluids engineers since the late seventies and has demonstrated its robust nature through many successful applications. The idea for the $K - \epsilon$ model originated after it was found that the turbulent energy equation performed better when coupled to a rate of change of the dissipation. For high Reynolds number, non-boundary layer (fully elliptic) flows, the turbulent energy and dissipation expressions are given according to the indexed expressions in equations 24 and 25.

$$\frac{DK}{Dt} \approx \frac{\partial}{\partial x_j}\left(\frac{\nu_t}{\sigma_k}\frac{\partial K}{\partial x_j}\right) + \nu_t \frac{\partial \bar{u_i}}{\partial x_j}\left(\frac{\partial \bar{u_i}}{\partial \bar{x_j}} + \frac{\partial \bar{u_j}}{\partial x_i}\right) - \epsilon \tag{24}$$

$$\frac{D\epsilon}{Dt} \approx \frac{\partial}{\partial x_j}\left(\frac{\nu_t}{\sigma_\epsilon}\frac{\partial \epsilon}{\partial x_j}\right) + C_1 \nu_t \frac{\epsilon}{K}\frac{\partial \bar{u_i}}{\partial x_j}\left(\frac{\partial \bar{u_i}}{\partial \bar{x_j}} + \frac{\partial \bar{u_j}}{\partial x_i}\right) - C_2 \frac{\epsilon^2}{K} \tag{25}$$

The effective Prandtl numbers relating the diffusion terms, K, and ϵ to the eddy viscosity are given in equations 26 and 27.

$$\sigma_K = \frac{\nu_t}{\nu_K} \tag{26}$$

$$\sigma_\epsilon = \frac{\nu_t}{\nu_\epsilon} \tag{27}$$

The eddy viscosity is given as

$$\mu_t = C_\mu \rho \frac{K^2}{\varepsilon} \tag{28}$$

where C_μ is usually given the value in the range of 0.05 to 0.09. The other emperical constants (a total of five exist in the model) vary according to the boundary layer conditions present.

This model has been designed for use in the overlap and outer layers in a fluid flow regime. In TASCflow, the use of log-law wall models is the preferred method for dealing with the turbulence occurring very near to the surfaces [1]. For further discussion on the use of wall functions, see Launder and Spaulding [24].

In addition to solving the turbulent and laminar forms of the conservation equations, TASCflow possesses other capabilities that make it particularly suitable for the problem of the post-crash vehicle fire. In the remaining sections of Part 2, discussion will be centered around the background and use of other major sub-models and features. These include:

- Conjugate Heat Transfer capabilities associated with heat transfer through the bulkhead
- Radiation modeling and Gibb's Diffusion Model
- Eddy Dissipation Combustion model (including plastics burning)
- Grid development tools specific to TASCflow

2.4 Conjugate Heat Transfer

The use of TASCflow may not be merited for $\bar{T}$ failures because of the time required to create a working grid which will allow for an accurate and well converged solution of the conservation equations and the associated scalar quantities. A $\bar{T}$ failure is a thermal failure where the thermal properties of barrier to the smoke and heat of a fire are such that a localized "hot spot" develops, allowing heat to move from one side of the barrier and cause an ignition on the other side of the barrier. The detail offered by TASCflow *does* become important when dealing with a combination of fluid flow through openings and around objects *combined with* conduction heat transfer (as in the $\bar{D}$ failure). A $\bar{D}$ failure is a durability failure where a structure that can be considered a barrier to the heat and smoke of fire has an opening or an open door that will allow heat and smoke to move from one side of the barrier to the other. The complicated nature of the engine compartment and bulkhead, and their influence on the conditions inside the passenger compartment warrant the use of the multiple control volume approach afforded by Computational Fluid Dynamics (CFD) modeling.

The proper application of TASCflow to bulkhead heat transfer depends on a number of parameters. In general, the fire scenarios have to be identified, the grid created, appropriate boundary conditions established, and thermally dependent properties determined before an iterative application of TASCflow can be affected. Issues such as varying time scales need to be considered when attempting a solid-fluid solution with a CFD model. As an example, the characteristic time associated with fluid flow and heat transfer in gases is considerably smaller than the time associated with conductive heat transfer. As a result of these differences, the time step required in the numerical solution should be different depending on whether a solid or fluid solution is desired. When a simultaneous solution is required, only one time step can be chosen and so the smaller of the two (usually fluid) will be chosen. The Conjugate Heat Transfer (CHT) capability available in TASCflow has been developed specifically to deal with the challenges associated with the solid-fluid interface where determining conduction through the solid is critical [1]. A discussion of CHT and the iterative application of this capability to the post-crash vehicle fire will be presented in Section 2.4.1. General CHT theory will be followed by a summary of boundary condition issues and then implementation considerations for bulkhead modeling *as well as* modeling that is covered in a report on windshield modeling.

2.4.1 CHT Theory

Conjugate Heat Transfer is characterized by heat transfer from a domain consisting of a fluid to a CHT solid and then conduction through that solid. In the fluid domain, the conservation equations are solved and the energy is transferred to the CHT solid at the interface between the two domains allowing for the subsequent characterization of conduction. The time averaged total energy equation is used in varying forms to describe the Conjugate Heat Transfer from the fluid through the solid domain. In the fluid domain (i.e. the interior of the engine compartment and on the exposed side of the bulkhead), TASCflow implements the time-averaged relationship described in equation 29 [1].

$$\frac{\partial}{\partial t}(\rho H) - \frac{\partial P}{\partial t} + \frac{\partial}{\partial x_j}(\rho u_j H) = \frac{\partial}{\partial x_j}(\lambda \frac{\partial T}{\partial x_j} + \frac{\mu_t}{Pr_t}\frac{\partial h}{\partial x_j} + S_E + \frac{\partial}{\partial x_j}\left[u_i\left[\mu_{eff}\left(\frac{\partial u_i}{\partial x_j} + \frac{\partial u_j}{\partial x_i}\right) - \frac{2}{3}\mu_{eff}\frac{\partial u_l}{\partial x_l}\partial_{ij}\right] + \mu\frac{\partial k}{\partial x_j}\right] \tag{29}$$

The indices i and j are Einsteinian (indexed) notations. T is the temperature, k is the kinetic energy, c is the specific heat, ρ is the density, λ and μ are Newtonian fluid viscosity terms, Pr is the Prandtl number, S_E is the source term, x is a directional term, and t is time. H represents the total enthalpy, and is expressed in indexed form in equation 30.

$$H = h + \frac{1}{2}u_i u_i \tag{30}$$

Alternatively, in the solid domain, transport of energy is accomplished solely by diffusion, expressed according to equation 31.

$$\frac{\partial(\rho c T)}{\partial t} = \frac{\partial}{\partial x_j}\left(\lambda\frac{\partial T}{\partial x_j}\right) + S_T \tag{31}$$

For bulkhead modeling, the following procedure is followed to solve the energy equations used in TASCflow [1]:

1. Assembly of the fluid energy equation for each active node in the fluid domain.

2. Assembly of the solid energy equation for each active node in the solid domain.

3. Specification of boundary conditions for fluid energy equation at each boundary face exposed to fluid and each boundary face exposed to the solid.

4. Application of the Conjugate Heat Transfer condition allowing energy flow from a fluid and a solid at the interface between fluid and solid boundaries.

5. Formation of aggregate fluid control volumes where grid embedding has been performed to deal with connections or detailed flows.

6. Solving of the coupled equations (given in general form in expressions 29 and 31) using the coupled multigrid solver

7. Determination of Conjugate Heat Transfer and solid dependent variables.

The interior discretization of the fluid control volume is not affected by the Conjugate Heat Transfer conditions described in Section 2.4.2. Likewise, the fluid specified boundary conditions are the same as for any fluid problem.

2.4.2 Conjugate Heat Transfer Boundary Conditions

Because of the structure of the Conjugate Heat Transfer (CHT) problem in TASCflow, interface boundary conditions are required to establish the relationship between the fluid and the solid. Of particular interest is the interface condition described by *many fluid boundary faces in contact with one CHT solid.* In the case of bulkhead modeling, it is convenient to specify the other materials in the engine compartment as either blocked out (non-reacting solid) or adiabatic (no heat loss). The bulkhead (exposed to fluid on two sides) is modeled using the CHT routines. As a result of this type of specification, it will be necessary to deal with the material dependent properties of the bulkhead only. A more detailed discussion of the boundary conditions used to solve the bulkhead heat transfer problem is given in Part 3.

2.5 Radiation Modeling

The modeling of radiation heat transfer in this work is important to current and future efforts because of the influence that this mode of heat transfer has on all of the fire scenarios used here. A generic discussion of the mean beam approximation for radiation will be supplemented by background on absorbing, emitting, and scattering media. Next, the diffusion model currently being used to model bulkhead heat transfer as well as the finite volume model being added to the package will be discussed in the context of their implementation in TASCflow. Finally, a discussion of the absorption model ABSORB and soot prediction tools will be provided.

2.5.1 Intensity and the Mean Beam Approximation

Fundamental to the characterization of radiation heat transfer, the concept of intensity will serve as the starting point in our discussion of radiation modeling. Sparrow and Cess give the intensity of radiation, i_r according to equation 32.

$$i_r = \frac{d\Phi_e}{dwcos\theta} \tag{32}$$

where i_r is defined as the radiant energy leaving a surface per unit area normal to the propagating radiation wave and Φ_e is the energy flux passing from the surface into the hemispherical space. The geometric interpretation of θ is shown in Figure 3.

Integrating with respect to θ, an expression for Φ_e is found accordingly in equation 33. The symbol $\cap$ denotes integration with respect to the solid angle, dw over a hemisphere.

$$\Phi = \int_{\cap} i_r cos\theta dw \tag{33}$$

By integrating over the hemisphere shown in Figure 3, the expression for Φ_e in equation 34 is found.

$$\Phi_e = \int_0^{2\pi} \int_0^{\pi/2} i_r cos\theta sin\theta d\theta d\phi \tag{34}$$

If the intensity is independent of direction, $\Phi_e = \pi i$, and the *total* intensity is then expressed according to equation 35.

$$i_r = \int_0^{\infty} i_\lambda d\lambda \tag{35}$$

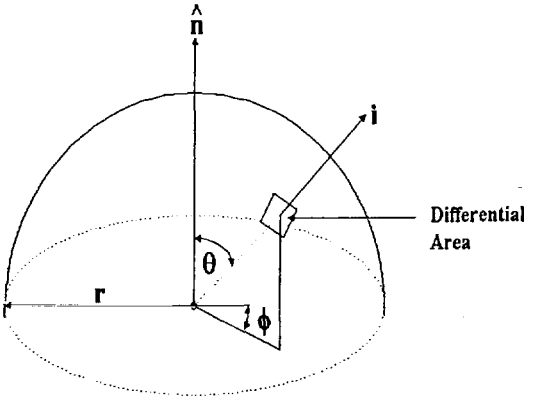

Figure 3: Integration of Intensity Over Solid Angle for a Hemisphere

While a discussion of intensity is certainly important to understanding the fundamentals of radiation and radiation properties, TASCflow has implemented a more practical approach in the modeling of radiation phenomena: the mean beam approximation. A mean beam approximation would be satisfactory for a well-mixed enclosure, such as a furnace, but more general analysis of radiation is required when the bounding surfaces are not all at the same temperature and the fluid volume is non-isothermal. The discrete transfer (not discussed) and diffusion models are currently the most popular among fire researchers, although the finite volume transfer method holds the promise of increased accuracy, especially for non-orthogonal grids. Following a discussion of the mean beam approach, the subject of the diffusion model currently implemented as well as the finite volume model will be discussed. A finite volume radiation model was implemented in TASCflow after the bulkhead research was completed.

For a beam of radiant energy of intensity, I, passing through a differential volume, the change in intensity is given as [25, 34]

$$\frac{dI}{d\ell} = -(K_a - K_s)I + K_a I_b(T) + \frac{K_s}{4\pi}\int_{4\pi} p(\theta', \phi' : \theta, \phi) I(\theta', \phi') d\omega' \qquad (36)$$

$d\ell$ is the length of the portion of the beam passing through the volume, K_a

and K_s are the gas absorption and scattering coefficients, $I_b(T)$ is the intensity associated with blackbody emission, $p(\theta', \phi' : \theta, \phi)$ is the probability that radiation incident in the (θ', ϕ') direction will be scattered in the θ, ϕ direction along the solid angle $d\omega'$ ($d\omega' = \sin\theta' d\theta' d\phi'$). Thus the terms that go into altering the intensity of the beam are attenuation due to absorption and scattering during travel along $d\ell$, emission and finally the radiation scattered along (θ, ϕ) from all directions. During an analysis of radiant heat transfer within the compartment, the definition of the extinction coefficient, $K_e = K_a + K_s$ will be important.

The models to be discussed provide the radiation source-sink term that goes into the energy equation solved for each control volume in the computational domain. For a control volume, the rate of net spectral radiation absorption is given by

$$\dot{R}_i = k_a \int_0^\infty \int_{4\pi} (I_\lambda(\theta, \phi) - I_{b\lambda}) d\omega d\lambda \tag{37}$$

where the integration of equation 36 gives $I_\lambda(\theta, \phi)$. Equation 37 as shown must be integrated over all wavelengths and around the sphere of 4π steradians. The radiation models to be discussed are all simplifications that relieve us from performing a triple integration for every control volume at each time step. For CFD modeling of fires, the temperature and species concentration distribution necessary to calculate the radiant transfer will be determined by a solution of the discretized conservation equations that include a number of approximations based on simplified models or experimental data.

2.5.2 Absorbing, Emitting, and Scattering Media

While the mean beam approximation provides an excellent basis for understanding the fundamental principals of radiation modeling, it is appropriate to offer further discussion on the nature of absorbing, emitting, and scattering in gases. The following explanation is intended to provide insight into the relationship between these three radiation parameters as well as their role in the modeling process. Furthermore, it is hoped that the reader will gain an increased understanding of the engineering simplifications used in radiation modeling.

Absorption in Media The primary gaseous products of combustion that are present in a test furnace or similar closed environment are CO_2, H_2O,

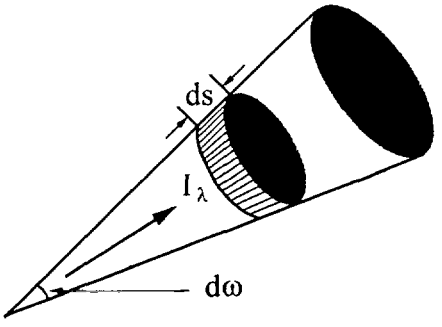

Figure 4: Geometric Interpretation of a Pencil of Radiation Rays

and CO (however, because of the particular structure of CO, this substance is a poor emitter). Because of the inherent nature of these gases, radiation will only be emitted and absorbed at certain wavelengths, much as if the gas barrier were acting as a window or other transparent barrier. In order to simplify the conglomerate effect that the furnace gases have on radiation transmission, modelers typically use a simplifying term known as absorptivity.

For radiation with an intensity of I_λ traversing a path length ds, the amount of absorption per unit time is assumed to vary according to the expression in equation 38.

$$\kappa_\lambda I_\lambda ds \tag{38}$$

The term κ_λ is defined as the monochromatic absorption coefficient of the media. By further simplification, the monochromatic absorption per unit time per unit volume due to the incident radiation beams is given by equation 39.

$$\kappa_\lambda \int_{4\pi} I_\lambda dw \tag{39}$$

The medium is assumed to be isotropic. Figure 4 shows the geometric interpretation of the terms dw, ds, and I_λ.

Scattering in Media In much the same way that the monochromatic absorption coefficient was derived, the monochromatic scattering coefficient may be found. Equation 40 characterizes the energy that is scattered per unit time per unit area per unit solid angle (of the hemisphere) normal to the rays.

$$E_{sc} = \gamma_\lambda I_\lambda ds \tag{40}$$

The variable, γ_λ is the monochromatic scattering coefficient. For the unit volume, this term is integrated, resulting in the total scattered energy given in equation 41.

$$E_{sc,tot} = \gamma_\lambda \int_{4\pi} I\lambda dw \tag{41}$$

By summing the absorption and scattering coefficients, the monochromatic extinction coefficient for participating media, β_λ, can be derivied.

$$\beta_\lambda = \kappa_\lambda + \gamma_\lambda \tag{42}$$

Emission in Media Sparrow and Cess [37] define the volumetric emission coefficient as $J_{\lambda,v}$, or the local emission from media per unit time per unit volume per unit solid angle. This parameter may be expressed in terms of the absorption coefficient, and Planck's function according to equation 43.

$$J_{\lambda,v} = \frac{\kappa_\lambda}{\pi} e_{b\lambda}(T) \tag{43}$$

Despite the ability to calculate these parameters over a large volume for a continuously varying gas or solid, reliance upon experimental data exists. Typically, the experimental measurements are complimented by analytical data, and extrapolations of the absorptive and emissive behavior of participating media may be made.

Using empirical coefficients, simultaneous gas and particle radiation can be calculated in a piece-wise method by summing the monochromatic absorption coefficients, or by determining the total emissivity for the two types of radiation and summing them. Accordingly, Paulsen has found that the total emissivity can be expressed according to equation 44:

$$\epsilon_{tot} = \epsilon_{g+p} = \epsilon_g + \epsilon_p - \epsilon_g \epsilon_p \tag{44}$$

where the subscript p denotes particle terms.

Using this total combined emissivity, it is usually practical to calculate the total radiation using the fundamental relationship given in equation 45:

$$Q_{tot} = \epsilon_{tot}\sigma T_g^4 \tag{45}$$

The total radiation is given as W/m^2. At this time, different approaches to modeling the fundamental phenomena associated with radiation heat transfer will be discussed.

2.5.3 Diffusion Model For Radiation

The choice of radiation model will have a significant impact on the accuracy of the results in any modeling effort. It is therefore important to choose the model based upon the expected conditions for the given problem. The significance of the impact of selecting radiation models was not quantified in this study. Two extremes are commonly recognized:

1. Transparent fluid where the boundaries play a dominant role via absorption and reflection. Energy is not directly transferred to the fluid in this case.

2. Optically dense fluid where scattering, absorption, and reflection by and of the particles and gases are the dominant mode of radiant energy transfer. Also known as the *diffusion limit*, this extreme implies that the radiant intensity is independent of direction and position.

In reality, the environment of interest will lie somewhere between the aforementioned extremes, though when considering high-soot-yield hydrocarbon-based fuels, the diffusion limit is appropriate. Certainly in the case of an automobile engine fire, the fluid may be observed to be optically thick due to incomplete combustion of solid *and* liquid hydrocarbon based fuels.

Gibb's [16] **Non-equilibrium Diffusion Radiation Model** is one model used in TASCflow that addresses the engineering simplification posed by the diffusion limit. Simultaneously, the form suggested by Gibb allows for a relatively simple (computationally speaking) solution. The practicality of employing this model has been found to depend largely upon the principle assumption of direction-independent radiative intensity. A brief overview of the theory and proposed implementation of this model now follows.

Integrating the radiant intensity, i, over all directions, we arrive at an expression containing the radiant temperature, T_r.

$$\frac{1}{4\pi}\int_{4\pi} i d\Omega = \frac{\sigma T_r^4}{\pi} \tag{46}$$

The radiant heat flux is defined in TASCflow according to equation 47.

$$q_r = \frac{4\sigma}{3K_e}\nabla T_r^4 \tag{47}$$

The fluid is considered optically dense for large values of K_e. Gibb defines the absorption as follows:

$$K_e = K_a + K_p^{'}(\epsilon_p + r_p(1 - f_{sc})) \tag{48}$$

The parameter K_a is the fluid absorption coefficient and $K_p^{'}$ is the particle cross-section per unit volume. The variable r is average reflectivity and ϵ is the emissivity. The scattering is accounted for through the parameter f_{sc}. After some manipulation, it is possible to obtain the net rate of energy transfer from the fluid to the radiant phase as well as the net rate of energy transfer from the particles to the radiant phase (equations 49 and 50).

$$\dot{Q}_f^r = 4\sigma K_a(T_f^4 - T_r^4) \tag{49}$$

$$Q_p^r = 4\sigma\epsilon_p K_p^{'}(T_p^4 - T_r^4) \tag{50}$$

The term in equation 49 is subtracted from the thermal energy expression used by TASCflow. Similarly, the term given in 50 is added during the temperature calculations.

Implementation of Gibb's Radiation Model The radiation only model acts as an energy transport mechanism. At this time, source terms (either positive or negative) can be added to this particular model via the TASCflow tool USRSRC. Because of the T^4 relationship, the expression in equation 46 will increase dramatically with T_r. Consequently, a poor initial guess can take some time to stabilize, especially in the case of combusting flows. Various tools have been developed in TASCflow to deal with stability problems introduced by the radiation model [9].

Parameters within the radiation routine can be modified for special conditions. Of interest to the problem of bulkhead heat transfer are the absorption and scattering parameters. Either constant or varying absorptivities and

emissivities can be implemented via regular user parameters or the Source Code Interface (SCI). Solid emissivities are dealt with via the boundary condition specifications in TASCBOB3D.

2.5.4 Finite Volume Model For Radiation

The **Finite Volume** radiation transfer model of Raithby [32] uses the same mesh developed by the user for the fluid flow prediction to produce a fully conservative set of relations for radiant heat transfer in non-isothermal participating media. Non-orthogonal grids that are difficult to use with most transfer methods are easily treated.

Starting from the expression written for the change in intensity of a pencil of radiation with cross sectional area dA^n as it passes through a hexahedral control volume, the intensity at node P from integrating the expression over a discrete solid angle ω is

$$\int_{\omega}\int_{A_{S,P}} I_S(\mathbf{s}\cdot\mathbf{n})dA_s d\omega = \int_{\omega}\int_{dV}\left[-(a+\sigma_s)I + aI_b + \sigma_s\bar{I}\right]dV d\omega \qquad (51)$$

$A_{s,p}$ and V are the surface area and volume of control volume P. Quadrature is performed by dividing $A_{s,p}$ into a finite number of surface panels each containing a centered integration point, f as shown in Figure 5. The ray passing through f is then traced back to a location, uf, where the intensity can be found by interpolation between nodal values. For simple two-dimensional enclosure problems containing a participating medium, very good agreement was observed with exact analytical solutions for course grids, with between linear and quadratic improvement in the prediction as the grid was refined. The model should not have any problem predicting transfer through non-isothermal gas volumes with different radiation property values throughout the fluid domain. The current surface to surface (optically thin) and diffusion (optically thick) models available in the structured version of TASCflow are not sufficient to properly address radiation when modeling flame spread. The finite volume or discrete transfer methods would be satisfactory for the calculation for radiation transfer.

2.5.5 Radiation Properties - ABSORB and RADCAL

The discussion in Section 2.5.2 provided a generic background on fundamental radiation properties. At this time, it is appropriate to offer background

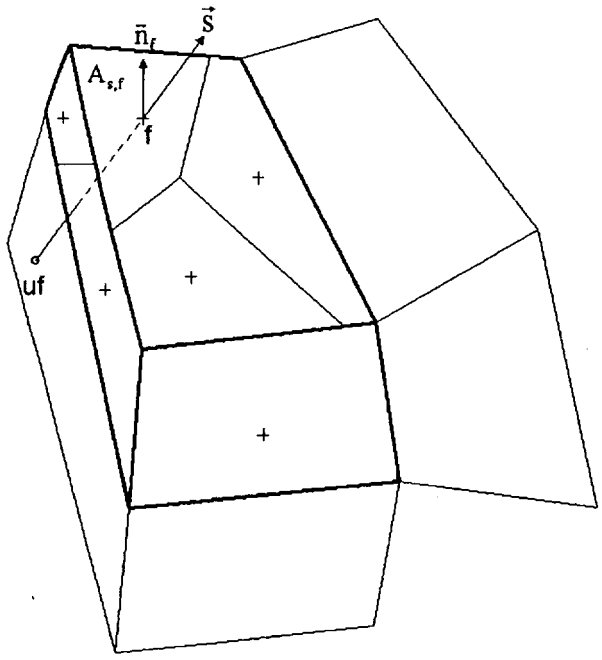

Figure 5: Finite Volume Transfer Method

on the implementation of radiation properties in TASCflow in the context of a model developed as part of the dissertation work of Pehrson [31]. The ABSORB model of Modak [28] is available to compute the absorptivity and emissivity of homogeneous isothermal mixtures of CO_2, H_2O and soot based on total emissivity curve fits of exponential wide band model results. Approximations are completed using three parameter (temperature, partial pressure and pressure path length) Chebyshev polynomials

$$\ln \epsilon_g = \sum_{i=0}^{2} T_i(x) \sum_{j=0}^{3} T_j(y) \sum_{k=0}^{3} c_{ijk} T_k(z) \tag{52}$$

with $x = 1 + \frac{\ln p}{3.45}$, $y = \frac{2.555 + \ln pl}{4.345}$, $z = \frac{T - 1150}{850}$, $T_o(x) = 1$, $T_1(x) = x$, and $T_{n+1}(x) = 2xT_n(x) - T_{n-1}(x)$. The absorptivity is then calculated from the emissivity using the approximation suggested by Hottel by taking into account the fraction of water vapor, $\zeta = \frac{p_w}{p_w + p_c}$,

$$a_g = \epsilon_g \left(\frac{T}{T_s} \right)^{0.65 - 0.2\zeta} \tag{53}$$

The curve fit relations are valid for temperatures of 300 K to 2000 K and pressure path lengths of 0.0011 to 1.0 atm meter. Soot absorptivity is approximated using the soot concentration, k_o, measured at wavelength, λ_o, the path length, l, and a blackbody source temperature, T_s:

$$a_s = 1 - \frac{15}{\pi^4} \psi^3 \left(1 + \frac{\lambda_o k_o T_s l}{c_2} \right) \tag{54}$$

The absorptivity of the mixture is then approximated as

$$a = a_s + a_g - a_s a_g \tag{55}$$

The quality of the agreement between the approximate absorption coefficient calculated by ABSORB and a full spectral integration for a mixture of CO2, H2O and soot is shown in Figure 6. The non-spectral calculations of ABSORB produce results in about two orders of magnitude less time than the full spectral calculation.

If the accumulated hot upper layer of gases in a compartment are considered well mixed (homogeneous), ABSORB is expected to give very good

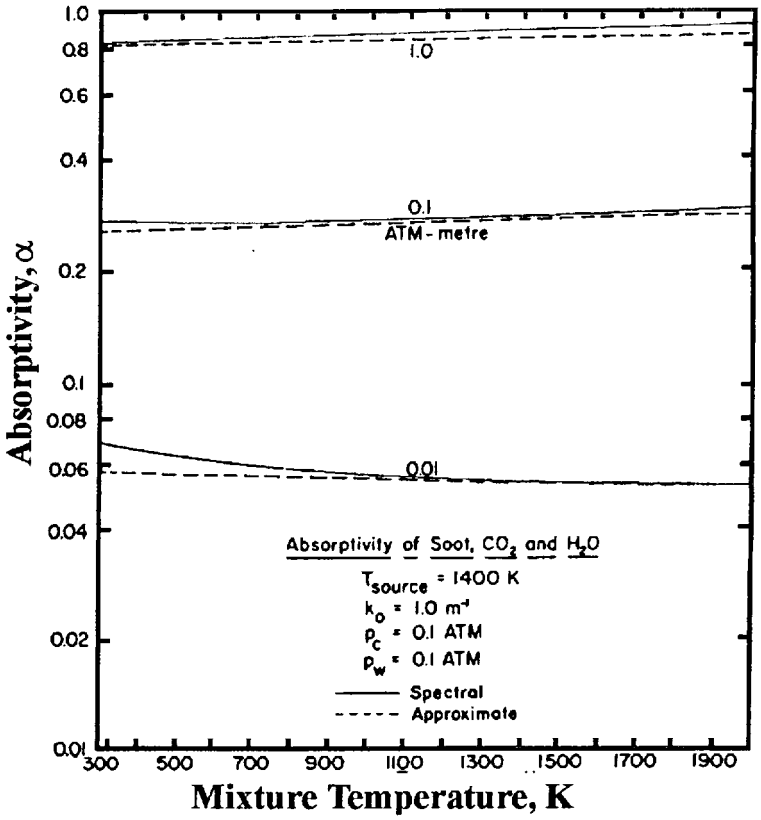

Figure 6: Modak ABSORB Wide Band Model Curve Fit Results Versus Spectral Calculations.

results. Path lengths will be on the order of about 1 to 3 meters, or pressure path lengths close to .3 atm-meter which are well in the region of close agreement between the exponential wide band model and ABSORB.

ABSORB has been used to predict the local absorption coefficient for each node throughout a discretized CFD domain based on local node fluid temperature, a blackbody source temperature, and concentration of soot, CO2 and H2O [44, 23]. The conditions throughout each control volume were considered homogeneous with representative path lengths on the order of .05 meters (approximate path length based on the size of each control volume). Pressure path lengths are now as low as .005 atm-meter which for temperatures expected in compartment fires, approach the lower limit of applicability. This is the same region where the agreement between the approximate calculation and the curve fit in ABSORB can be as great as 25 %. For pressure path lengths less than .0011 atm meter, ABSORB assumes the absorptivity is zero. Also, the radiation source temperature, T_s, is required for determining the absorption coefficient from the emission coefficient in Equation 53.

One step below line by line models and above wide band models in terms of resolution are the narrow band models. Instead of carrying out the spectral integration over each line, the spectrum for each species is divided into intervals on the order of 25cm^{-1} in which the spectral lines are assumed to have a random distribution. With the strength of the band following an exponential probability distribution, the emissivity for the interval, $\Delta\nu$, is [12]

$$\epsilon_{\Delta\nu} = 1 - \exp\left[-\frac{\left(\frac{S}{d}\right)X}{\sqrt{1+\left(\frac{S}{d}\right)\left(\frac{X}{B_d P_e}\right)}}\right] \tag{56}$$

when the path is homogeneous. Averages for the mean line intensity to spacing ratio, $\frac{S}{d}$, taken along a path provide the Curtis-Godson approximation for non-homogeneous mixtures. Grosshandler [18] has assembled a narrow band model called RADCAL using both theoretical approximations and tabulated spectral properties. The results of this model have been used to generate input data for simpler models, and also serve as a benchmark to models for non-homogeneous gas volumes [17].

The range of path lengths accepted by RADCAL to assure the model stays close to experimental data is 10^{-4} to 10^{3} meters. Characteristic lengths associated with discretization of compartments for fire prediction are well within this range. Clearly RADCAL would not have a difficulty in predicting accurately the radiation properties in each control volume, the drawback is significantly increased computer time demands. The Curtis-Godson approximation along with the Goody statistical narrow band model has been shown to have calculation times approaching two orders of magnitude longer than a simplified method such as the total transmittance non-homogeneous model [19], and approximately one order of magnitude over ABSORB.

2.5.6 Soot Production

The characteristic luminosity of a diffusion flame is due to the presence of glowing carbonaceous particles in the range of 10 to 100 nm. In fact, it is the collective effect of these particles, or soot, that accounts for over 70% of total emitted radiation from solid fuels. Acting as a gray body, soot particles will continue to play a role in the combustion process by way of producing what is commonly known as smoke [14]. Emitting over a continuous spectrum, the modeling of soot deserves special attention because of its impact on the

overall heat transfer process. Particularly in small enclosures such as those expected in a post-crash vehicle fire, the effect of soot on the radiation (and *re-radiation*) cannot be ignored.

From a theoretical standpoint, the modeler can look towards the *flamelet model* if soot prediction is of interest. This model relates the soot source terms to the mixture fraction in the fuel using kinetic rate equations (describing chemical reactions during pyrolysis and combustion). Whereas a multi-step turbulent reaction process needs to be specified in the flamelet model, various reaction libraries are available in TASCflow for simple fuels. At this time, reaction libraries have to be constructed for some of the more complicated fuels that would be present in the fire scenarios of interest for the post-crash vehicle environment. Another more simplified approach commonly employed in soot modeling is the use of soot yield rates, Y. These rates are often specified as a constant value for a given fuel, despite the fact that actual soot yields will vary as a result of environmental and material characteristics. Because the accuracy afforded by these techniques has not been adequate, a more recent trend in soot modeling has been to use empirical data. This approach will now be discussed in brief.

According to Drysdale [14], theory indicates that for particulate that has a diameter less than the radiation wavelength, the emission coefficient is proportional to the soot volume fraction, or proportion of a flame that the particulate occupies. Hence, if the ability to measure the soot volume fraction exists, then the ability to model the emission coefficient and therefore the absorption and scattering coefficients exists. Arising from this knowledge, two methods stand out as being particularly useful. In the past, the soot volume fraction could be obtained from what is known as the *optical density.* Optical density, D, may be obtained experimentally from readings using a photocell receiver and light source. Equation 57 shows the relationship between the initial intensity, I_o, and the intensity at the photocell, I.

$$D = -10 \log_{10} \frac{I}{I_o} \tag{57}$$

where D is given in decibels (db). More commonly, the *extinction area* is used in place of the soot volume fraction to characterize soot yield. This quantity, much like the optical density, may be obtained experimentally by using a monochromatic laser through a cross-section of typical products of combustion. Equation 58 denotes the extinction area (smoke per unit mass

of fuel burned) for a generic material.

$$\sigma_f = -\frac{\dot{V}}{L\dot{m}} \ln\left(\frac{I}{I_o}\right) \tag{58}$$

Mulholland found that the variation in specific extinction area with scale was small [29], which is important since no other variable used to characterize smoke shares this feature [5].

The use of the cone calorimeter has become a common method for measuring the extinction area in the past 10 years. The monochromatic laser included with the cone's instrumentation package has the capability of dynamically measuring the extinction area for well-mixed smoke traveling through the duct of the apparatus. Using typical data recording devices, the calorimeter will provide a characteristic soot production rate as a function of time. Because soot yield data tends to scale quite well, this data can then be plugged into the Computational Fluid Dynamics code in lieu of using a less accurate and less fuel specific theoretical model. Currently, these techniques have been successfully employed in work at Worcester Polytechnic Institute and will be used more extensively in future work for the post-crash fire modeling effort. Figures 7 and 8 show typical soot yields for materials similar to those found in modern automobiles.

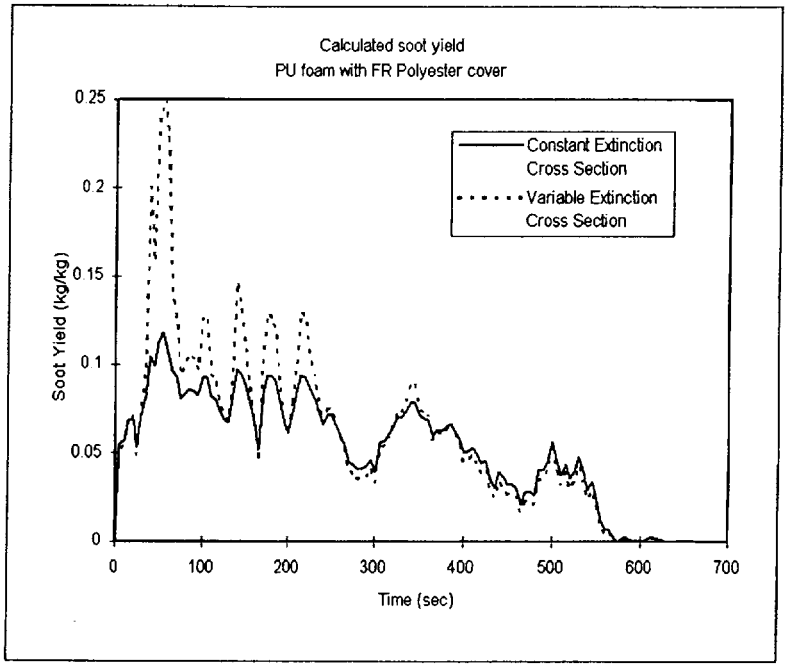

Figure 7: Typical Cone Calorimeter Data For Soot Yield

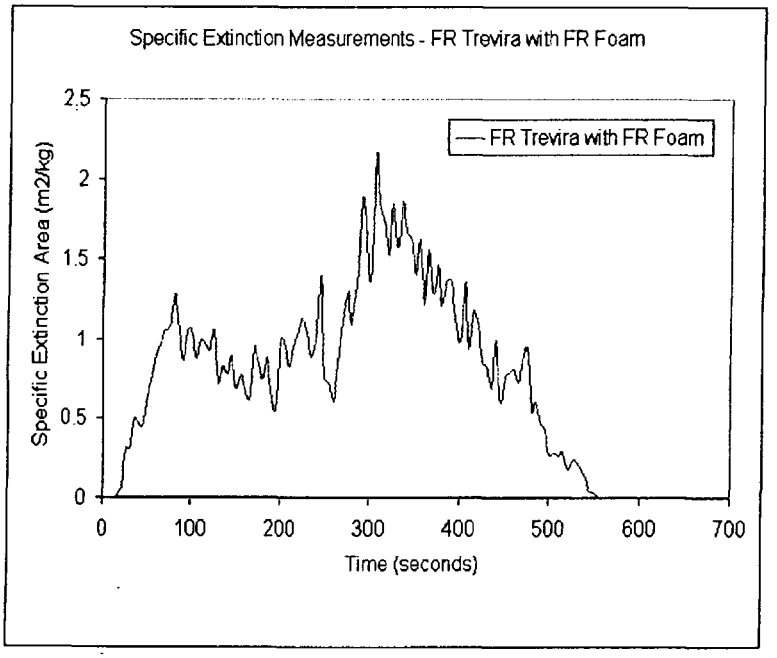

Figure 8: Typical Cone Calorimeter Data For Specific Extinction Area

2.6 Combustion Modeling

In order to effectively model the design fire scenarios, it is necessary to give proper consideration to the tools available in TASCflow. Specifically, the nature of combustion modeling, species production, as well as plastic melting and dripping should be explored. Combustion modeling will now be introduced in the general form that it will be implemented in the CFD code *TASCflow*.

The Eddy Dissipation Combustion model (EDC), which simulates reactions occurring in the flames, has been extensively used for industrial combustion applications. This model originates from the research efforts of Magnussen and Hjertagen [26]. The driving assumptions are listed below:

- This combustion model may only be used for turbulent flows. With respect to the problem of bulkhead heat transfer in controlled environments (furnace applications) and uncontrolled environments (automobile engine compartments), it is expected that this assumption will hold true for the types of fires or combustion processes that have been observed.

- The model assumes a single-reaction for up to 100 scalar quantities. Multiple stage reactions can be modeled, but simplifications must be made to represent the reactions as a single stage process. Major species that are typically produced in fire (CO_2, CO, H_2O, etc.) have been successfully modeled using the simplifying approaches described above.

- The chemical reactions are assumed to occur very fast relative to the mass and heat transport processes (i.e. as soon as components are present in sufficient quantities, the reaction can and does occur). More specifically, the reaction rate is directly related to the time required to mix the reactants at the molecular level. This time is determined by the turbulent eddy properties, K, and ϵ. Equation 59 shows this relationship.

$$rate_{rxn} \propto \frac{\epsilon}{K} \tag{59}$$

With an appreciation of the fundamental nature of this model, it is now logical to explore how this model has been implemented in TASCflow. The effect of the model may be seen on two fronts:

1. The advection-diffusion expressions for mass fractions

2. The conservation of energy equations.

The EDC model is used to determine the value of R_i (source term) in expression 60. (indexed notation)

$$\frac{\partial(\rho Y_i)}{\partial t} + \frac{\partial(\rho u_j Y_i)}{\partial x_j} = \frac{\partial}{\partial x_j}\left(\Gamma_{i,eff}\frac{\partial Y_i}{\partial x_j}\right) + R_i \tag{60}$$

The variable Y_i represents the mass fraction of each species. The variable x denotes the length quantity (where the velocity, u, is a vector). The effect of the combustion model on the energy equation is manifested in equation 61 [1]. Essentially, the chemically stored energy is converted to heat.

$$\frac{\partial}{\partial t}\left[\rho\left(H - \frac{P}{\rho}\right)\right] + \frac{\rho u_j H}{\partial x_j} = \frac{\partial}{\partial x_j}\left(\lambda\frac{\partial T}{\partial x_j} + \frac{\mu_t}{Pr_t}\frac{\partial h}{\partial x_j} + \sum_i \Gamma_i h_i \frac{\partial Y_i}{\partial x_j}\right) + S_e - \sum_i h_i R_i \tag{61}$$

The term $\sum_i h_i R_i$ represents the conversion of chemical energy to heat energy.

Because of the highly non-linear nature of expressions 60 and 61, it is useful to linearize the combustion source terms in order to better achieve numerical convergence. Problems such as the production of negative concentrations of reactants may arise if linearization techniques are not employed. It should be noted that the combustion terms introduce a very strong coupling between the scalar values (species, etc.) and the energy and momentum equations. Continuity is affected because the combustion reactions have large density gradients associated with them and these gradients can therefore cause problems with numerical stability in the solution of the continuity expression.

The implementation of this model is fairly straight forward [4]. The user needs to define the reactant and product scalars of the reacting flow (up to 100 scalars may be defined). Once this is accomplished, the component attributes need to be defined and boundary conditions assigned to each of the scalars. Depending on the desired level of control, other parameters may be assigned, though this subject will not be discussed at this time. Finally, the initialization can be carried out and the run may be started as for non-combusting cases.

2.6.1 Plastic Burning Model

The thermal decomposition of plastics is fairly complex in part because of the many forms that the pyrolysis process can assume. When a plastic is

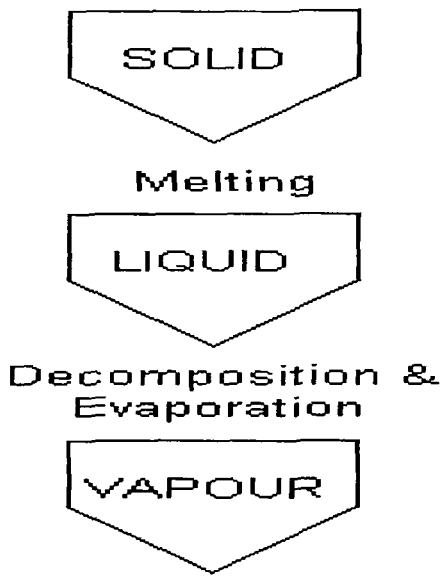

Figure 9: Production of Fuel Vapour From Solids

heated, vaporization is triggered by scission of the polymer bonds within the plastic. The vaporized particles are then free to undergo combustion above the surface if the proper concentrations and thermal conditions can be satisfied. Three common reverse-polymerization processes are (1) end-chain scission, (2) random-chain scission and (3) chain stripping [14]. Further complicating the process, certain plastics melt (e.g. polystyrene) and then vaporize while other plastics char (e.g. phenolic resins) as they are vaporized. Various environmental factors such as the presence of water complicate the scission process (which in turn affects the combustion of the plastic). Figure 9 shows one possible decomposition process of a thermosetting plastic [14].

One way to categorize plastics is as polar or non-polar. Non-polar plastics are typically immiscible with water, while polar plastics will readily mix, thus changing thermal and chemical properties. When considering the combustion process (where condensation is frequently encountered), the interaction between the plastic and its surroundings should be considered. The density and specific heat need to be adjusted to reflect varying concentrations of water and plastic in the solid.

A Plastics Combustion Model (PCM) has been implemented in TASCflow [8]. Principally designed for non-polar, non-charring materials, the PCM

available in TASCflow may be customized to a fairly high degree (via FORTRAN subroutines) to allow for a more accurate representation of the plastics combustion process as seen in various automobile engine compartment environments. Treated as a CHT solid, the plastic is heated to the vaporization point, $T_{v,plastic}$, and then begins to lose mass according to equation 62.

$$\dot{m}_p = -A_p \Gamma \frac{\partial P_v}{\partial x} \tag{62}$$

In this expression, $\dot{m}_p$ is the mass loss rate of plastic, A_p is the exposed surface area of the plastic, P_v is the vapor pressure at the surface (expressed as a gradient in equation 62), and Γ is the binary diffusion coefficient. A constant volume has been assumed. As a result of this assumption the density is adjusted to reflect the mass loss due to vaporization.

2.7 Grid Development

One major advantage of TASCflow is the ability to construct complicated grids which retain qualities conducive to numerical convergence. Many steps have been taken in order to simplify the process and promote accurate representations of and solutions to the modeling problem. The sub-program TASCgrid has been used to generate structured grids for the problem of post-crash vehicle fires. The use of structured grids in the solution of the problems associated with this research is appropriate for a few reasons:

- The relatively simple geometries are very easily parameterized using the structured approach, allowing for more flexibility with regards to the type of vehicle being modeled
- Stability of the solution is enhanced for problems involving highly coupled relationships such as those induced by combustion, turbulence, etc.
- There is a strong association between the computational domain and the physical domain. As a result, visualization of the computational grid is much easier, thus facilitating the analysis of any problems that may arise.

A discussion of the grid development process implemented in TASCflow [2] will now be provided.

There are four principle phases involved with grid development in TASCflow. These include the (1)**Geometry Phase**, (2)**Curve Development Phase**, (3)**Surface Generation Phase**, and (4)**Interior Node Distribution Phase**. Each of these will now be discussed in turn.

Geometry Phase - The physical domain is described in this phase of grid development. It has been suggested that this process is analogous to CAD surface modeling. The geometric entities are specified by way of the following general structure:

- The **type** of entity (i.e. point, curve, or surface)
- The **label** defining the entity with respect to other entities in the grid
- **Parameters** which define how the entity is interpolated, etc.

- Use of **raw data points** which are used to define special physical locations or surfaces in the grid

Various curve definitions may be utilized including linear, spline, or radial. In addition to these basic types of curves, control curves and composite curves can be constructed if the need exists. Typically, it is beneficial to define the physical geometry in terms of the surfaces as opposed to the curves (wire frame) which define the surface. A general description of surface generation follows.

Four methods of surface generation are currently supported by TASCflow for the geometry phase:

1. Surface by points
2. Surface by parametrically parallel curves
3. Bilinear surfaces
4. Surface by rotation

The surface by points is described by an array of raw data points. The space between these points is described by a given interpolation scheme and the array is transformed into a 2D or 3D surface. The generation of a surface by parametrically parallel curves is more common, though it has not been chosen as the primary means for defining surfaces for this effort. A list of previously defined curves is combined with an interpolation scheme to join points on the curves resulting in an elegantly defined surface. The bilinear surface, or Coons patch, is a surface defined by four curves connected via a bilinear interpolation method. The curves are listed from head to tail and blended to form the surface. This method has been chosen as the most expedient technique for defining simple surfaces. The surface by rotation is created by rotating a previously defined curve around an axis through a user-defined number of radians. This type of surface construction is very effective for defining cylindrical shapes as well as any non-continuous curvilinear shapes.

Connectivity descriptions supply logical links between different points, curves, or surfaces in the grid. This information is in turn used to define the grid during later phases. Two types of connectivity are used in TASCflow:

- implicit connectivities
- explicit connectivities

The implicit connectivities arise from relative definitions used in creating the curves and surfaces. At times, when a logical connection between surfaces is desired, the explicit user-defined connection is appropriate.

Vertex Entities are those places where nodes must be placed according to the specified geometry (e.g., vertexes are always placed on the four corners of each surface). Default locations for vertex placement include intersections between two or more curves, floating ends of curves, and user-defined locations. The specification of vertices will not be discussed in detail at this time.

Curve Development Phase - Distribution of the nodes on the curves is the primary goal in this phase of grid construction. For the post-crash vehicle fire scenario, simple geometries have been chosen to most efficiently promote the development of the model. Typically, simple distributions of the nodes on the curves have been affected. It is very likely that more complicated distributions will be created as the need to better capture small scale reactions, turbulent flows, wall phenomena, etc. becomes more prominent.

Determination of grid dimensions, location of vertex attachments (attaching grid nodes to the physical vertices), and finally node distributions comprise the principle activities that are accomplished in the curve development phase. A brief description of these elements follows:

Grid Dimensions - The grid dimensions are defined in terms of variable definitions, thus introducing the physical coupling of the nodes and the actual problem geometry. The values for ID, JD, and KD describe the value assigned for each of the principal Cartesian orientations (x, y, and z).

Vertex Attachments - The vertex attachment portion of the curve development phase couples the corners of the grid with specific geometric locations. Strictly speaking, the curves joining the vertexes then act as the "edges" of the domain, which are important in defining the boundary conditions later in the modeling process.

Node Distribution - Node distribution along the "edges" may be accomplished in many ways (remember that the edge is defined by its end vertices). It is crucial to obtain a distribution of nodes that will allow for accurate solution of the fluids/heat transfer problem according to the varying length

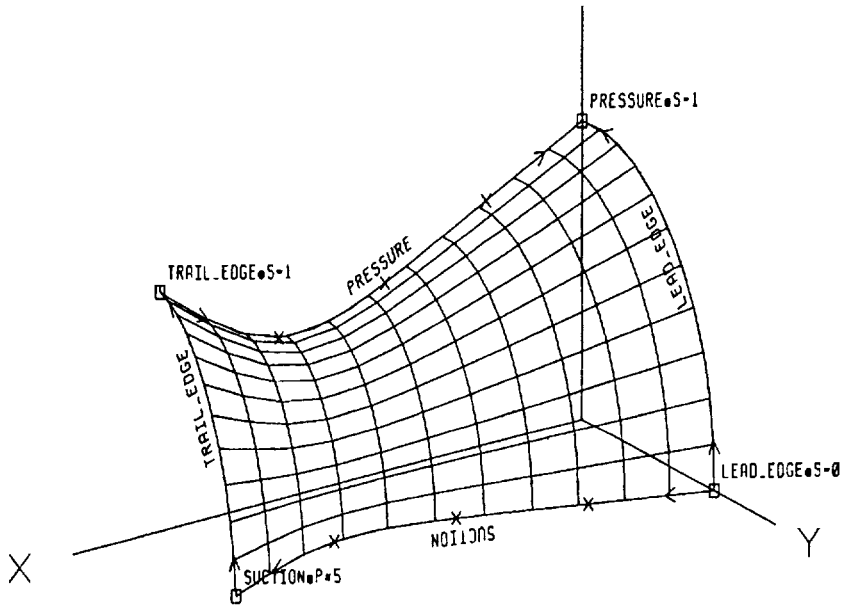

Figure 10: Distribution of Nodes on a Surface With Internal Curves

scales. For example, it is important to have more nodes near the walls of a compartment in order to properly resolve the effects of turbulence and heat conduction where large temperature gradients may exist.

Surface Generation Phase - The nodes are distributed on the surface regions (a collection of nodes that are logically connected on a particular surface) generated from the curves in this phase. In many cases, the distribution of the nodes on the surfaces will be different from that of the edges because of surface artifacts such as openings or internal curves. Figure 10 [2] shows a surface with an internal curve that is interpolated in TASCgrid. Figure 11 [2] demonstrates how surface distribution of the nodes may be affected by the specification of openings along the surface.

Interior Phase - The final step in defining the complete grid file is to assign values for node locations to the interior points (bounded by the surfaces). It is important to realize that the assignment of interior node locations can only be executed if the boundary nodes have already been defined (in the

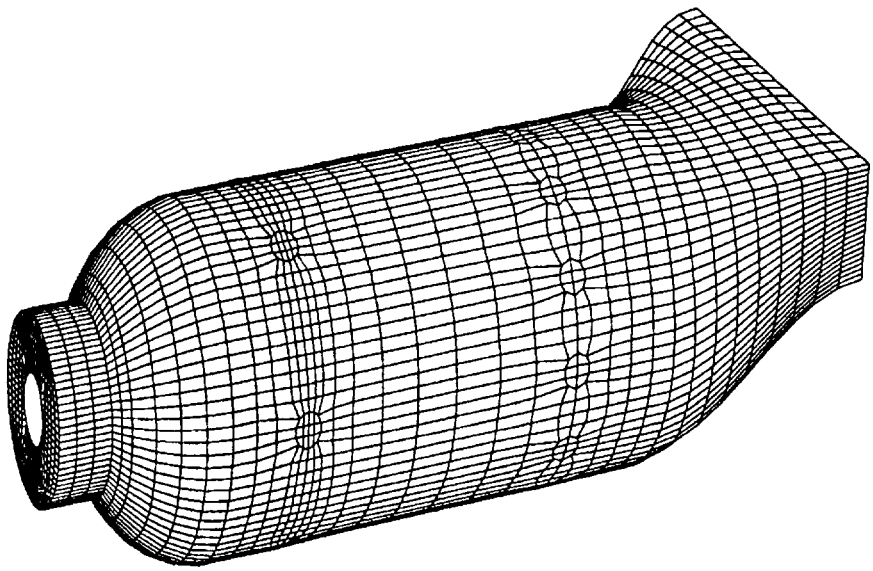

Figure 11: Distribution of Nodes on a Surface with Openings

previous phases). This phase is usually executed automatically by the code so long as the regions and preferred interpolation schemes are provided. The interpolation methods that are available include:

- transfinite
- semi-iso-geometric
- iso-geometric
- elliptic

At this time, only the elliptic scheme will be discussed as it has been chosen for the modeling problem at hand. Elliptic interpolation is accomplished by solving a coupled system of non-linear partial differential equations for the coordinates in a region. This method has been chosen because it is best suited for rectangular grids, allowing for more accurate solutions for the interior grid distribution within the same space of time than other methods. The interior grid distribution becomes very important when such factors as skew and aspect are considered (these factors generally affect the ability of the solver to converge).

Upon completion of the **Interior Phase** portion of grid design, the modeler is left with a grid to which the boundary conditions may be applied and from which the solution may be consequently obtained. Figure 12 demonstrates the data flow used to achieve the grids used in the post-crash vehicle fire modeling problems.

Other capabilities provided in TASCflow's boundary conforming grid construction ensemble which make it particularly useful for modeling the post-crash vehicle fire are grid embedding and grid attachment. A need for resolution (finer grid construction) often arises because of the very different length scales associated with fluid flow and heat conduction or turbulence. Grid embedding will be performed in areas near the openings around general surfaces in order to improve the resolution at those locations. The process of creating a module for grid embedding is more or less mechanical and so will not be discussed at this time.

Grid attachment, or the creation of multi-block grids (see Figure 13 [10]) will prove to be a useful means of creating more complicated geometries using the structured approach to setting up the problem. As the physical domain changes, grid attaching allows the modeler to change various components

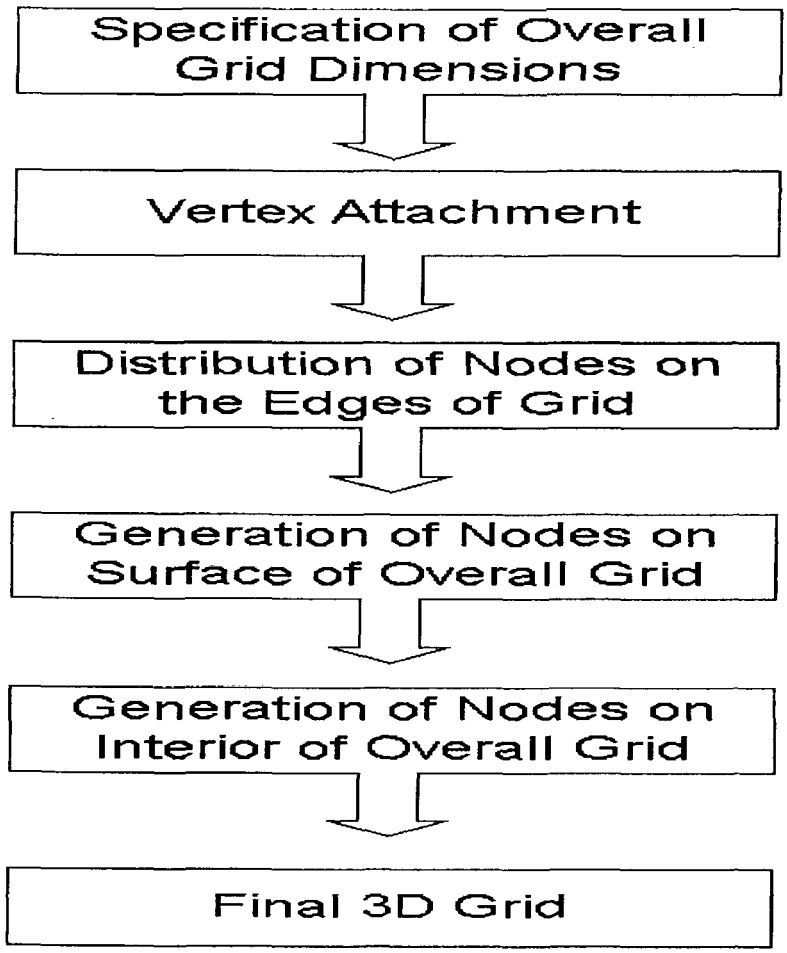

Figure 12: Data Flow Diagram for Grid Construction

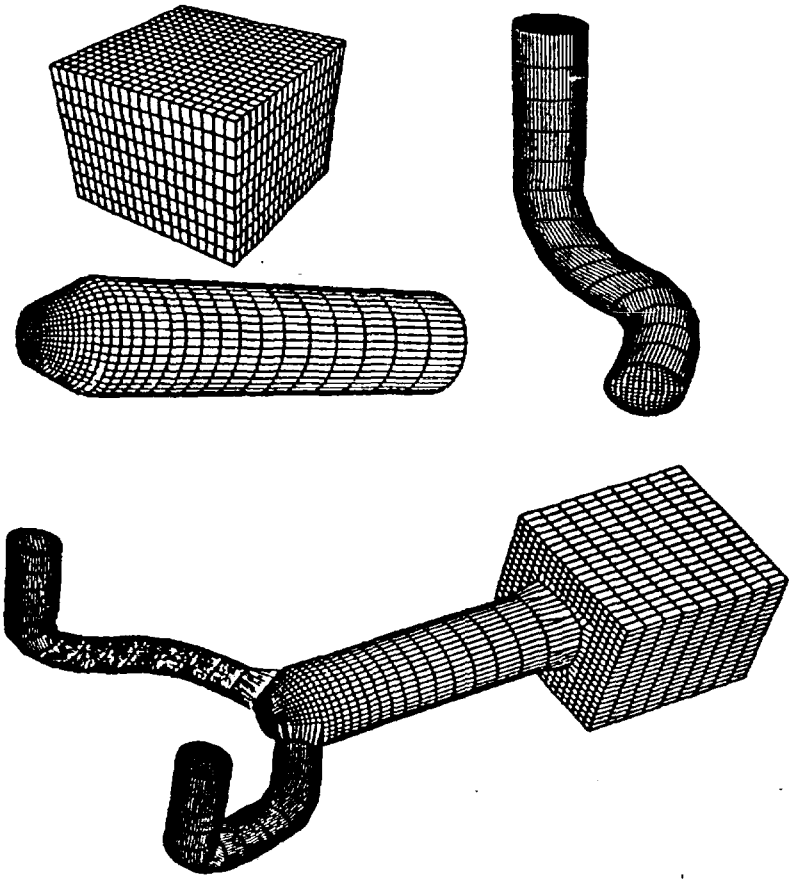

Figure 13: Grid Attaching

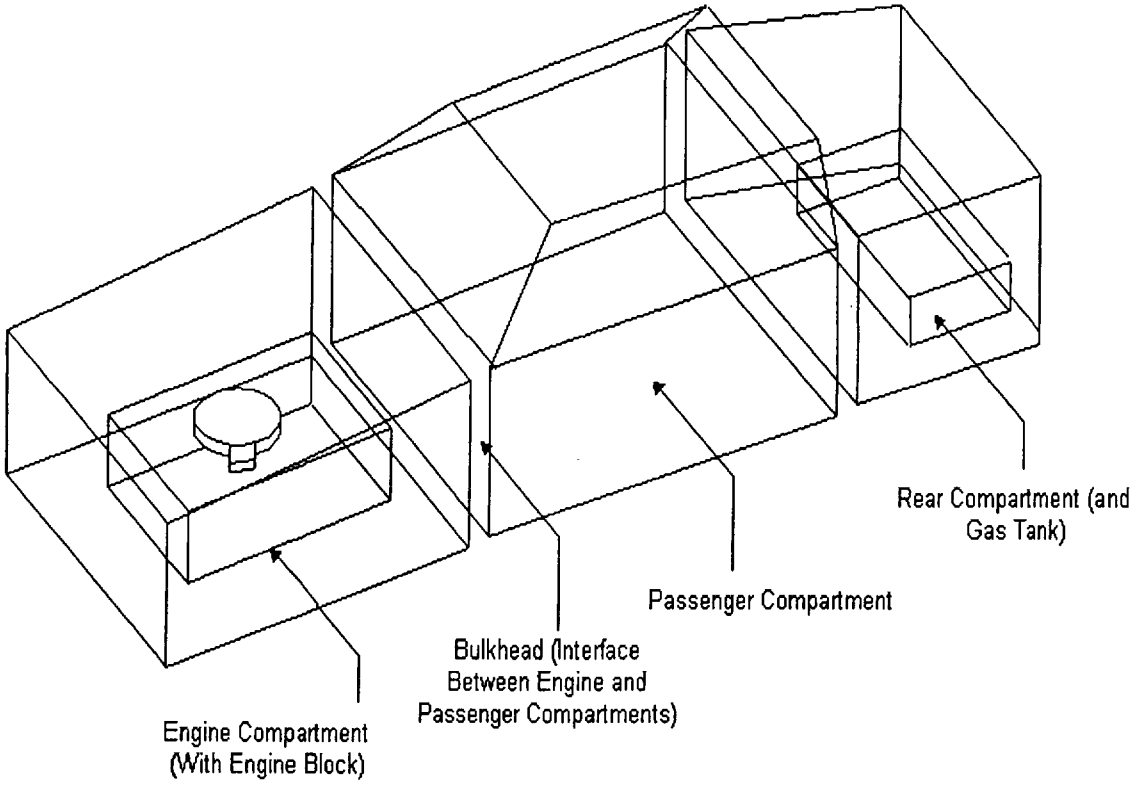

Figure 14: Grid Attaching - Vehicle Grid

in a piece-wise manner using separate grids. As a result, development and solution problems associated with overly complicated grids can be reduced by way of grid attachment. Figure 14 demonstrates three modules that are under development for the post-crash vehicle fire.

2.8 Discretization and Solver

The discretization method in TASCflow is the *finite volume method.* The particular application of this method ensures that the conservation equations discussed in Section 2.3 are implicitly satisfied since they are solved in conservative form. In particular, there exist a few features of the solver which endear TASCflow to the modeler [10]:

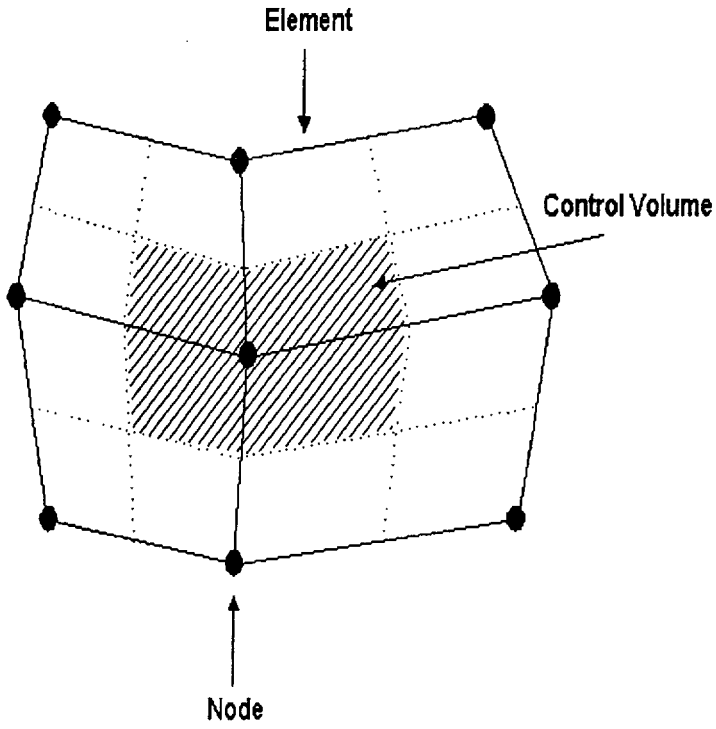

Figure 15: Finite Volume Definition

- Pressure de-coupling is used in lieu of the traditional staggered grid approach, where the pressure is coupled with the velocity. For a more in depth explanation, refer to ASC technical documentation [10].

- Discretization is accomplished by way of (1) a mass-weighted skew scheme and (2) a second-order-accurate upwind skew scheme. These methods have lead to improvements in performance on the order of 10-100 times conventional models.

- The multi-grid solving method is used. The solution is obtained using the *additive correction multi-grid method.* Based on the concept of the Algegraic Multigrid [10], the multigrid method creates coarser grids from the finer grids specified by the user. It is through this process that errors that would normally be allowed to propagate through the grid are substantially reduced. Furthermore, a notable decrease in solution times may be observed for larger grids where block iteration methods such as the multigrid method are used.

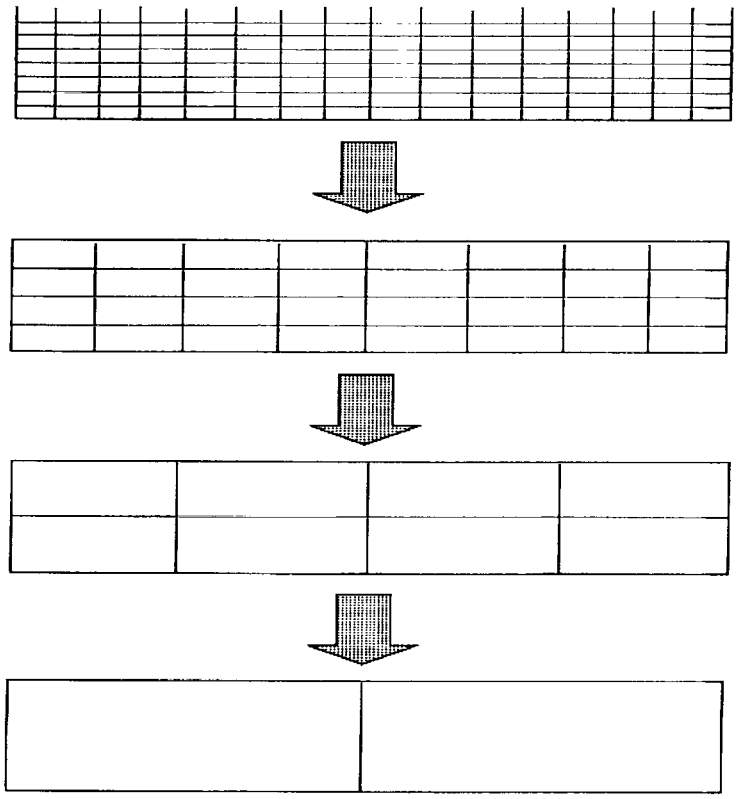

Figure 16: Multi-Grid Method

Part III
Boundary Conditions and Fire Scenarios

3 Boundary Conditions and Fire Scenarios

One of the principal objectives of this deliverable is to establish boundary conditions for bulkhead heat transfer and research potential fire scenarios which would serve as the source for gaseous combustion products, flame, smoke, and hot gases. These fire scenarios could then be implemented into future modeling efforts in place of the currently used simplified heat sources. In Section 3.1, nine common heat transfer and fluid flow boundary conditions are discussed. Section 3.2 focuses on boundary condition attributes and specific conditions applied to bulkhead heat transfer (the first modeling task in this deliverable). The attachments applied to the problem of bulkhead heat transfer (further discussed in Part 4) are outlined in Section 3.3. Lastly, the concept of the design fire (typical fire scenario expected to provide a substantial life and fire safety challenge) is explored via the available fuels, potential ignition sources, and likely scenarios in Section 3.5.

3.1 General Description of Fluid and Heat Transfer Boundary Conditions

The equations of motion, mass conservation, and energy require "mathematically tenable and physically realistic" [40] boundary conditions to achieve accurate and sound solutions. The five most common boundary conditions for fluid transport include:

1. Solid surface (porous or non-porous)
2. Free liquid surface
3. Liquid-vapor interface
4. Liquid-liquid interface
5. Inlet or exit section

These conditions are supplemented by the four established heat transfer boundary conditions [27]:

1. First kind (or Dirichlet)
2. Second kind (or Neumann)

3. Third Kind (or mixed)

4. Fourth Kind (or radiation)

While there are other types of boundary conditions in real situations, they are usually some variations of those listed above. The boundary conditions listed above for fluid and heat transfer will now be explained in turn.

Solid surface - The use of this boundary condition depends on whether a liquid or a gas is in contact with the surface in question. This is also known as the no-slip or no-temperature-jump condition. Exceptions to both of these boundary specifications do exist, but will not be discussed because they are not relevant to the setup of the bulkhead heat transfer analysis.

Free liquid surface - There are two cases for a free liquid surface: (a) The ideal or classic free surface exerts a known pressure on the liquid and (b) The atmosphere exerts a pressure and shear, causes heat and mass flux at the surface.

Liquid-vapor interface - In this type of interface, the vapor and fluids are strongly coupled. Kinematic qualities, stress, and energy constraints are shared. It is useful to note that the slopes for the velocity and temperature gradients do not necessarily match from layer to layer, but they must be continuous. This type of interface becomes important in processes involving evaporation, condensation, or chemical kinematics.

Liquid-liquid interface - This type of interface is similar to the liquid-vapor interface.

Inlet or exit section - This boundary condition is used primarily to simplify calculations by way of limiting the domain. To achieve mathematical exactness, the velocity, pressure, and temperature must be known at all points in the inlet and outlet. In reality, it is not usually possible to obtain these values and so approximations (such as a constant pressure over the opening) are used to simplify the calculation, thus enabling the modeler to obtain a workable solution.

Fixed Temperature (Dirichlet) - This condition is characterized by a specified temperature at a surface. The surface is typically gaseous, but this is not a requirement. Equation 63 describes this boundary condition with respect to a one dimensional Cartesian coordinate system.

$$T|_{x=L} = T_s \tag{63}$$

Heat Flux (Neumann) - The Second Kind boundary condition denotes a specified heat flux at a surface, as represented by equation 64.

$$-k \left.\frac{\partial T}{\partial x}\right|_{x=L} = q_s \tag{64}$$

Mixed - For a solid-fluid interface, the surface may be described using Newton's Law of Cooling. For the case of convective cooling, this relationship may be reduced to the expression in equation 65.

$$-k \left.\frac{\partial T}{\partial x}\right|_{x=L} = h_c(T|_{x=L} - T_\infty) \tag{65}$$

Radiation - The radiation heat loss boundary condition is similar to the mixed boundary condition above, except that the convective term in Newton's Law of Cooling is replaced by a radiation term.

$$-k \left.\frac{\partial T}{\partial x}\right|_{x=L} = \sigma(T^4|_{x=L} - T_\infty^4) \tag{66}$$

3.2 Attributes and Boundary Conditions for Bulkhead Heat Transfer

A discussion of the attributes and boundary condition specification for the problem of bulkhead heat transfer follows. At this time, the boundary conditions required to solve problems where openings in the bulkhead exist and combustion is occurring will not be discussed.

3.2.1 Attributes

The attributes describe the general assumptions that were made in solving the modeling problem. Within the confines of TASCflow, the specification

of attributes will directly influence the options that exist for boundary condition specification. The following list describes those attributes used to define the bulkhead heat transfer problem (definitions provided from user documentation provided by ASC) [3].

Flow field solution is required - Typically, the flow field solution will be required unless the exact nature of the flow can be specified. As a result of this requirement, hydrodynamic boundary conditions will be necessary.

Flow is incompressible - This attribute is appropriate when dealing with a gaseous fluid medium, such as air or gaseous products of combustion. As a result, the Navier-Stokes equations will not include compressible flow terms.

Flow requires thermal energy equation solution - As with the hydrodynamic flow field, the solution to the thermal energy equation is also necessary. The heat transfer influences flow characteristics and will often be the focus of the simulation efforts.

Flow is turbulent - Typical fire-related scenarios will be characterized by turbulent flow and so the omission of the phenomena associated with turbulence can lead to inaccurate predictions. When the turbulence model is active, specification of other variables will be required to achieve closure for the hydrodynamic and thermal equations.

Flow is non-reacting - Kinetic chemical reactions are not being modeled for the case of bulkhead heat transfer. Such reactions will be modeled for later simulation scenarios but are not included at this time in order to keep the simulations as simple as possible while various heat transfer phenomena are isolated. Reacting flows introduce an added tier of instability in the solution that may lead to poor convergence in the transient case.

Flow does not include additional scalar transport equations - If a tracer gas or dye is required, then this attribute can be changed. Whereas heat transfer by way of diffusion is more of a concern in the case of an impervious bulkhead, monitor points have been established to allow for transient monitoring of the fire-related phenomena.

Diffusion model for radiation is active - Gibb's model for diffusion radiation has been employed using small absorption coefficients. It has been firmly established that in typical bulkhead heat transfer situations, the effects of radiation heat transfer cannot be ignored. A semi-diffuse environment has been assumed to exist.

Flow does not include Lagrangian tracking - The conditions for specification of particle generation at all boundaries are enabled when this attribute is set. However, for the simulation conducted as part of the first deliverable, particle tracking is not required.

The domain is stationary - This attribute may be changed if a rotating coordinate system is preferred (e.g. turbomachinery simulations). Absolute coordinate systems are used for the bulkhead heat transfer model as well as post-crash vehicle fire simulations.

Walls are stationary - This is appropriate for simulations where the position of the boundary walls is not expected to change during the course of the fire simulation. Specification of this attribute for moving walls may prove to be useful for certain cases of decomposition or simulation of massive failure of the windshield or bulkhead. At this time, this option is not selected.

User specified profile boundary conditions are not read - This specification is primarily used when time-periodic boundary conditions are desired. This is not to be confused with temperature-dependent boundary conditions that exist in any heat transfer problem; temperature-dependent thermal properties are read in through other FORTRAN subroutines not related to the profile boundary conditions.

Transient boundary conditions are required - This is necessary for simulations where time-dependent heat transfer behavior is present. This condition is also required for the validation of the TASCflow solid diffusion model (tested over a one hour period). In line with the objective of developing an engineering design tool, transient simulations will nearly always be required.

3.2.2 Boundary Conditions for Post-Crash Vehicle Fire Modeling

Four types of boundary conditions have been used:

1. Adiabatic walls
2. Conjugate heat transfer solid with CHT exterior heat transfer
3. Inlet with prescribed flow and temperature (ISO 834)
4. Outlet (a function of the flow field solution)

A Discussion of these conditions with respect to how they relate to both bulkhead heat transfer and the previously discussed general boundary conditions follows.

Wall Boundary Condition Stationary, smooth, adiabatic walls were chosen as the default condition. Fluid exchange cannot occur across the surface of a solid wall, thus establishing the physical bounds of the fluid and heat transfer. The choice of a smooth wall affects the turbulence modeling for those materials that comprise bulkheads.

Conjugate Heat Transfer Solids This boundary condition was attached to the bulkhead specimen. Boundary conditions for the mass, momentum, K, ϵ, and Φ conservation relationships are not required on the exterior surface due to the lack of fluid interaction. The temperature values on the unexposed surface were plugged into an heat flux expression utilizing a simplified heat transfer coefficient and the bulk heat loss was calculated over the surface.

Inlet Boundary Condition This condition was prescribed for the base of the computational domain within the fluid region. The flow of the gases was specified according to a specific subsonic velocity parallel to the bulkhead surface (Cartesian coordinate system). The temperature was specified according to the ISO 834 heating curve. The relationship given in equation 67 was used to model this variable temperature specification.

$$T = 750\left(1 - \exp\left[-3.79553\left(\frac{t}{3600}\right)^{0.5}\right]\right) + 170.41\left(\frac{t}{3600}\right)^{0.5} + 298 \quad (67)$$

Turbulence was modeled using $K - \epsilon$ expressions. Equations 68 and 69 describe the k and ϵ relationships found in TASCflow.

$$k_{inlet} = 3/2(T_u|V|)^2 \tag{68}$$

$$\epsilon_{inlet} = \frac{k_{inlet}^{3/2}}{L_\epsilon} \tag{69}$$

The variable T_u is the turbulent intensity and L_ϵ is the length scale (typically specified as 0.05 - 0.09 and 0.03 - 0.05, respectively). The boundary velocity, or the local magnitude of the inlet velocity, is denoted by $|V|$. The velocity was specified using Cartesian coordinates normal to the boundary surface.

Outlet Boundary Condition The outlet boundary condition is created as a direct result of the flow field solution. The pressure was assigned a value of 101,326 Pa and the velocity (normal to the boundary) was between 3 and 8 m/s out of the domain.

3.3 Boundary Condition Attachments

Attachments refer to the assignment of specific boundary surfaces to specific boundary conditions. Prior to discussing the nature of these attachments, it is useful to consider the definition of a boundary face. Recalling that the computational grid is composed of nodes that are arranged in such a way so as to form six-sided elements, a boundary face may be considered to be any one of the exterior faces of the exterior elements in the domain. Boundary faces may also exist on the exterior faces of objects within the domain. Figure 17 depicts the smallest possible boundary face, or flux element, that is allowed [3].

Four methods are available to the user to attach boundary conditions to the boundary faces:

1. Declaration of the boundary condition as the default condition
2. Declaration of the boundary condition as the default condition of an object within the domain
3. Specification of the boundary condition to be attached to a specific region within or on the domain (attaching to specific nodal coordinates over a point or surface)

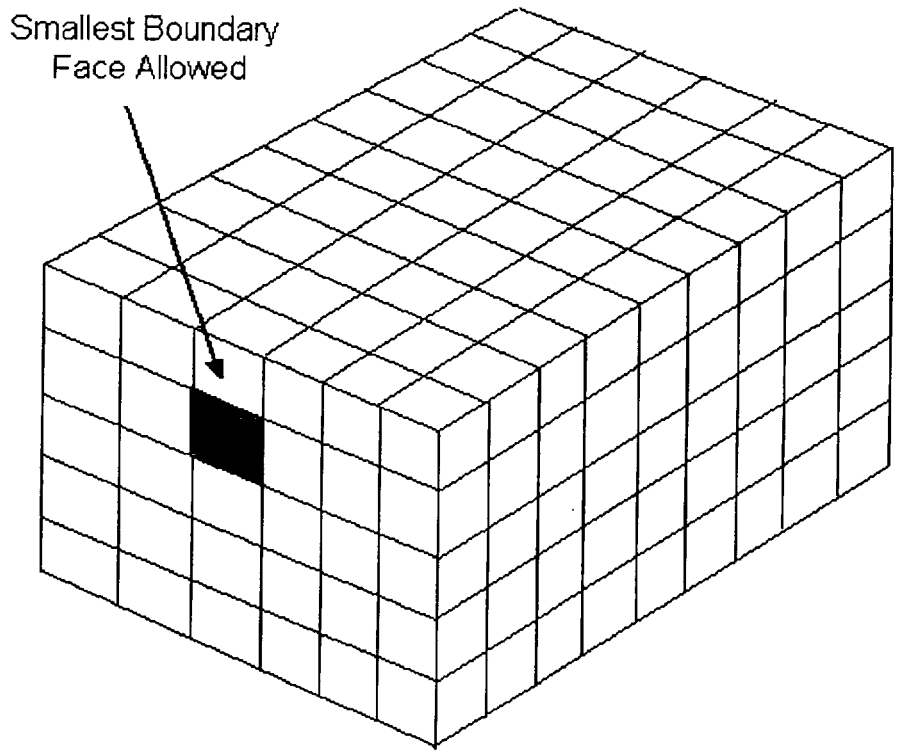

Figure 17: Boundary Faces

4. Utilization of profile boundary conditions

Items (1) and (3) were employed during the specification of boundary conditions for the bulkhead heat transfer calculation. Specifically, the adiabatic walls were chosen to be the default condition for all surfaces. Also, the default condition for the CHT solid was chosen where a heat transfer coefficient was specified for exterior CHT elements. Inlet and outlet conditions were prescribed over the upper and lower fluid faces. For further discussion of the boundary conditions, refer to Section 3.2.2

3.4 Boundary Conditions - Future Modeling Efforts

Boundary conditions for (1) generic modeling conditions and (2) bulkhead heat transfer in TASCflow have been discussed thus far. It is appropriate to provide an overview of those boundary conditions within the TASCflow environment that will likely play a role in the future modeling of the post-crash vehicle fire. Accordingly, Table 1 lists six types of boundary conditions and the nature of those boundary conditions with respect to their use in future work. Note that virtually all of the generic boundary conditions discussed in Section 3.1 above have been incorporated in the TASCflow boundary condition specification.

TASCflow Boundary Conditions		
Boundary Condition	**Where Used**	**Possible Specifications**
Wall	Compartment walls for engine and passenger compartments	Adiabatic, heat flux specified, or temperature specified
Inlet	Engine compartment or interface between compartments. Also used for openings	Velocity, mass, or pressure specified. Temperature or turbulent intensity also can be specified
Outlet	Accompanies inlet boundary condition	A function of inlet boundary condition
Openings	Openings or post-crash cracks, etc. Flow is likely to be bi-directional. Used with natural entrainment.	far field entrainment or re-circulating flow
Symmetry	Depends on geometry and complexity of scenario	None
CHT Exterior	Used for bulkhead or undercarriage. May also be used on exterior areas where fire is on interior of engine or passenger compartments	Adiabatic, temperature or heat flux specified. Exterior heat transfer coefficient can be specified

Table 1: Boundary Conditions - Future Work

3.5 Formulation of Fire Scenarios

The proper modeling of a post-collision automobile fire must involve fire scenarios that can be expected for this situation. The fire scenarios considered in this work involve the engine compartment and the fuel tank/line. The following section of the report will present the plastics and liquids that may be used in cars, the material properties that are associated with these substances, and the possible ignition sources for fires in the engine compartment and fuel line/tank. This will allow for development of reasonable fire scenarios in the modeling process.

In order to formulate a reasonable model that can be used as a tool for evaluating the fire safety of vehicles, the materials used that could be ignited must be identified. These materials will include plastics, rubber, and flammable and combustible liquids. The thermal properties of each material must be accounted for in order to properly construct the fire scenarios required for the model. A general description of the behavior of liquids and plastics subjected to fire conditions is provided in the following section.

3.5.1 Liquids Subjected to Fire

The ignition of a liquid fuel involves three steps [13]. The first step is dominated by the generation of combustible vapors by a heating source or by evaporation. The source of heat can be a flame or hot engine components. Liquids are classified as being volatile if their boiling point is relatively low. This makes a volatile liquid produce a greater amount of combustible vapors at ambient conditions than liquids with higher boiling points. An important property for this step is the liquid's flashpoint, the temperature at which enough vapors are produced for a possible ignition.

The second step of the ignition process is the mixture of the combustible vapors with oxygen, the necessary component of combustion. At the surface of the liquid, the vapor mixture is very concentrated and does not contain enough oxygen for combustion. As the vapor rises it mixes with oxygen from the surrounding air and the oxygen concentration increases. Once the mixture of combustible vapor and oxygen is within the flammable range, which is characteristic for each liquid fuel, and this mixture is at a high enough temperature or comes into contact with a spark of sufficient energy, ignition can occur. The lower flammable limit is the minimum volume percentage of the vapor in air, meaning there is just enough oxygen for the given amount of

vapor for ignition to take place. The upper flammable limit is the maximum volume percentage of the vapor in air that will support combustion, meaning that ignition cannot take place for any greater amount of vapor because there will not be enough oxygen to for combustion.

With a vapor-air mixture that is within the flammable limit the third and final step, ignition, can take place if this mixture is at a high enough temperature or comes into contact with a source of sufficient energy. The flame can be sustained if the temperature of the surface (and volatiles) is at or above the fire point, the temperature at which enough vapors are produced to fuel the flames. Once ignition has begun and a flame has been sustained, the local temperature of the liquid increases. This leads to an increase in the vaporization rate of the liquid and supplies more fuel to the fire.

A vehicle collision can cause flammable liquids to come into contact with the open air, to be subjected to heat sources, and to be exposed to flames or sparks. A collision can cause fuel lines to be severed, and since fuel lines operate under pressure, a fine spray can result. The spray is made up of atomized liquid particles and greatly increases the vaporization rate of such particles due to the increased ratio of surface area to volume. Fuel containers such as the gas tank or parts of the engine can become compromised in an accident, causing gasoline, oil, or antifreeze to leak. The leaking flammable liquids can be exposed to the heat of engine components by direct or indirect contact. In the event of a vehicle collision electrical wires can be severed and create sparks with enough energy to ignite the combustible mixture of vapors and air from any spraying or leaking fuel. The probability of this scenario was not quantified in this study. A list of flammable and combustible fluids used in vehicles is given below along with available material property data.

Liquids By far, the most easily ignited and ample fuels in a post-crash vehicle are the various liquids used in the drive train, coolant, power, and comfort systems.

1. *Gasoline* - has a spontaneous ignition temperature, depending on the octane rating, of 280-456° C [33], h_c (net) = 43.7 MJ/kg, ρ = 680.3 kg/m^3, $\mu \times 10^4$ = 2.9 Pa sec [13]. The flashpoint is about -40° C. The contents and properties of gasoline are likely to vary considerably according to the blend, octane rating, etc.

2. *Engine oil* - operates normally at 110-120° C but can reach temperatures as high as 150° C [43]. It has a piloted ignition temperature

around 400° C [33].

3. *Automatic transmission fluid (ATF)* - Dexron^{TM}, industry standard, operates normally at 110° C and as high as 160° C [43].

4. *Power steering fluid* - operates normally at 110-115° C and as high as 160° C [43]. Its piloted ignition temperature is 310° C [33].

5. *Engine coolants* - consist of a mixture that is 50% water and 50% ethylene glycol [33] that typically operates at 88° C [43]. Despite the fact that half of this mixture is water, engine coolants have a piloted ignition temperature around 380° C [33]. Property data for Ethylene glycol: MW=62.07, h_c=17.05 MJ/kg, oxygen/fuel=1.289, T_{boil} =197.5° C, h_v = 800 kJ/kg c_{pl} = 2.43 kJ/kg C, c_{pv} = 1.56 kJ/kg C. Polyglycol-in-Water: H_t=11.0-14.7 kJ/g, H_{ch}=10.4-12.2 kJ/g.

6. *Compressor lubricants* - typically polyalkylene glycol, polyalpha-olefins, or alkylbenzenes [43].

7. *Brake fluid* - Polyethylene glycol [6].

8. *Battery Acid* - sulfuric acid [6].

3.5.2 Plastics Subjected to Fire

Plastics, like liquid fuels, undergo the same three step ignition process of vaporization, mixing with oxygen, and coming into contact with sufficient heat or spark energy for ignition (see Section 2.6.1). However, plastics can melt when subjected to heat which makes them more complex as a fuel for fire. If the plastic is subjected to a temperature above its melting point, combustible vapors will be given off as the solid makes the transition to the liquid state. Once melted, the liquid plastic from the engine can drip and form a pool on the ground below the vehicle which could involve the heating of the gas tank, brake lines, or engine. Plastics melting within the interior of the vehicle can drip onto the floor or seats and bring about a more rapid rate of flame spread and toxic product generation. A list of plastics used in the engine, interior and exterior of vehicles with available material property data is given below.

Plastics in the Engine - A wide variety of plastics can be found under the hood. The list that follows is for the base polymer and does not account for additives that may be present in some motor vehicle plastic parts.

1. *Polyethylene* - used to make gas tanks [20]. H_t=43.6 kJ/g, H_o=12.8 kJ/g, H_{co2}=13.9 kJ/g, H_{co}=11.8 kJ/g, H_{ch}=38.4 kJ/g, H_{con}=21.8 kJ/g, H_{rad}=16.6 kJ/g, y_{co2}=2.76 g/g, y_{co}=0.024 g/g, y_s=.060 g/g.

2. *Polyproylene* - gas tanks [20], battery cases, air intake ducts, fan shrouds, and blades [36]. H_t=43.4 kJ/g, H_o=12.7 kJ/g, H_{co2}=13.8 kJ/g, H_{co}=11.7 kJ/g, H_{ch}=38.6 kJ/g, H_{con}=22.6 kJ/g, H_{rad}=16.0 kJ/g, y_{co2}=2.79 g/g, y_{co}=0.024 g/g, y_s=.059 g/g.

3. *Fluoroelastomers* - gaskets and seals [15].

4. *Nylon 4,6* - used for top of valve spring retainers with 50% glass filled nylon 4,6 for bottom. Nylon 4,6 is also used in chain tensioners, bearings, covers, clips, and liquid connectors in the engine, filters, thrust washers, and mechanical components of the transmission, and connectors, small motor gears, bearings, end laminates, sensors, tubing, ties, and bobbins in the electrical system.

5. *Nylon 6,6* - glass reinforced and used for intake manifolds. Glass reinforced nylon 6,6 is also used for water outlet housings [36]. Some engines contain valve lifter guides composed of nylon 6,6 filled with glass reinforced molybdenum disulfide.

6. *Vinyl ester* - used in valve covers in certain vehicles. Vinyl ester retains its material properties well at temperatures as high as 177^o C because the plastic is thermosetting. At high enough temperatures the polymer chains crosslink and harden [36].

7. *Epoxy ester resin* - used for valve covers. Typical characteristics of epoxy: H_t=28.8 kJ/g, H_o=12.1 kJ/g, H_{co2}=10.8 kJ/g, H_{co}=6.9 kJ/g.

8. *Flouropolymers* - investigations are being made for its suitability for use in fuel lines, fuel rails, impeller shafts, intake manifolds, valve covers, gaskets, and camshafts [42].

9. *Polyphenylene sulfide* - investigations are being made for its suitability for use in fuel lines, fuel rails, impeller shafts, intake manifolds, valve covers, gaskets, and camshafts [42].

10. *Polyphthalamide* - investigations are being made for its suitability for use in fuel lines, fuel rails, impeller shafts, intake manifolds, valve covers, gaskets, and camshafts [42].

11. *Liquid-crystal polymers* - investigations are being made for its suitability for use in fuel lines, fuel rails, impeller shafts, intake manifolds, valve covers, gaskets, and camshafts [42].

12. *Nitrile-butadiene rubber (NBR)* - fuel hoses and hydraulic hoses [6].

13. *Polychloroprene (Neoprene)* - wire insulation [6].

14. *Styrene-butadiene rubber (SBR)* - sealants and tubing [6].

Plastics Used for Interiors - An understanding of interior plastics is required to properly assess the fire hazard in the passenger compartment. Some plastics commonly used in the interior of vehicles that may influence the tenability include *Flexible polyurethane foams*, *Polyvinyl chloride*, and *Polypropylene*. The list that follows is for the base polymer and does not account for additives that may be present in some motor vehicle plastic parts.

1. *Flexible Polyurethane Foams* - H_c=16.4-19.0kJ/g, Y_s=0.131-0.227 g/g.

2. *Polyvinyl chloride* - H_c=5.7kJ/g, Y_s=0.172g/g.

3. *Polypropylene* - H_c=38.6kJ/g, Y_s=0.007g/g.

3.5.3 Ignition Sources

In order to properly utilize the material property data presented in the previous section, the ignition sources must be identified. This allows for the determination of the first object to be ignited and is useful in assessing the spread of the fire within the point of origin. Ignition sources will include the two origins of interest; the engine compartment and the fuel tank/line.

Engine Compartment Over two-thirds of all post-collision vehicle fires begin in the engine compartment [11]. Hot components of the engine can cause the insulation of electrical wires to degrade and, in the case where bare wire is exposed, can result in an electrical fault [33]. Electrical faults, or arcing, can occur in any component of the electrical system. The probability of this scenario was not quantified in this study. Another potential source of ignition for the engine compartment are hot surfaces, although most engine parts have a normal operating temperature that is below the ignition temperature of gasoline [33], these surfaces can be ignition sources for other fluids present in the engine compartment.

Fuel Tank/Line The integrity of fuel tank can be compromised in a car crash and result in a fuel leak. The gasoline may form a pool below the vehicle. If the fuel vapor comes into contact with an ignition source the subsequent fire has the potential of coming into contact with the underside of the vehicle. A possible ignition source for this situation is the catalytic converter, which normally operates at a temperature above the ignition temperature for gasoline [33].

A failure within the fuel line can involve a variety of situations. At one extreme is the complete severing of the fuel line causing gasoline to discharge under pressure. The gasoline must undergo vaporization before it can be ignited if the surfaces it contacts are below the ignition temperature of the fuel. The other extreme involves a small hole in the fuel line. A small leak under pressure causes the gasoline to atomize, making it easier to ignite because it is in a vapor form [20]. The use of electronic fuel injection and pollution control measures in automobiles has resulted in fuel lines that operate at pressures in the range of 15 to 90 psi [20]. This high pressure may be an important feature when considering even small leaks in the fuel line. When fuel or any other flammable liquid is issued out of an opening and comes into contact with any hot surface in the engine that is at a temperature above the liquid's flashpoint, ignition of the liquid will occur.

Part IV
Heat Transfer Properties

4 Thermal Properties

The specification of temperature-dependant thermal properties for heat transfer modeling can have a significant impact on the quality of CHT results. The *thermal conductivity*, *specific heat*, and *density* are perhaps the most important properties with regards to the modeling of heat transfer through the automotive bulkhead. Proper identification of these properties will have a more significant impact on the prediction of conduction through solid materials than almost any other modeling parameter.

In Part 4, the fundamental thermal properties including conductivity, specific heat, density, absorptivity, and emissivity are discussed as they pertain to the post-crash vehicle fire. The relationship between these properties and bulkhead heat transfer is the focus of the research. The implementation of these thermal properties into the current modeling efforts are considered in Section 4.6.

4.1 Thermal Conductivity

The thermal conductivity describes the rate of energy conduction through a given solid and has the units W/mK. In equation 70, the thermal conductivity is represented as k, the constant of proportionality between the heat flux per unit area and the rate of temperature change in a solid with respect to position in that solid.

$$q(T) = -k(T)\frac{dT}{dx} \tag{70}$$

In steel, the thermal conductivity will vary according to the exact composition or blend in the steel at lower temperatures, but will tend to approach more or less the same values at elevated temperatures [38]. Specifically, the transient values used in TASEF-2 [30] have been chosen to represent the thermal conductivity of steel. Figure 18 shows the magnitude of k as a function of temperature. These values were implemented into TASCflow via a FORTRAN subroutine, PROPT.f and run in conjunction with the bulkhead heat transfer problem. The data from this curve was then applied at different temperatures during the conduction of heat through the various layers of the bulkhead. The values used in the PROPT.f routine are shown in Figure 19.

Recent research into the thermal properties of mineral wool insulation has demonstrated that the temperature-dependent thermal properties are

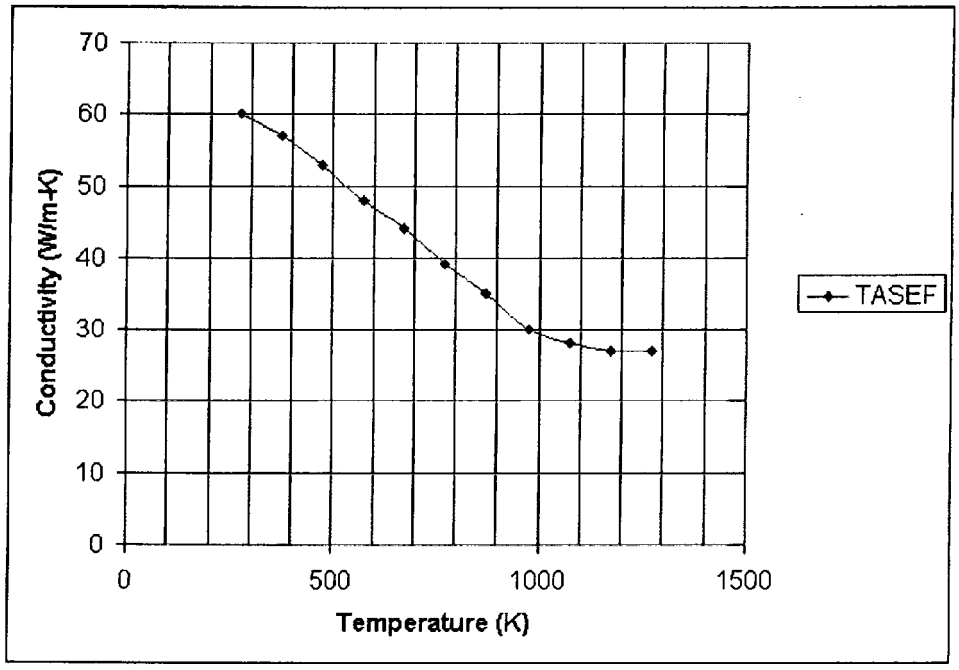

Figure 18: Thermal Conductivity of Steel

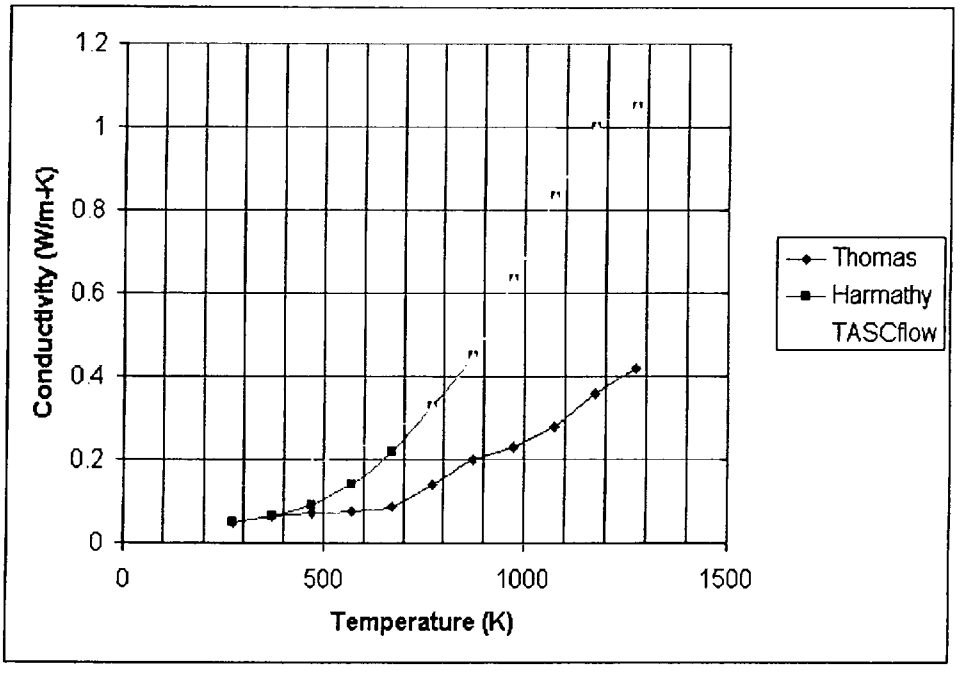

Figure 19: Thermal Conductivity of Insulation

not well known for this type of material despite its widespread use. According to Spinn [38], the thermal properties for these types of materials are generally not available for temperatures greater than 700° C. Consequently, determination of these properties tends to be speculative in the absence of accurate, experimentally derived data. Furthermore, the available data varies *considerably* depending on when it was recorded and by whom. Because of these discrepancies, it is advisable to determine the thermal properties for each specific insulating material if the design tolerances are minimal and the exact composition is not known. The data used in this research to create temperature dependant curves for the thermal conductivity was derived from TASEF-2 [30], Harmathy [21], Thomas [39], SwRI [7], and Holometrix [22]. The thermal conductivity curve for insulation shown in Figure 19 depicts the values input into the TASCflow PROPT.f files for the two-layer bulkhead. The values chosen to represent the thermal conductivity at temperatures less than 700 K were slightly higher than those used by Thomas or Harmathy. It was discovered in earlier test runs that the conduction wave propagated too slowly for very small values of conductivity, and while the values for the insulation was not known exactly it was reasonable to adjust the low end values to reflect the thermal response of insulation that was observed.

4.2 Specific Heat

Specific heat is defined as the amount of energy required to raise a unit mass of a substance by 1° C. More practically speaking, this quantity (typically with units J/kgK) may be used in combination with the thermal conductivity and density to characterize the resistance of a material to a given energy flux (via the thermal diffusivity or thermal inertia, as defined in Section 4.4). Specific heat may be measured at a constant volume, c_v, or a constant pressure, c_p. For solids, the values for c_p and c_v are equal, but for gases and liquids this is not usually the case.

The values of specific heat for steel vary widely in literature [38]. At about 540°C, the phase change in steel causes the specific heat to change substantially. Despite this change, the overall effect on conductive heat transfer is not thought to be too dramatic. Values used by the program TASEF-2 for steel have been employed in TASCflow [30], and may be seen in Figure 20.

Characterization of the specific heat in the insulation was particularly important because this thermal property largely accounts for the heat wave propagation through the solid by way of the thermal diffusivity. As a result

of the sensitivity to this value for large insulative material thicknesses, the proper determination of specific heat of insulative materials proved to be more challenging. Values from Harmathy [21], Hansson and Rehn (default values in TASEF-2) [30], Holometrix [22], and SwRI [7] once again provided a range of data that was then used to determine the most suitable values for the conjugate heat transfer problems studied in this deliverable. A brief examination of the data shows that the agreement at lower temperature values is good, but the measured values of specific heat begin to diverge after the temperature exceeds about 500 K. In cases where the data did not cover the required temperature range, linear curve fitting was performed to obtain values of specific heat at increased temperature levels. Figure 21 shows the values employed in TASCflow. While extrapolating data for increased temperatures is sufficient for the present work, there are dangers associated with this practice. Specifically, the material behavior may not behave in the fashion predicted using standard linear or power-law curve fitting techniques, but may instead behave more or less unpredictably. To remedy this challenge, it is advisable to conduct appropriate tests up to the maximum temperatures expected in fire conditions on those materials which will play the most significant roles in conduction heat transfer.

4.3 Density

Density values for steel and insulation were assumed to remain constant over the temperature range experienced in one hour ISO 834 test (see Figure 24). Such an assumption was deemed to be valid in light of evidence pointing to a *maximum* density change of 5% in insulative materials [38]; steel density variations are assumed to be far smaller [38]. Harmathy [21] reported no change in linear dimensions of insulative materials over a substantial temperature range, but this data was in conflict with observations at SwRI. Nevertheless, the impact of a maximum density variation equal to 5% was not deemed to be significant in this modeling effort and was confirmed in transient simulations where the density was varied as much as 5%.

4.4 Thermal Diffusivity and Thermal Inertia

Equations 71 and 72 depict the two parameters that appear most frequently in thermal properties calculations associated with conduction. Thermal dif-

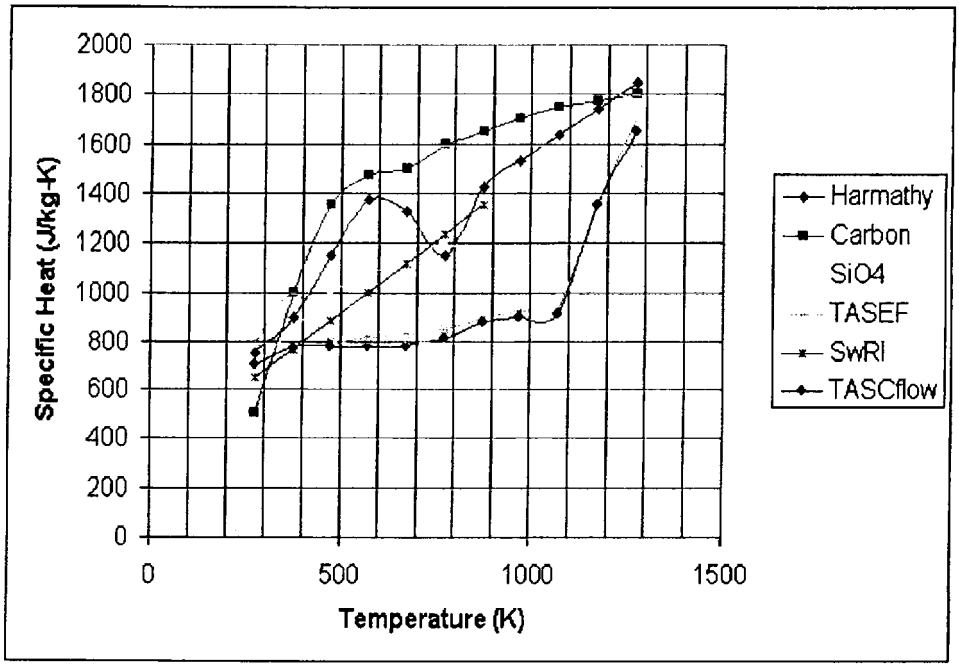

Figure 20: Specific Heat of Insulation

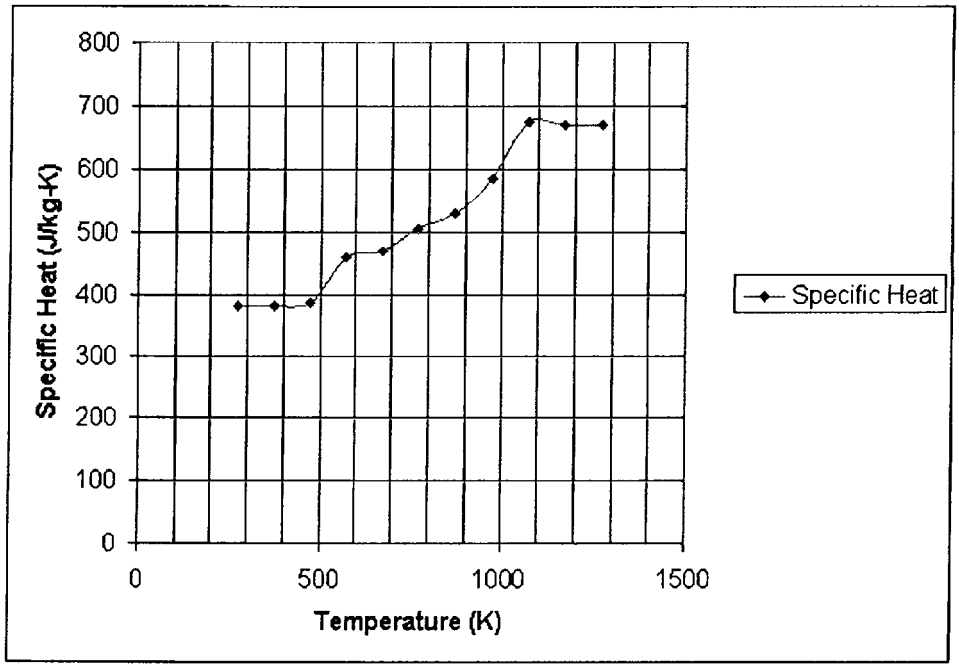

Figure 21: Specific Heat of Low Carbon Steel

fusivity, α, is given by the following expression:

$$\alpha = \frac{k}{\rho c_p} \tag{71}$$

Thermal inertia, δ_t, is given in equation 72:

$$\delta_t = \sqrt{k\rho c_p} \tag{72}$$

The thermal diffusivity is the controlling transport property for transient conduction described by Fourier's Equation. Typically, the values for k, ρ, and c vary independently according to temperature.

4.5 Emissivity, Absorptivity, and Reflectivity

The majority of formal research into emissivity, absorptivity, and reflectivity focuses on the nature of those properties in gases, and how they influence radiative energy transfer. At this time, the nature of these thermal properties as they relate to surface characteristics will be discussed. For a more in depth discussion of emissivity and absorptivity in gases, see Section 2.5.2 or refer to source material by Drysdale [14].

For a non-black surface, the emissivity, ϵ_λ of the surface is a function of T, λ, and the material itself. In general form, emissivity is then given according to equation 73.

$$\epsilon_\lambda = \frac{e_\lambda}{e_{b,\lambda}} \tag{73}$$

where e_b is the black body radiation or energy usually prescribed according to the simplified form in equation 74.

$$e_b = \sigma T^4 \tag{74}$$

The variable e_b is given in W/m^2, σ is 5.6696 $\times 10^{-8}$ W/m^{2}K^4. Temperature, T, is given in Kelvin. Many times, ϵ_λ is approximated as constant over a broad temperature range and for all wavelengths when in fact, emissivity is quite sensitive to all of these variables in addition to other less obvious parameters. As an example, the dependence of emissivity on wavelength is illustrated in Figure 22. The emissivity of a diffuse gray surface will obey Lambert's Law that states that the intensity of radiation leaving a surface is independent of the direction. In actuality, the emissivity of a real diffuse

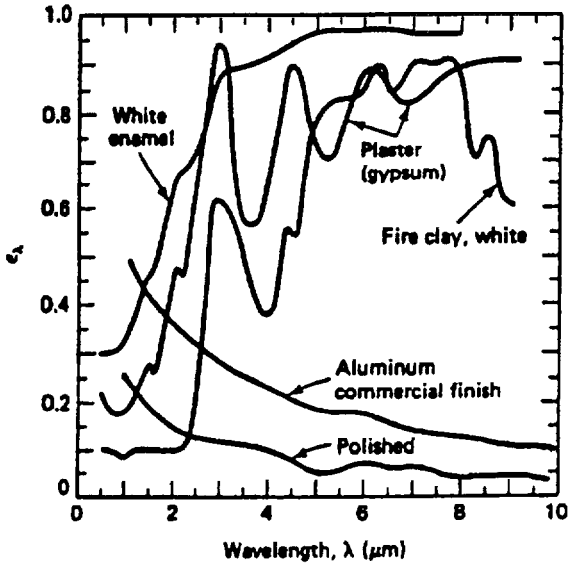

Figure 22: Wavelength Dependence of Emissivity For Various Materials

gray surface is influenced by the zenith angle, ϕ at which the pencil ray of radiation approaches it (see Figure 3 for visualization of this quantity) [14]. Figure 23 illustrates the dependence of several common material surfaces on this angle [14].

With regards to this modeling effort, it is necessary to determine the emissivity of a variety of surfaces including metals and non-metals. While metals generally exhibit low emissivities, non-metals have higher emissivities. Oxidized surfaces have similar properties as non-metals, and thus have high emissivities (i.e. 0.7 - 0.8 for steel). Painted surfaces have also been shown to be good emitters, the emittance principally being a function of paint color and texture.

The energy that is not emitted by a surface as a result of radiation heat transfer is either absorbed or reflected.

While the entire spectrum is absorbed by a black surface, the absorption of a gray surface is given according to the expression in equation 75 for a given wavelength, λ.

$$\alpha_\lambda = \frac{rad_{absorbed}}{rad_{incident}} \tag{75}$$

According to Kirchoff's Law for gray surfaces, $\alpha_\lambda = \epsilon_\lambda$. This assumption is

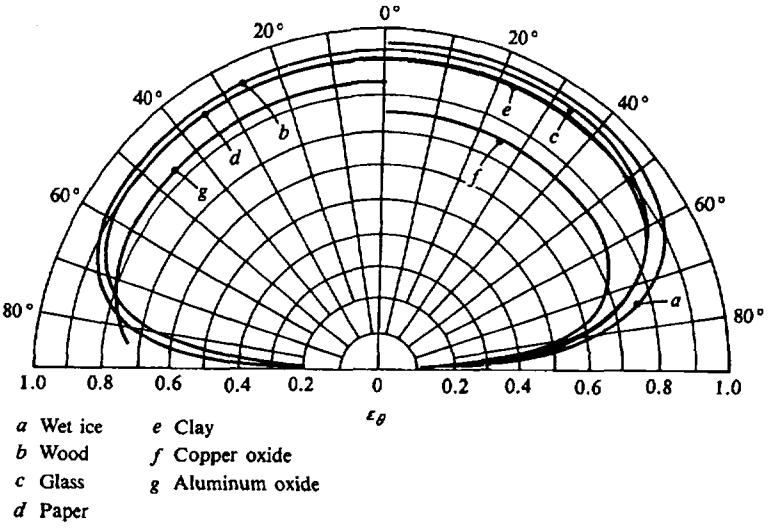

Figure 23: Dependence of Emissivity on Zenith Angle For Various Materials

deemed acceptable for the case where the radiation incident to a surface is in the same wavelength range as radiation emitted from the surface [37]. At this time, the surfaces inside of an automobile engine compartment can be considered to be gray surfaces, meaning that they will have approximately equal absorptivities and emissivities.

Reflection accounts for the remaining energy interacting with a real surface ($H = \rho H + \alpha H + \tau H$). Sometimes referred to as ρ_λ, reflection for a given wavelength is described in equation 76.

$$\rho_\lambda = \frac{rad_{reflected}}{rad_{incident}} \tag{76}$$

Table 2 lists various emissivities for various metals and non-metals associated with the problem of the post-crash vehicle fire [37]. The absorptivities and reflectivities can be determined according to the assumptions that one makes about the surface.

4.6 Implementation Of Thermal Properties into Current Work

Thus far, thermal properties have been used to study the sensitivity of the CHT and flow code in TASCflow to user inputs for those materials directly

Emissivity of Metals		
Surface	**Temperature (°C)**	**Emissivity**
Polished Aluminum	200-600	0.04-0.06
Heavily Oxidized Al	90-540	0.20-0.33
Mild Steel, polished	150-480	0.14-0.32
Stainless, after heating	230-900	0.50-0.70
Emissivity of Non-Metals		
Surface	**Temperature (°C)**	**Emissivity**
Asbestos	40	0.93-0.97
Smooth Glass	40	0.94
Pyrex Glass	260-540	0.94-0.74
Black Gloss Paint	40	0.90
White Paint	40	0.89-0.97
Rubber	40	0.86-0.94
Water (> 0.1 thick)	40	0.96

Table 2: Emissivities of Various Metallic and Non-Metallic Surfaces

exposed to the fire environment. Values for thermal conductivity, specific heat, density, emissivity, absorptivity, and reflectivity in the solids *and* gases are required for the accurate solution of the radiation routines, combustion, and various other sub-models in the package which supplement the solution of the basic conservation equations. Consequently, it is in the best interest of the modeler to choose those values that will most accurately represent the problem. The accuracy of the results can be verified with comparisons to appropriate experimental data. Such a comparison was not conducted in this study. As research for this project continues, more will be learned about the exact nature of the materials that are likely to have a significant impact in the post-crash vehicle fire environment.

Part V
Applications of TASCflow

5 Application of TASCflow to the Bulkhead Modeling Problem

One of the principal objectives of this deliverable was to apply TASCflow to the problem of heat transfer through a generic bulkhead. In Chapter 5, an explanation of the modeling sequence will be complimented by a description of the specific bulkhead modeling performed as part of this deliverable. Results for the two-layer bulkhead modeling will be presented in the context of those parameters that were varied and then compared with results obtained using the finite element model, TASEF-2, a previously validated heat conduction code. The structure of TASEF-2 will be compared and contrasted with that of TASCflow, and results of a previously performed bulkhead modeling effort will be discussed with respect to the simulations performed in TASCflow. Following the comparison of TASCflow with the empirical and modeling results obtained from TASEF-2, discussion of the results of a three-layer bulkhead will follow. Features of the three-layer model will be compared with the two-layer model in the context of bulkhead heat transfer. Sensitivity of the thermal response of bulkhead materials to thermal and environmental properties will be established through the runs performed using TASCflow.

5.1 Explanation of Modeling Sequence

Because of the complicated nature of Computational Fluid Dynamics and the wide variety of challenges that may be encountered while setting up an intricate modeling problem, it is widely recognized that an iterative approach should be adopted during the initial phases of development. Consequently, a piece-wise approach is being used to obtain a reasonable simulation of the post-crash vehicle fire scenario in such a manner so as to ensure that each aspect of the problem can be resolved adequately and checked for accuracy with comparisons to appropriate experimental data. Such comparisons were not made in this study. The following list highlights the major succession of steps in the procession that will end with a tool that can predict species concentrations, presence and nature of toxic, superheated gases, as well as the spread of fire into the passenger compartment for the engine fire scenario:

- **Bulkhead Heat Transfer** - This is the first step involving modeling of a variable heat source adjacent to a solid bulkhead. The intricacies

of temperature-dependent thermal properties and transient CHT can be examined in this context.

- **Bulkhead with Combustion Source** - The addition of a combustion source will introduce species concentrations and the associated intricacies of dealing with the chemical production of heat from fuels in the engine compartment. The effect of turbulence and the parameters specified for the radiation model on the production of heat will be of considerable interest.

- **Bulkhead with Openings** - The modeling of a bulkhead with openings opens the possibilities associated with flow through the bulkhead, and sheds light upon the effects of cracks and holes in the bulkhead on the spread of flame and heated gases into the passenger compartment via those paths. The use of combustion modeling will better enable the user to predict the effect of combustible openings and the effect of the fire position on the spread of fire.

- **Bulkhead Adjacent to Engine Compartment** - The addition of the engine compartment allows the modeler to simulate the effects of the engine on the flows in the compartment adjacent to the bulkhead and out of the compartment adjacent to the windshield. In the post-crash scenario, it is important to consider the nature of convective flows as well as the impact of the corresponding radiation on the heat transfer through the aforementioned barriers.

- **Bulkhead Separating an Engine and Passenger Compartment** - It is of interest to predict the effects that a fire in the engine compartment will have on the conditions of the passenger compartment. The addition of a passenger compartment allows for more realistic accumulation of products of combustion (heat, gaseous species) in addition to improving the ability to model the influence of the materials in the passenger compartment on the overall tenability of that space.

5.2 Description of Bulkhead Modeling - Two Layer Bulkhead

The two-layer bulkhead was modeled as a vertical plate with a 0.127 meter layer of insulation and a .006 meter layer of steel. The thermal properties

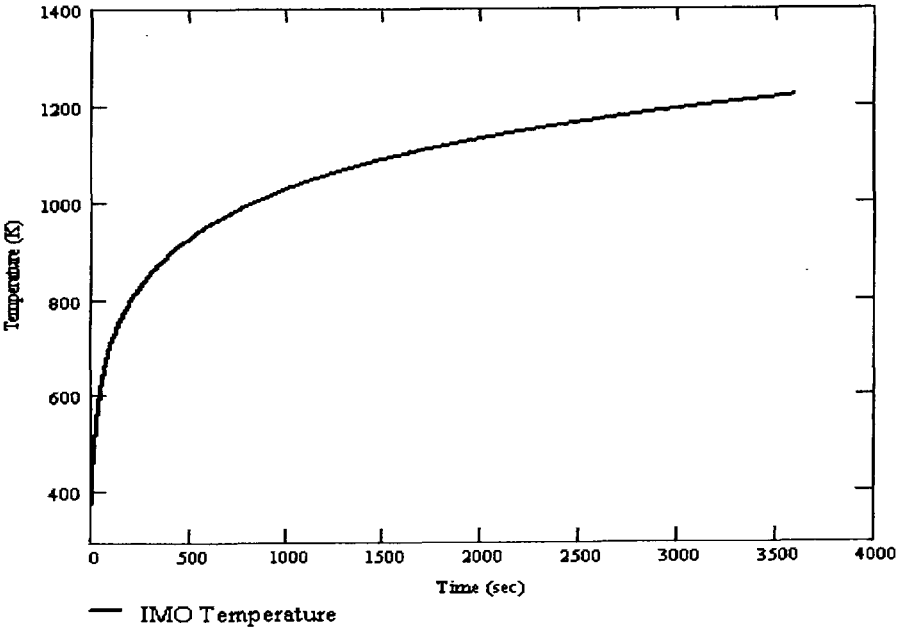

Figure 24: ISO 834 Heating Curve

associated with these materials are given in Part 4. A stream of air moving at a constant velocity parallel to the bulkhead flowed through an inlet on the bottom face of the fluid control volume and out of an outlet boundary at the top face of the same control volume. The bulkhead itself was treated as a CHT solid with a constant heat transfer coefficient on the unexposed face of 7.8 W/m^2K and exhibiting adiabatic behavior on the edges. The value for the heat transfer coefficient was chosen to match the average value found in TASEF-2 on the unexposed face. The ambient temperature was assumed to be 298 K while the temperature of the fluid passing by the bulkhead was assumed to vary according to ISO 834 (See Figure 24). Figure 25 shows the general control volume used in TASCflow.

Figure 28 depicts the boundary conditions for the two-layer bulkhead. In the x-direction, 15 nodes were assigned to the fluid (with decreasing spacing nearer to the interface according to an expansion factor of 0.1), 24 nodes were used in the insulation, and 8 nodes were placed in the steel. Because the conduction characteristics were not of particular interest (i.e. only a small gradient exists over the surface) in either the y and z orientations, only 9 nodes were required over each of these axes. Furthermore, examination of the conductive behavior demonstrated only minor temperature differences across the unexposed face of the bulkhead, thus validating the previous assumption. It is worthwhile to note that no less than nine nodes could be employed due to aspect ratio considerations (aspect influences the ability to resolve the fundamental relationships for each control volume). Figure 27 shows the grid detailing node distributions for the two-layer bulkhead and Figure 26 depicts an actual grid as displayed in TASCflow.

Among those parameters that were of interest are the *turbulent intensity*, *emissivity* of the walls, *absorptivity* of the gases, *velocity* of the gases, *thermal conductivity* of the insulation, and *specific heat* of the insulation. Each of these variables has the potential to play a significant role in determination of the heat transfer from the fluid (gases heated according to ISO 834) to the bulkhead. In table 3, a matrix is provided which shows how the turbulent intensity, wall emissivity, gas absorptivity, and gas velocity alter the temperature response of the unexposed surface of the bulkhead over the one hour test period for the ISO 834 heating curve. The effect of varying thermal properties may be seen in Figure 34. While the velocity can realistically be expected to vary between 1 and 10 m/s, values between 3 and 8 have been highlighted in the sample runs. The initial turbulent intensity may be expected to be between 1 and 10 % for most engineering applications, where

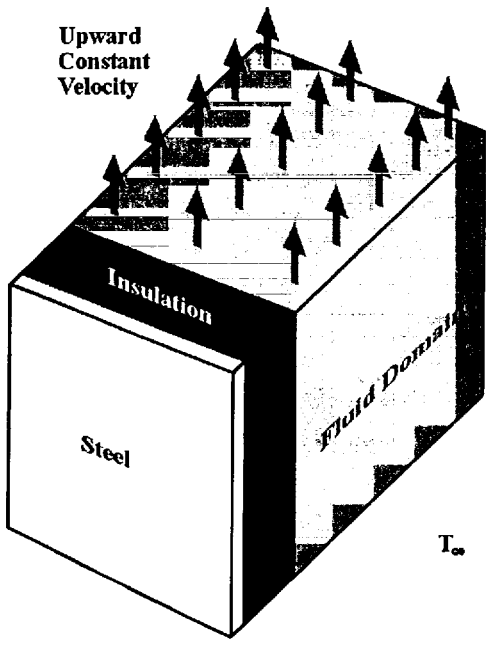

Figure 25: Two Layer Bulkhead - General Control Volume

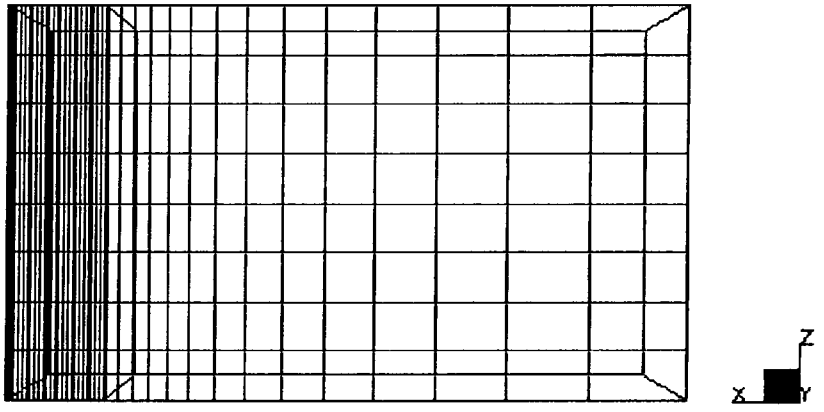

Figure 26: Two Layer Bulkhead - Actual TASCflow Grid

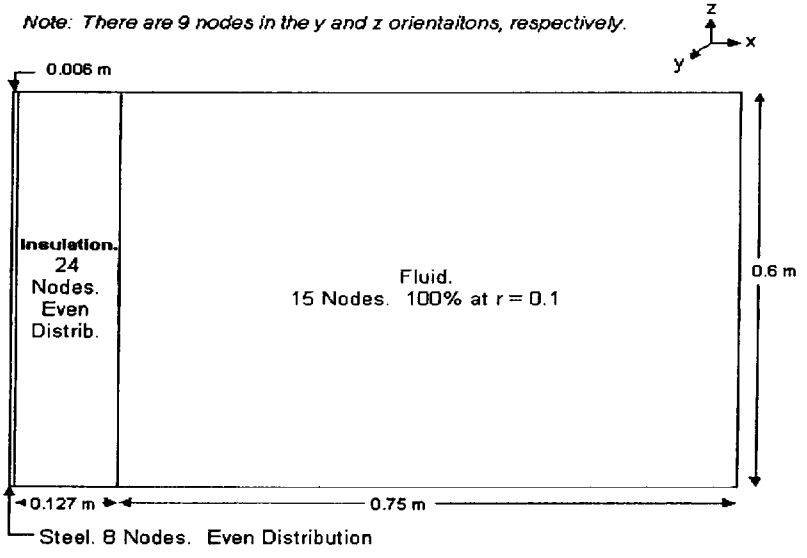

Figure 27: Two Layer Bulkhead - Grid

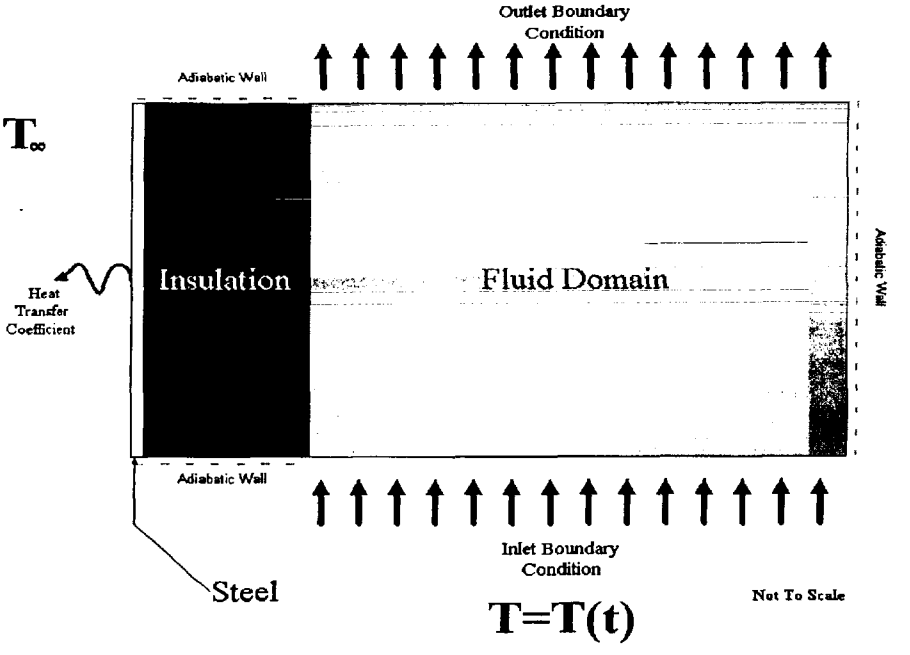

Figure 28: Two Layer Bulkhead - Boundary Condition Layout

Two-Layer Bulkhead Matrix				
Run A-F	**Velocity** m/s	**Turbulent Intensity** 0.01 – 0.2	**Emissivity** 0.0 – 1.0	**Absorptivity** 0.0 – 1.0
A	8	0.09	1.0	1.0
B	8	0.1	1.0	1.0
C	3	0.1	1.0	1.0
D	5	0.06	0.8	0.7
E	3	0.05	0.8	0.5
F	5	0.05	0.3	0.3

Table 3: Run Matrix For TASCflow - Sample Runs

5% is the median value used in typical fire modeling problems. Accordingly, the effect of turbulent intensity for values between 5 and 10% was examined. Emissivity and absorptivity both will fall between 0 and 1. Whereas the slightly higher emissivities are expected, the full range of absorptivities was examined.

5.2.1 Results of Two-Layer Bulkhead Analysis

Approximately 50 runs were completed where the effect of varying the aforementioned parameters was examined. Additionally, several runs were dedicated to ensuring that the results of the simulations were insensitive to the size of the grid (i.e. the number of nodes used in the x, y, and z directions) as well as the magnitude of the timestep. As a result of the runs dedicated to studying grid sensitivity, the size of the grid has been optimized to allow the modeler to appropriately deal with the effects of turbulence and large gradients associated with thermal properties and the rapid temperature changes. The timestep sensitivity study was performed using 0.5 second, 1 second, and 2 second units. Whereas the bulk of the runs were completed using the 1 second timestep (using up to 10 iterations per second), it was necessary to ensure that the results would not change when a smaller timestep was used. At all times over the one hour simulated test period, the difference in the temperature response of the unexposed side of the bulkhead never exceed 0.1 Kelvin. Accordingly, the 1 second timestep was deemed sufficiently small to obtain accurate results. For the 2 second timestep, the differences in the temperature response where all other variables were held constant was also

minimal. This result suggests that for simple modeling cases, larger timesteps might be employed to reduce computation time. However, as the modeling problem becomes more involved (i.e. combustion and species concentrations are being predicted), smaller timesteps will inevitably have to be utilized.

The results for each of six sample runs where environmental parameters were varied are presented in Figure 29 and are described in Table 3. The variation of the response of the unexposed surface of the bulkhead is presented with respect to the empirical data collected by the United States Coast Guard for a bulkhead with the same cross-sectional dimensions and material configurations. Because only one set of experimental results has been used, the data has been bounded by $\pm 5\%$ error bars indicating the minimum range that would likely be encountered. It is quite apparent that no single parameter, when varied within the range of typical conditions that may be expected, has a tremendous influence on the heat transfer *through* the solid. Any changes in the parameters listed in Table 3 will have an impact on the transfer of energy from the gas *to* the exposed surface of the bulkhead (as opposed to the propagation of the heat wave *through* the solid).

Increasing the velocity increases the heat transfer to the exposed bulkhead plate (bulk flow transfers energy to the surface of the bulkhead). Likewise, increasing the turbulent intensity will have a small effect on the heat transfer by way of increasing the amount of energy that is dissipated due to turbulent fluctuations. Changing the emissivity of the exposed surface will have an impact on the amount of heat energy that the surface can emit (and hence absorb or reflect). Increasing the absorptivity of the furnace gases plays a role in Gibb's diffusion radiation model, where greater absorptivities lead to more energy being transferred to the radiant phase from the furnace gases. The more energy that impinges on the exposed surface, the greater the intensity of the heat wave propagating through the solid. Depending on the thermal properties of the solid, the increased intensity may lead to a greater and/or quicker temperature rise on the unexposed surface. Despite a wide variation in the critical surface properties, it is apparent that the transient temperature response of the solid is only slightly affected for the case of a temperature-specified gas flowing over the bulkhead face.

5.3 Comparison of TASCflow and TASEF-2

In an effort to validate the results obtained for this modeling effort, it was deemed appropriate to compare the results from the TASCflow simulations

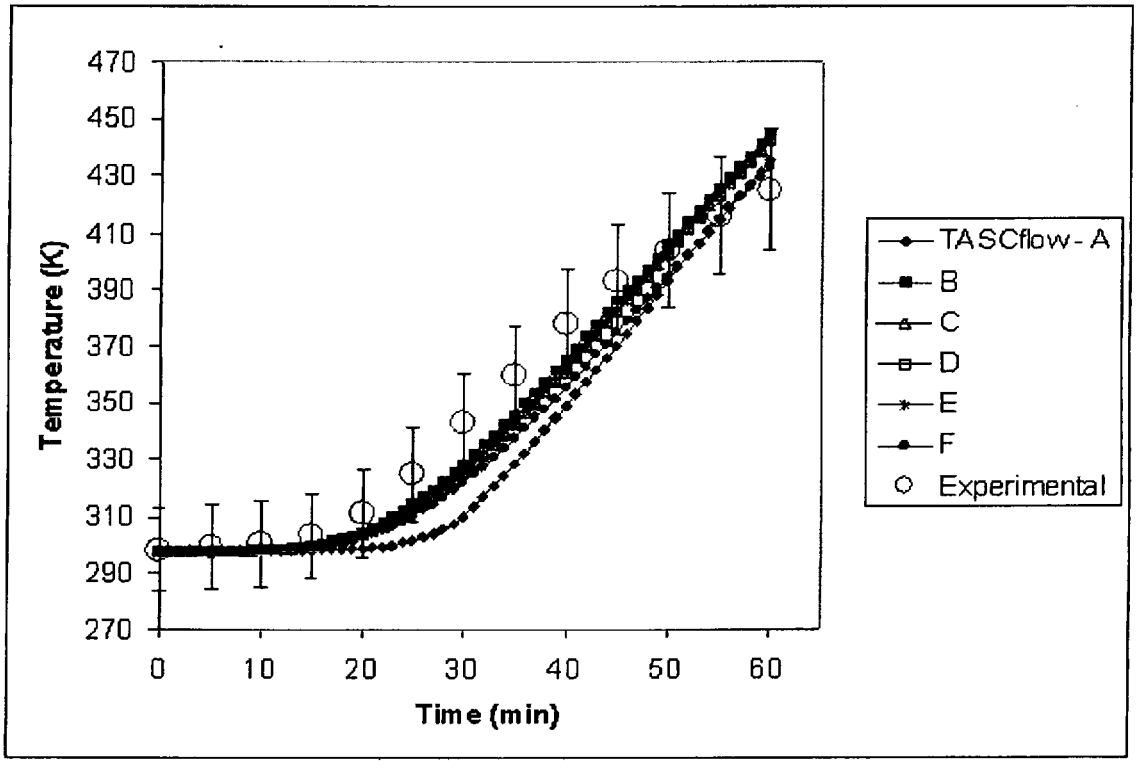

Figure 29: Two Layer Bulkhead - Results for One-Hour Transient Simulation

with empirical data *and* the results obtained using the finite element model TASEF-2. The simulations using TASEF-2 were performed in 1996 by Paul Spinn and are presented in his Masters Thesis [38]. Only the results from the runs where the insulation was exposed to the furnace gases (ISO 834 heating curve) will be compared with those obtained using TASCflow. The empirical data is given for a similar bulkhead setup with typical insulative properties, given as hollow red circles and bounded by $\pm 5\%$ error bars. Section 5.3.1 will introduce the reader to the mathematical basis of TASEF-2, while Section 5.3.2 will provide a point-by-point comparison of the solution methodologies employed by each program.

Modeling heat transfer at the bulkhead using TASEF-2 requires a different approach from that used to model the Conjugate Heat Transfer problem in TASCflow. Inherently, TASEF-2 cannot solve the detailed fluid flow equations associated with fluid-solid interaction, and hence the use of TASEF-2 to model fluid flow through the bulkhead is not possible. Nevertheless, TASEF-2 *may* be used to explore the conduction heat transfer using a heat source on one side of the bulkhead. If the flow through the bulkhead is minimal (as determined experimentally and with TASCflow), then the results from TASEF-2 should compare favorably with those obtained with the much more complicated and computationally expensive CFD code.

5.3.1 Bulkhead Modeling Approach of TASEF-2

The background material presented in this section is taken from the TASEF-2 manual, *Pre- and Post-Processor For Finite Element Analysis on Non-Linear Transient Heat Conduction* [30]. Because of the nature of TASEF-2, the ability to model an actual *combustion* source does not exist. Accordingly, a specified heat source (either constant or growing) has been used. Time-dependent thermal properties can also be applied according to available data or preset parameters provided in the code. A two-dimensional grid can also be specified, where various nodes may be coupled to simplify calculations even further. The relationship described in equation 77 is used to formulate a solution to the heat transfer problem for an arbitrary small area, A.

$$\frac{\partial}{\partial x}\left(k\frac{\partial T}{\partial x}\right) + \frac{\partial}{\partial y}\left(k\frac{\partial T}{\partial y}\right) + Q = \rho c\frac{\partial T}{\partial t} \tag{77}$$

Q represents heat flux, and x and y are directional terms. The exact form of equation 77 is not used, but is discretized to arrive at the final form of

this relationship that TASEF-2 uses to solve for the conduction through the solid. Similar types of simplified expressions are used to describe radiative and convective heat transfer boundary conditions. Equation 78 describes and convection heat transfer,

$$q_{con} = h(T_s - T_g)^{\alpha} \tag{78}$$

and equation 79 is used to approximate the radiative heat transfer.

$$q_r = \sigma \epsilon T^4 \tag{79}$$

The indices s and g denote surface and gas respectively. The variable α is a power for the convective heat transfer (usually equal to one for linear heat transfer). The parameters σ and ϵ are the Stefan-Boltzmann constant and total emissivity respectively. Finite element discretization is then used to solve conduction equations according to Euler's method of forward differencing. When applicable, the convection and radiation relationships are used to approximate heat flux boundary conditions that govern the conduction through the solid.

The following types of input parameters are successively entered into the TASEF-2 input program:

1. Input and output file specifications
2. Geometry of analysis regimes (including the main region and all sub-regions)
3. Specification of coupled nodes
4. Material properties for various layers in the main and sub-regions specified in the geometry
5. Initial temperature and radiation constant specification
6. Boundary node groups
7. Prescribed heat transfer boundary conditions
8. Prescribed temperature boundary conditions
9. Prescribed heat flux boundary conditions

10. Specification of voids

11. Time related parameters

12. Fire history (ISO 834)

The output is given in table form over a series of time intervals. A matrix of temperatures describes the heat transfer through the solid for each time interval. The nature of the results depends heavily upon the thermal properties (expressed either as constant or time-dependent) and the size of the grid. It is further possible to examine localized hot spots on the bulkhead as a result of the specified heat source.

5.3.2 Inputs For TASCflow and TASEF-2

Input broken down into six major logical groups within TASCflow and TASEF-2 will be reviewed and compared in this section. The principle objective is to provide a mechanism to make a comparison between the modeling techniques. The following areas will be discussed with some detail:

1. Geometry Input

2. Material Input

3. Heat loads

4. Internal conditions

5. Boundary conditions

6. Time integration

Typically, the ability to model fire phenomena is more limited in TASEF-2 then in TASCflow. Accordingly, the comparison will not be directed towards the abilities of TASCflow, but rather towards those limitations imposed by the structure of TASEF-2. Further information about these logical groups with respect to TASCflow is offered in section 2.

Geometry Input TASEF-2 uses mainly orthogonal shapes in the grid formulation, though it is possible to have triangular shapes. It is recommended that more elements be used on the x-axis than for the y-axis so that the details of conductive transfer can be adequately captured. Three-dimensional grids cannot be constructed in TASEF-2, thus limiting the ability to predict conduction over the surface *and* through the surface simultaneously. Alternatively, constant flux boundary conditions are usually assumed for the exposed surfaces.

TASCflow can be used to create two and three-dimensional grids, either rotating or fixed. Non-orthogonal shapes and curvilinear connections between points can be made. The individual elements can be orthogonal or non-orthogonal (such as hexahedral) in nature. Furthermore, it is possible to have boundary fitted elements, embedded grid refinement for localized areas, and grid attachment. There is no grid that can be generated in TASEF-2 that cannot be generated in TASCflow.

Material Input The material properties of the solid area being modeled in TASEF-2 are entered for (1) the main region and (2) all other sub-regions. The thickness, thermal conductivity, as well as thermal capacitance ($\rho \cdot c_p$) are typically given as either constant or temperature dependent. The use of conductivity-temperature graphs may be employed to describe the variation in the said property. Likewise, the thermal capacitance may be described as independent of temperature, linearly related to temperature, or linearly related to enthalpy, h. The sub-regions can either be specified to have different material properties or modeled as voids with prescribed or radiative/convective boundary conditions.

TASCflow can mimic the conditions given above exactly, albeit the means to arrive at those conditions are much more elaborate. A wide variety of mathematical descriptions of the material properties as well as data points (such as those obtained from material property graphs) can be entered into the routines. TASCflow reads in these routines during its execution. In addition to voids, materials of varying porosity can be designated. The use of a main region and sub-regions does not explicitly exist in TASCflow, but any point can be specified to have any material properties that the user requires. The thermal capacitance is indirectly solved for using the momentum, continuity, and energy equations.

Heat Loads In TASEF-2, heating can be specified according to a prescribed or calculated flux or temperature to a node, line, or area. The ability to model heat sinks exists, where heat sinks are simply described as negative heat sources. In TASCflow, similar boundary conditions can be provided, though the ability to model source terms is much more advanced. For example, source terms in TASCflow can be modeled as flux or combustion sources (using such models as Eddy-Breakup), depending on which version of the code is used. Furthermore, the effect of distance and view factors on the surface is considered. The use of convection and radiation boundary conditions as well as mass flow boundary conditions is common. Despite the advanced features that can be employed, it is still possible to model simple distributed or point sources at one or any boundaries.

Internal Conditions Internal conditions in TASEF-2 refers to the relationship between specific nodes in the finite element mesh. Such factors as equal temperature nodes and prescribed temperature nodes are defined under the auspices of internal conditions. In TASCflow, this type of situation is dealt with on a node by node or regional basis. It is possible to obtain the same ends, though the means are significantly more versatile in TASCflow.

Boundary Conditions TASEF-2 defines a boundary as a set of straight lines, not necessarily connected, with the same boundary conditions. Accordingly, the number of boundaries is set, and the following types of conditions may be specified:

- Prescribed temperature
- Prescribed heat flux (per unit length)
- Linear convective heat exchange
- Non-linear convective heat exchange
- Radiative heat exchange
- Combined radiative and convective heat exchange

Boundaries without heat exchange need not be specified.

In TASCflow, if a heat flux source is given, the temperature, etc. can be calculated. Nevertheless, it is possible to use prescribed temperature

or flux boundary conditions in the same manner. In the conjugate heat transfer problem, the convective exchange is not typically specified, but can be calculated by the code based upon local fluid conditions. In the case where the fluid is not being considered, but the heat transfer to the fluid is under consideration, it *is* possible to specify a heat transfer coefficient. Equation 80 describes the relationship used by TASCflow in this case.

$$q = h(T - T_{ref}) \tag{80}$$

The heat transfer coefficient, h, and the reference temperature, T_{ref} are specified in the boundary conditions. Further information about boundary condition specification is available in Part 3.

Time Integration The time bounds of the problem are designated in this part of TASEF-2. Maximum times, time increments, and time steps are also defined here. In TASCflow, the issue of time integration is quite different because of the coupled equations and the difficulties that arise when trying to achieve closure. Nevertheless, while the modeler is wise to consider the intricacies associated with choosing the best possible time step, time integration will only become an issue for runs in TASCflow that are far more complex than what TASEF-2 can accommodate.

Graphical Comparison of Results Results for a two layer bulkhead simulation obtained from TASEF-2 [38] and TASCflow are depicted in Figure 30 for the one hour test associated with the ISO 834 heating curve. Also presented in Figure 30 are experimentally derived results taken from Spinn's Master Thesis [38]. The two runs shown ("Spinn 1" and "Spinn 2") were obtained for two sets of thermal conductivity data derived from TASEF-2 and Harmathy (see Part 4). Typical composite values have been used in TASCflow, the results of which may be seen from the sample TASCflow curve included (labeled "A", described in Table 3). The results obtained from TASCflow compare quite favorably with the experimental data, and reasonably well with the runs produced in TASEF-2. The differences, which principally arise between twenty and 45 minutes, can primarily be attributed to varying thermal properties, the significance of which is discussed in more detail in Section 5.4. Though not presently confirmed, it is believed that varying the diffusivity of the insulation will largely account for the observed discrepancies in the propagation of the heat wave through the material.

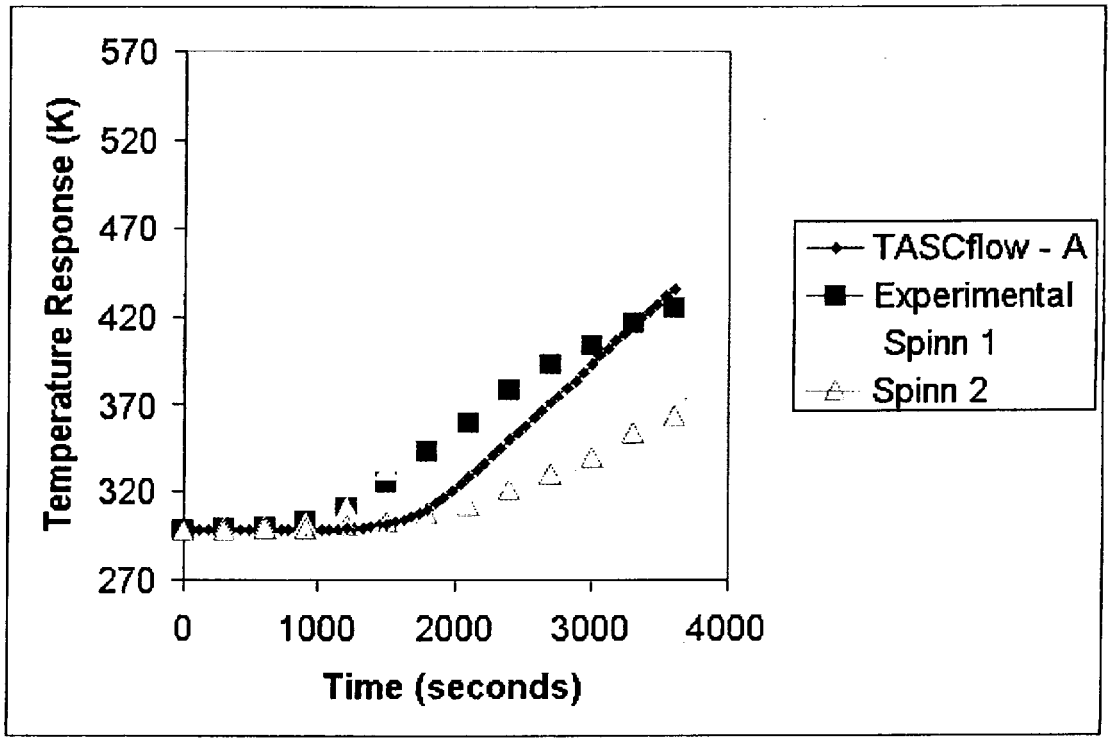

Figure 30: Two Layer Bulkhead - Comparison of Results from TASCflow and TASEF-2

5.4 Description of Bulkhead Modeling - Three Layer Bulkhead

The three layer bulkhead modeling problem was set up in a similar fashion to the two-layer problem, the principal difference being the addition of a layer of insulation on the unexposed surface. For this configuration, 15 nodes were placed along the x-axis of the fluid, 17 nodes were in the cross-section of the first layer of insulation, 3 nodes in the steel, and 12 nodes were in the cross-section of the second layer of insulation. This particular modeling effort focused on determining the effect of varying the thermal properties of the insulation as well as how the arrangement of the insulation and steel would impact the heat transfer *through* the bulkhead over a one-hour test period. Accordingly, the parameters that were varied in these runs primarily included the thermal conductivity and specific heat of the insulation. The specific heat curve was held constant in runs A-G while the conductivity curve was varied. In runs H, I, and J, the specific heat curve was varied while the conductivity curve was held constant. As a result, it was possible to examine the effect of each of these major thermal properties on the conduction through the layered bulkhead separately.

Table 4 shows the matrix used in the modeling process to demonstrate the nature and arrangement of materials can influence the thermal response of the specimen. Figure 34 shows the generic setup of the three layer bulkhead with respect to the modeling effort. Thermal properties for insulation used in each of the sample runs are presented in Figures 31, 32, and 33. Where the thermal properties were different for each of the two insulation layers, the values are given in Figure 31. Figure 32 shows the conductivity of the insulation where both layers of insulation possessed identical properties (hence only one value for each run is given). Figure 35 shows the temperature response of the unexposed surface of the bulkhead over the one hour test period for each of seven sample runs described in the matrix where the thermal conductivity curve was varied. Figure 36 shows the temperature response on the unexposed surface of the bulkhead for each of four different specific heat curves shown in Figure 33.

The average conductivity and specific heat of the insulation was increased and then decreased by way of altering the property curves (see Figures 31, 32, and 33). The purpose for this variation was to point out the sensitivity of the conduction response to the user input for thermal conductivity and specific heat. The thermal properties of the steel were not varied because

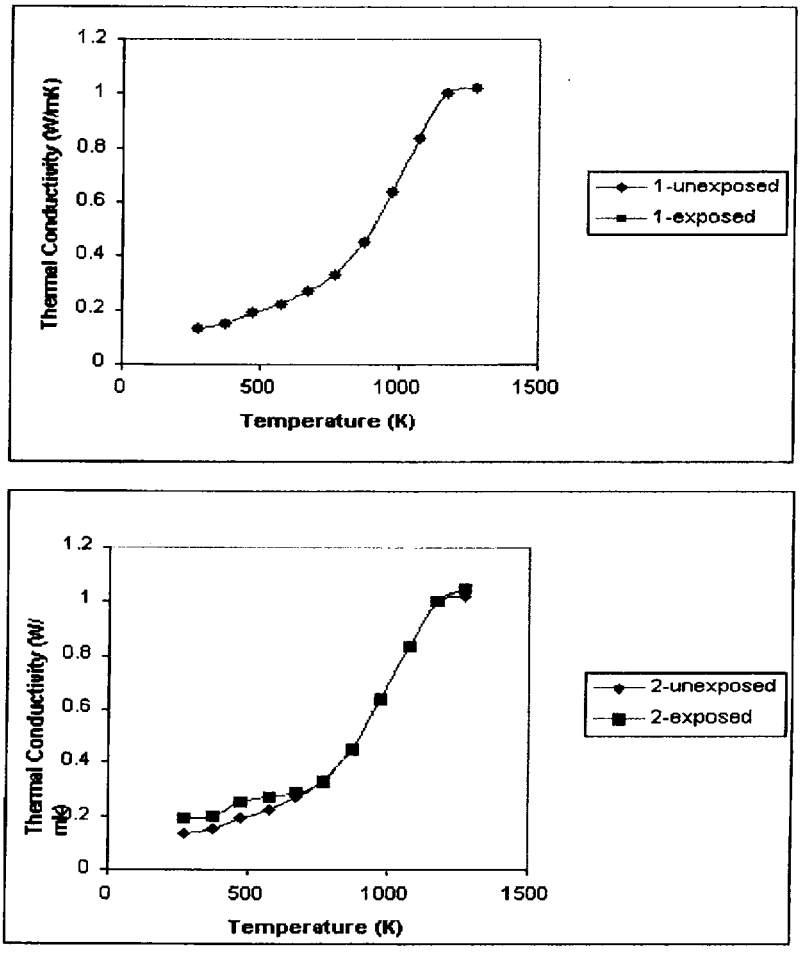

Figure 31: Thermal Conductivity of Insulation - Varying Conductivity in Each Layer

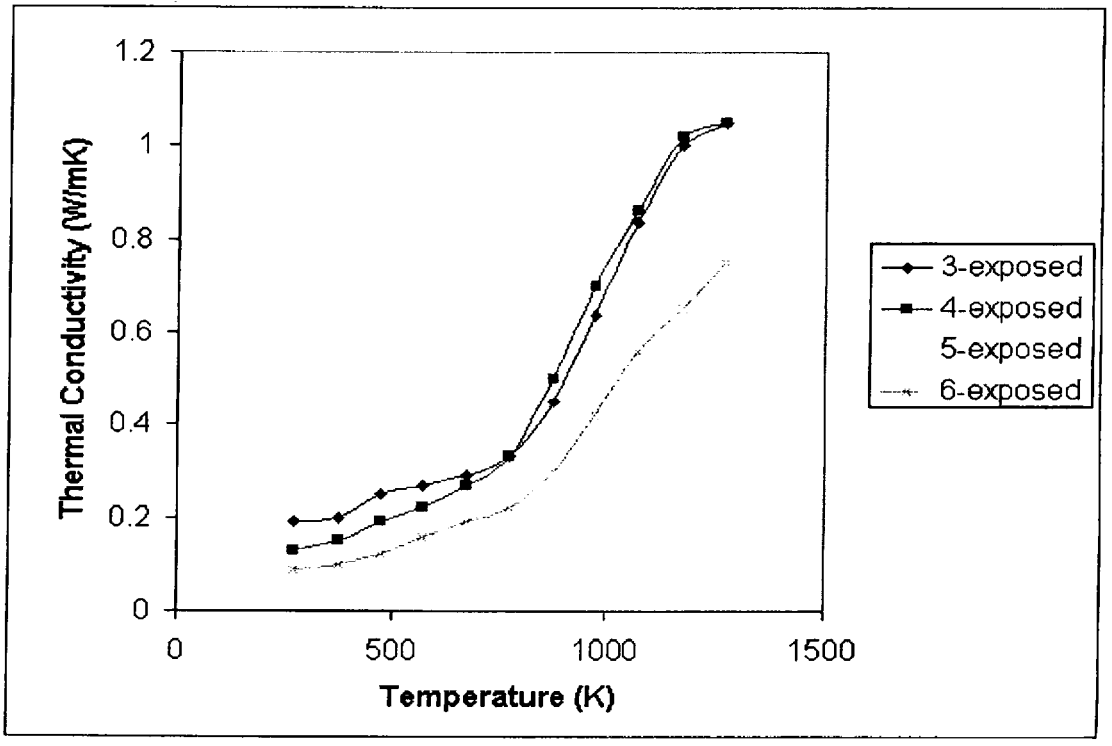

Figure 32: Thermal Conductivity of Insulation - Identical Conductivity in All Layers

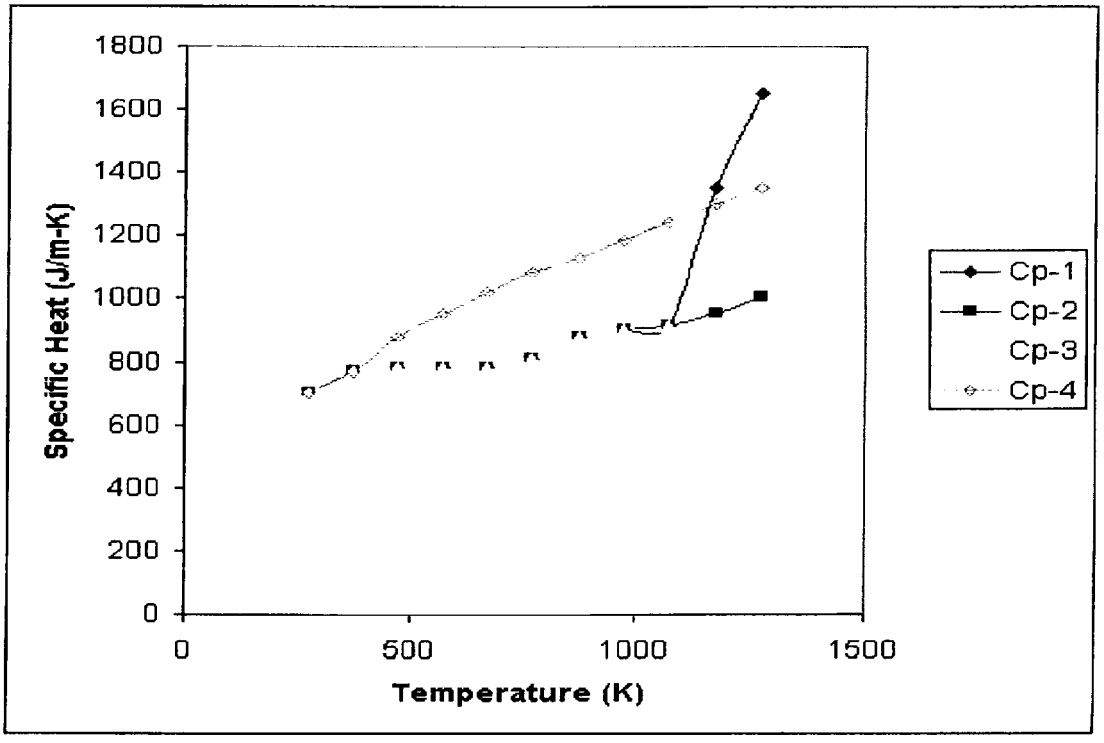

Figure 33: Specific Heat of Insulation

Three-Layer Bulkhead Matrix			
Run **Run** A - F	**Insulation Density** kg/m^3	**Insulation Conductivity** A - F	**Insulation Specific Heat** A - F
A	137	1	Cp-1
B	137	1	Cp-1
C	137	2	Cp-1
D	137	3	Cp-1
E	137	4	Cp-1
F	137	5	Cp-1
G	137	6	Cp-1
H	137	4	Cp-2
I	137	4	Cp-3
J	137	4	Cp-4

Table 4: Run Matrix For TASCflow - Sample Runs

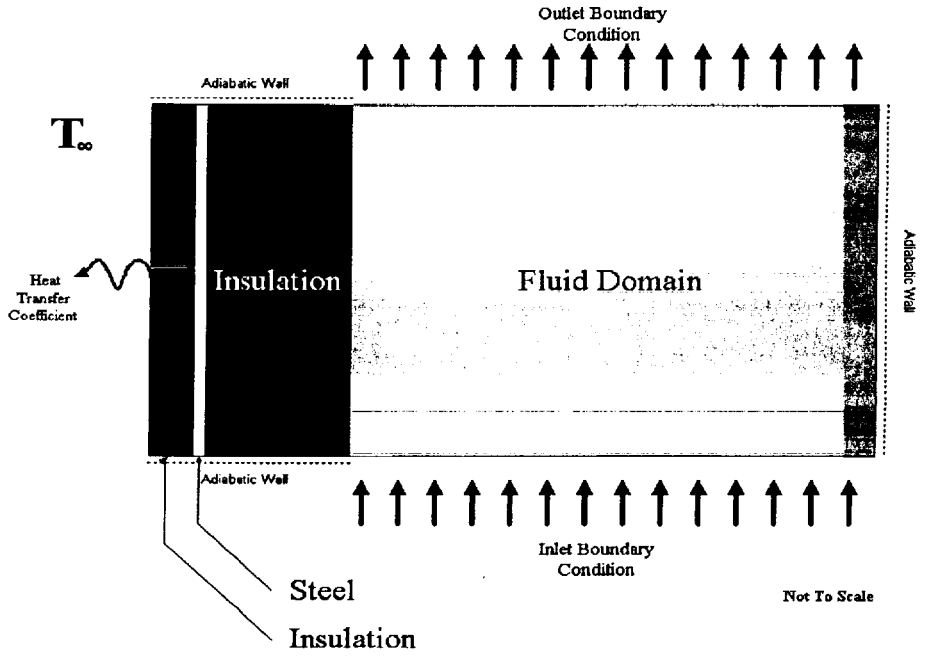

Figure 34: Three Layer Bulkhead - General Control Volume

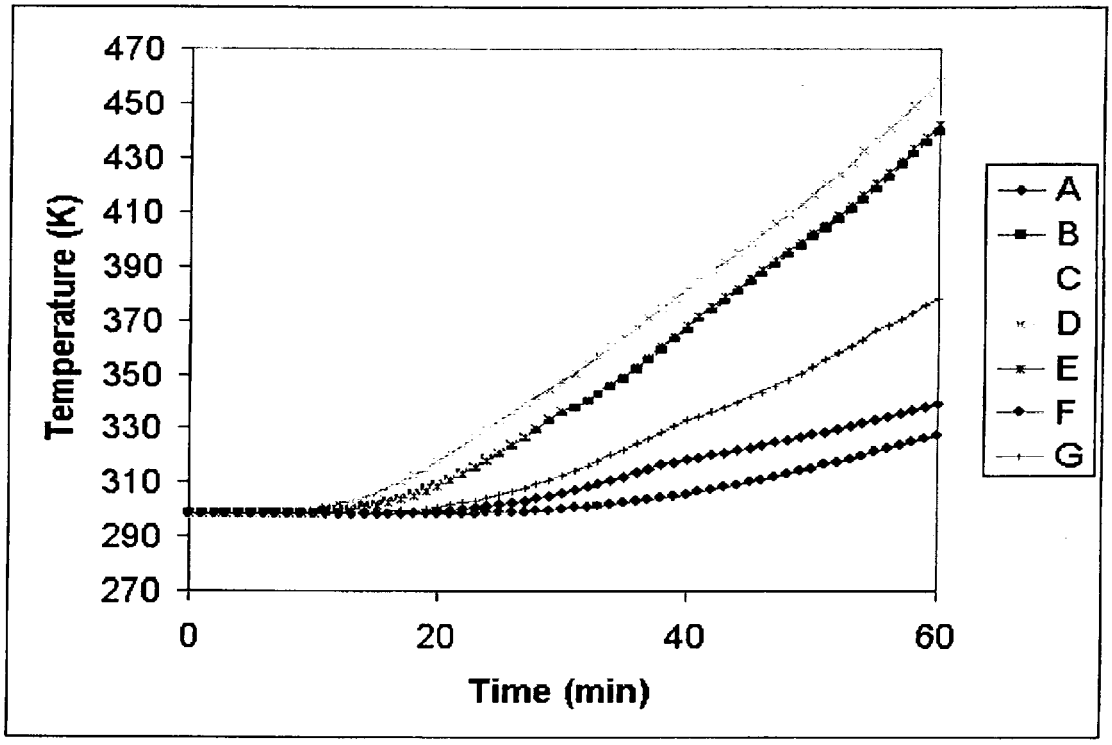

Figure 35: Three Layer Bulkhead Modeling Results- Thermal Conductivity Variation

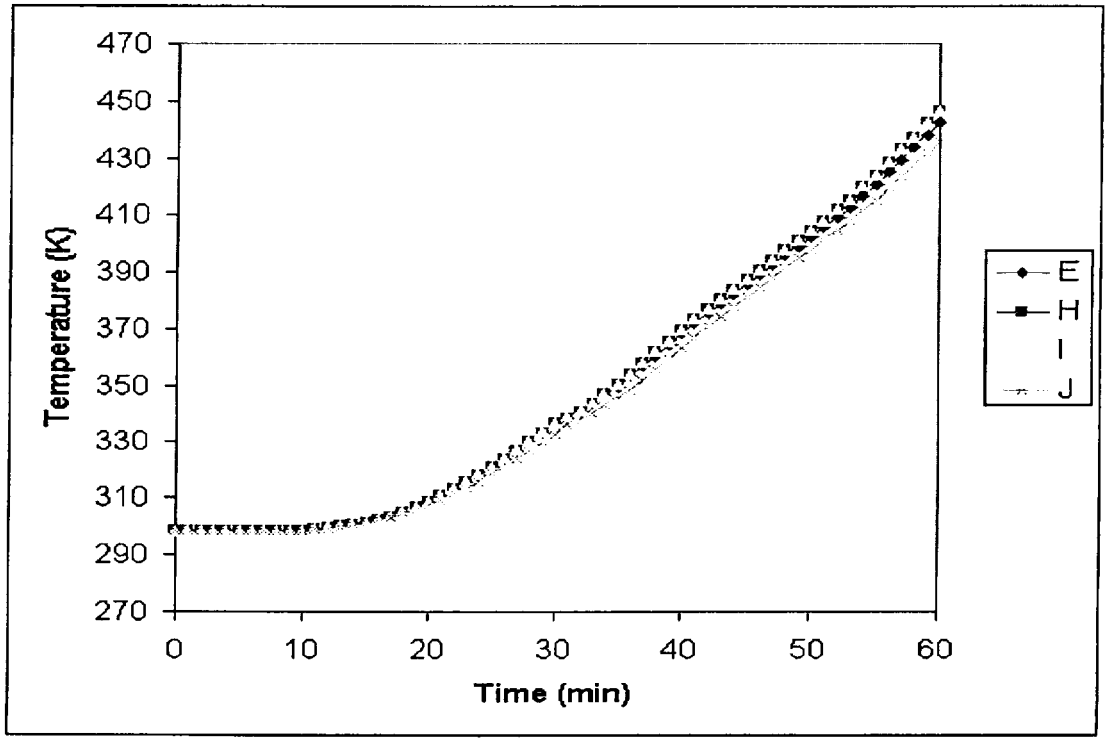

Figure 36: Three Layer Bulkhead Modeling Results - Specific Heat Variation

values are well established in the literature and it is likely that the steel would have a minimal influence on the heat conduction through the bulkhead in this particular problem. The variations in conduction through the solid may indeed be seen to vary according to the thermal diffusivity ($k/\rho c$), where the influence of the thermal conductivity is particularly strong relative to the influence of specific heat. The substantial variations in the temperature on the unexposed side of the bulkhead demonstrate the need to carefully establish and then implement thermally-dependant properties in the code. Recommendations concerning thermal properties may be found in Part 5.

Part VI
Required Further Development

6 Required Further Development

With respect to occupant safety in the post-crash vehicle fire environment, a couple of fire scenarios stand out as having potential to cause harm to the occupants via toxic species production, hot gas generation, and spread of flame. Specifically, the under-carriage pool fire scenario and the engine compartment flame spread through the windshield would seem to be appropriate cases (determined from observation of tests and experience). Accordingly, it may be appropriate to conduct additional modeling projects on these scenarios. The following list identifies work that may be helpful in future modeling projects:

1. **Presence of openings in bulkhead** - The state of fluids modeling in CFD is fairly advanced at this time and allows for prediction of flows through deliberate openings and environmentally-induced cracks alike. However, the accuracy of these flows depends largely upon the initial prediction of the heat/mass source in the engine compartment. Consequently, it would be helpful to gain an understanding of the fire scenarios that will drive the flows and heat transfer (and more specifically, the associated heat and mass release rates).

2. **Effect of engine on the convective flows inside the engine compartment** - The blockage provided by the engine can have a significant impact on the entrainment and consequently the nature of the flows and associated heat release rates in a real fire. Furthermore, where the engine can actually act as a heat source or heat sink, proper modeling of this mass and the associated fuel loads will help develop a reasonable estimate for the post-crash vehicle fire.

3. **Melting of the windshield** - Although it may not be possible to model the melting of windshield glass from first principles at this time, concessions can be made whereby the condition of the windshield is dependant on the flux to the surface. The flux to the surface is directly related to the radiation and convective flows originating from the engine compartment, which may be reasonably predicted using TASCflow. A component to effectively model this phenomena will be flux vs. failure data for those materials commonly used in windshields.

4. **Pool fire under the vehicle** - At this time, CFD modeling technology will support research into pool fires extremely well. Modeling of

specified heat and mass release rates can be enhanced by knowledge of the fuel (such as gasoline) and the nature of the spill. In addition to data gathered for this project, a wealth of empirical data already exists for various pool fire scenarios. The choice of radiation model will likely have an impact on the results for this type of fire scenario.

5. **Combustion and Toxic Species Modeling** - Though primarily dependent on the specified values for mass and heat release, the ability to model simple combustion via a one or multi-step reaction is fairly robust. The correlation between heat and mass release rates and toxic species is not so clear, but may be approximated for the less complex fire scenarios with considerable accuracy. For fire scenarios where multiple complex fuels are involved, it is not computationally practical to arrive at detailed predictions of species production. Furthermore, the data for validation does not currently exist in any great quantities.

6. **Effect of combustible lining materials** - The key to modeling combustible lining materials is in the proper specification of thermal and combustion properties. At this time, it is not reasonable to assume that an adequate and computationally economic solution for CFD modeling of flame spread and combustion will exist for the types of materials used in automobiles. Consequently, the modeler is dependent on experimental data to provide key rates of heat and mass production for various supposed orientations of the material in question.

7. **Plastics combustion and associated melting** - As with gasoline, plastics can significantly affect the integrity of the passenger compartment when they melt and form pools which can then combust and lead to further spread of the fire. Currently, plastics melting models exist in TASCflow, though the level of complexity of these models does not always support the requirements of the fire scenario. Consequently, it will be necessary to enhance these models by way of continued development or better specification of mass and heat release as well as production of toxic species.

In order to realistically address these challenges for the purposes of creating an effective engineering tool, more data needs to be collected. While it is possible to formulate estimates that may be used in the specification of heat and mass release, etc., the unique nature of the post-crash vehicle fire

warrants specific testing with respect to the design fire scenarios discussed in Section 3.5. Where scaling of toxic species production is particularly difficult for most fuels, and mass and heat release will be a challenge with many solid fuels, careful consideration should be made with respect to what is measured and which methods are used. It is widely recognized in the modeling community that the quality of results is dependant in large part on the quality and applicability of the inputs (which in this case is characterized by the fire scenario and its associated heat and mass release rates).

The success of a CFD effort depends largely upon the development of realistic fire scenario data as well as proper representation and use of thermal properties. Whereas the work to date has shown that the thermal response of the materials associated with the spread of heat and flame into the passenger compartment is highly sensitive to the thermal properties, it is useful to collect data for automotive insulations, lining materials, etc. up to 1300K. Currently, most data scarcely applies past 600K. The use of small scale material data obtained from such sources as the cone calorimeter may prove to be highly useful.

References

[1] Advanced Scientific Computing. 1995. TASCflow3d User's Documentation, Theory, Version 2.4 Edition. Thry. ASC, 554 Parkside Drive, Unit 4, Waterloo, Ontario, Canada N2L 5Z4.

[2] Advanced Scientific Computing. 1995. TASCflow3d User's Documentation, Volume 1, Version 2.4 Edition. Intro, Overview, Graph, Grid. ASC, 554 Parkside Drive, Unit 4, Waterloo, Ontario, Canada N2L 5Z4.

[3] Advanced Scientific Computing. 1995. TASCflow3d User's Documentation, Volume 2, Version 2.4 Edition. Bob, Tool, TDI. ASC, 554 Parkside Drive, Unit 4, Waterloo, Ontario, Canada N2L 5Z4.

[4] Advanced Scientific Computing. 1995. TASCflow3d User's Documentation, Volume 3, Version 2.4 Edition. Parm, Flow, SCI, AddCap, ACL. ASC, 554 Parkside Drive, Unit 4, Waterloo, Ontario, Canada N2L 5Z4.

[5] Babrauskas, V. 1994. "Describing Product Fire Performance-Manufacturers' Versus Modelers' Needs," Fire and Materials, 18:289-296.

[6] Bauccio, M. 1994. ASM Engineered Materials Reference Book, 2nd Edition. ASM International.

[7] Boyer, L. 1993. Thermal Radiation From Marine Fire Boundaries. Technical Report CG-D-01-94, United States Coast Guard, Research and Development Center.

[8] Advanced Scientific Computing. Development of a Plastics Combustion Model: Combustion Modeling. ASC, 554 Parkside Drive, Unit 4, Waterloo, Ontario, Canada N2L 5Z4.

[9] Advanced Scientific Computing. TASCflow3d User's Documentation, Radiation: Diffusion Radiation Model. ASC, 554 Parkside Drive, Unit 4, Waterloo, Ontario, Canada N2L 5Z4.

[10] Advanced Scientific Computing. Technical Summary of ASC's CFD Technology. Technical Summary. ASC, 554 Parkside Drive, Unit 4, Waterloo, Ontario, Canada N2L 5Z4.

[11] Conley, C. 1996. "Deadlier Than You Think," NFPA Journal, 90(5):79.

[12] deRis, J.N. 1979. "Fire Radiation - A Review," Seventeenth Symposium (International) on Combustion, The Combustion Institute, pp. 1003-1015.

[13] DiNenno, P. J., Editor. 1995. SFPE Handbook of Fire Protection Engineering, 2nd Edition, Society of Fire Protection Engineers and National Fire Protection Association.

[14] Drysdale, D. 1985. An Introduction to Fire Dynamics, 1st Edition, Wiley Interscience.

[15] Fire, F. 1992. "Anatomy of an Urban Myth," Fire Engineering, 145(2):59.

[16] Gibb, J. 1973. Internal Note, MRM 85, Central Electricity Board.

[17] Grosshandler, W. L. 1980. "Radiative Heat Transfer in Nonhomogeneous Gases: A Simplified Approach," International Journal of Heat and Mass Transfer, 23:1447-1459.

[18] Grosshandler, W. L. 1993. "RADCAL: A Narrow Band Model for Radiation Calculations in a Combustion Environment," Technical Report NIST Technical Note 1402, Building arid Fire Research Laboratory, NIST.

[19] Grosshandler, W. L. and A. T. Modak. 1981. "Radiation From Nonhomogeneous Combustion Products," Eighteenth Symposium (International) on Combustion, The Combustion Institute, pp. 601-609.

[20] Gustin, B. 1996. "New Fire Tactics for New-Car Fires," Fire Engineering, 149(4):43.

[21] Harmathy, T. 1983. DRB Paper No. 1080 NRCC 20956, Technical Report, National Research Council of Canada, Ottawa, Canada.

[22] Hunt, S.P. 1991. A Finite Element Analysis of a Barrier Subject to an ISO Fire, Master's thesis, Worcester Polytechnic Institute, Worcester, MA, USA.

[23] Kumar, S. and G. Cox. 1989. "Radiation and Surface Roughness Effects in the Numerical Modelling of Enclosure Fires," Fire Safety Science-Proceedings of the Second International Symposium, pp. 851-860.

[24] Launder, B. E and D.B. Spaulding. 1972. Lectures in Mathematical Models of Turbulence, Academic, New York.

[25] Lockwood, F. C. and N. G. Shah. 1981. "A New Radiation Solution Method for Incorporation in General Combustion Prediction Procedures," Eighteenth Symposium (International) on Combustion, The Combustion Institute, pp. 1405-1414.

[26] Magnussen, B. F. and B. H. Hjertager. "On Mathematical Modeling of Turbulent Combustion with Special Emphasis on Soot Formation and Combustion," Symposium (International) on Combustion, The Combustion Institute, pp. 719-729.

[27] Mills, A. F., Editor. 1992. Heat Transfer, Irwin Publishing, Boston, MA.

[28] Modak, A. T. 1979. "Radiation from Products of Combustion," Fire Research, 1:339-361.

[29] Mulholland, G. W., V. Henzel, and V. Babrauskas. 1988. "The Effect of Scale on Smoke Emissions," Fire Safety Science - Proceedings of the Second International Symposium, Hemisphere Publishing Corp., pp. 347-357.

[30] Paulsson, M. 1983. Postprocessor for Two Dimensional Heat Flow Analysis, Lund Institute of Technology, Division of Structural Mechanics.

[31] Pehrson, R. D. 1999. Prediction of Fire Growth on Furniture Using CFD, Ph.D. Dissertation, Worcester Polytechnic Institute, Worcester, MA, USA.

[32] Raithby, G.D. and E. H. Chui. 1990. "A Finite-Volume Method for Predicting a Radiant Heat Transfer in Enclosures with Participating Media," Journal of Heat Transfer, 112:415-423.

[33] Roberts, C. C. Jr. 1991. "Motor Vehicle Fire Analysis," Automotive Engineering and Litigation, 4.

[34] Sarofim, A. 1986. "Radiative Heat Transfer in Combustion: Friend or Foe," Twentyfirst Symposium (International) on Combustion, The Combustion Institute, pp. 1-23.

[35] Schlichting, H. 1979. Boundary Layer Theory, Pergamon.

[36] Smock, D. 1994. "Plastics Rev Up Engines," Plastics World, 52:26.

[37] Sparrow, E. M. and R.D. Cess. 1978. Radiation Heat Transfer, Hemisphere Publishing Corporation, Washington.

[381 Spinn, P. 1996. Semi-Empirical Heat Transfer Design Technique for Fiberous Insulation, Master's Thesis, Worcester Polytechnic Institute, Worcester, MA, USA.

[39] Thomas, G. C. 1995. Private communication with Paul Spin, Ph.D. Candidate at the University of Canterbury, New Zealand.

[40] White, F.M. 1991. Viscous Fluid Flow, McGraw-Hill, Inc.

[41] Wilcox, D. C. 1993. Turbulence Modeling for CFD, DCW Industries, Inc.

[42] Winter, D. 1993. "Automakers Order Engine Materials From Long Menu. Ward's Auto World, 29(6):47.

[43] Winter, D. 1993. "Plastics Gaining Under the Hood," Ward's Auto World, 29(9):58.

[44] Yan, H. CFD Room Fire Growth on Wall Lining Materials, Unpublished.

Appendix A -- Description of the Modeling Process

Introduction

The Computational Fluid Dynamics procedure used to establish a model for the heat transfer to a three-layer passenger vehicle bulkhead consists of two main areas; grid generation and boundary conditions. Additionally the Parameter File and FORTRAN subroutines used in the investigation of the bulkhead heat transfer calculation are also explained. The specifics of each are demonstrated in an example using the general purpose fluid modeling software package TASCflow. It should be noted that although this procedure can be applied to other CFD codes, results may vary due to differences that may exist for various physical phenomena or numerical solvers.

Grid Generation

The process of grid generation allows the user to specify the geometry of the physical domain as well as the number and distribution of nodes in the computational domain. Grid generation can be accomplished with various commercially available software packages such as PowerMesh, however, the grids generated for the bulkhead heat transfer calculation were done using the command line-based TASCgrid grid generation utility that is included with TASCflow. This utility consists of four parts; the geometry phase (tascgridg), the curve phase (tascgridc), the surface phase (tascgrids), and the interior phase (tascgridi). Each phase requires a user specified definition file which are explained in greater detail in the following sections.

Geometry Phase (Tascgridg)

The geometry phase requires a geometry definition file (*gdf*) that is used as input for *tascgridg*. The *gdf* file used for the bulkhead heat transfer calculation is called *bulkhead_9.gdf* and is shown in Appendix A. The geometry of the three-layer bulkhead, which is under the heading "VARIABLE DEFINITIONS" in the *bulkhead_9.gdf* file, used in the model is;

- Fluid region
  - Length (x direction) = *0.750 m*
  - Width (y direction) = *0.600 m*
  - Height (z direction) = *0.600 m*
- Insulation layer:
  - Thickness (x direction) = *0.1 m*
  - Width (y direction) = *0.600 m*
  - Height (z direction) = *0.600 m*
- Combined steel/insulation layer
  - Thickness (x direction) = *0.033 m*
  - Width (y direction) = *0.600 m*
  - Height (z direction) = *0.600 m*

Based on the above geometry, points in three-dimension space are defined in order to describe the three-layer bulkhead and a region of fluid. This geometry follows a convention of describing three-dimensional space in terms of west to east for movements in the positive x direction, south to north for movements in the positive y direction, and bottom to top for movements in the positive z direction. The geometric points associated with the corners of the fluid region, insulation, and steel can be found under the heading "POINT" in the *bulkhead_9.gdf* file. The *bulkhead_9.gdf* file also contains instructions to construct linear curves between define points and surfaces from the linear curves. This information is used in the curve and surface phases of the TASCgrid utility and will be explained in greater detail in the appropriate sections.

Once the necessary information about the problem geometry has been specified, then *tascgridg* can be executed. The geometry for the problem is processed and the curve phase can begin.

Curve Phase (Tascgrigc)

The curve phase requires a curve definition file (*cdf*) that is used as input for *tascgridc*. The *cdf* file used for the bulkhead heat transfer calculation is called *bulkhead_9.cdf* and can be found in Appendix A. This file defines the number of nodes required in the computational domain under the heading "Grid Dimensions" in the *cdf* file and also distributes nodes along the edges of each element using the specified vertices form "Vertex Attachment". For the bulkhead heat transfer calculation, the computational domain consists of the following;

- Nodes in the x direction : *47*
- Nodes in the y direction: *9*
- Nodes in the z direction: *9*

The number of nodes used in the y and z directions, corresponding to the width and height, is the same throughout the computational domain for the fluid region and each layer of the bulkhead. The number of nodes used in the x direction for each element of the model is shown below.

- Nodes in fluid region length: *15*
- Nodes in insulation layer 1: *17*
- Nodes in steel/insulation layer: *15* (3 for steel, 12 for insulation)

The nodes in the fluid region are distributed at an expansion factor of 0.1, meaning that the nodes are spaced closer together as we move in the positive x direction. This is done to capture the large gradients that exist for temperature and density at the fluid/bulkhead interface. The expansion factor for all other elements in all three directions is unity, which denotes equal node spacing. The expansion factors for all node distributions are shown in *bulkhead_9.cdf*.

Surface Phase (Tascgrids)

The surface phase requires a surface definition file (*sdf*) that is used as input for *tascgrids*. The *sdf* file used for the bulkhead heat transfer calculation is called *bulkhead_9.sdf* and can be found in Appendix A. This file describes the surfaces that comprise the computational domain, distributes nodes along each surface, and defines the control volume for the problem.

Interior Phase (Tascgridi)

The interior phase requires an interior definition file (*idf*) that is used as input for *tascgridi*. The *idf* file for the bulkhead heat transfer calculation is called *bulkhead_9.idf* and can be found in Appendix A. This file defines the west south bottom and east north top corners of the computational domain and nodes are distributed to the interior regions. A number of iterations is sometimes required depending on the complexity of the geometry specified and a convergence criteria is established for the amount of error that can be allowed in the x,y, and z directions. The final grid file is generated with the proper geometry and nodal distributions.

Specification of Conjugate Heat Transfer Solid Objects

The individual layers of the bulkhead are specified using solid block-off regions in the *tascbob3d* utility and can be found in the *bulkhead_9.bcf*. These regions are

- Insulation layer 1: [16:32,1:9,1:9], CHT solid
- Steel: [32:35,1:9,1:9], CHT solid
- Insulation layer 2: [35:47,1:9,1:9], CHT solid

Boundary Conditions

After the grid file has been generated, the boundary conditions are specified for the bulkhead heat transfer calculation. The attributes, required in TASCflow, of the problem are shown below;

- Flow field solution is required
- Flow is incompressible
- Flow requires thermal energy equation solution
- Flow is turbulent
- Flow is non-reacting
- Flow does not include additional scalar transport equations
- Diffusion model for radiation active
- Flow does not include Lagrangian tracking
- The domain is stationary
- User specified profile boundary conditions are not read
- Transient boundary conditions are required

This bulkhead heat transfer calculation uses four types of boundary conditions; adiabatic walls, conjugate heat transfer solids, an inlet condition with a temperature profile that is a mathematical representation of the ISO 834 heating curve, and an outlet condition. The specifics of these boundary conditions are described in detail in the *bulkhead_9.bcf*, and are summarized in the following section.

Wall Boundary Condition

The wall is stationary, adiabatic, and has an emissivity of 0.8. The wall model used is a log-law assuming a smooth surface. This boundary condition is the default boundary condition for all unspecified regions.

CHT Exterior Boundary Condition

This condition treats the external surfaces of the CHT solids in the bulkhead as being adiabatic surfaces. The surface [47,1:9,1:9], the back face of the second insulation layer, has a specified heat flux of

$$q = \alpha\left(T_{wall} - T_{ref}\right)$$

where $\alpha = 7.8$, T_{wall} = temperature of the front of the bulkhead, $T_{ref} = 298K$.

Inlet Boundary Condition

The inlet condition used in this problem is a temperature specified in accordance to the ISO 834 heating curve shown below.

$$T = 750\left(1 - \exp\left[-3.79553\left(\frac{t}{3600}\right)^{0.5}\right]\right) + 170.41\left(\frac{t}{3600}\right)^{0.5} + 298$$

The velocity components for this inlet condition were U=0 m/s, V=0 m/s, and W = 5.0 m/s with turbulence conditions for the k-ε model of a turbulent intensity of 0.07 and an eddy length scale of 0.03. An emissivity of 0.8 was used for the bulkhead heat transfer calculation. For this study of the bulkhead, turbulent intensity values ranged from 0.05 to 0.09 and eddy length scales from 0.03 to 0.05. This boundary condition is applied to the bottom face of the fluid region, [1:15,1:9,1].

Outlet Boundary Condition

A constant static pressure condition of 101325 Pa is applied at the top face of the fluid region, [1:15,1:9,9], with an emissivity of 0.5.

Parameter File

The parameter file used for the bulkhead heat transfer calculation is called *bulkhead_9.prm* and can be found in Appendix A of this report. The *prm* file describes the various parameters and subroutines used in this simulation. An explanation of the essential features of this file is described in the section that follows.

absorption = 0.7 This is the absorption coefficient for the fluid (air).

bcinfo = t This sets the boundary condition information to true, so boundary conditons can be written to the output file for the flow field solution.

cvfld = 735. The specific heat at constant volume for the fluid (air).

cpfld = 1141.7 The specific heat at constant pressure for the fluid (air).

condfl = .06752 The thermal conductivity of the fluid (air).

ertime = .001 The target maximum residual for the flow field solution.

iskew = 2 The advection type for all transport equations except for the k-e turbulence model. Type 2 refers to a Mass Weighted Scheme that is more accurate than the Upwind Differencing Scheme (UDS) and is blended with 5% UDS for added robustness.

knttrn = 30 The transient information of the flow field solution is written to the results file after every 30 time steps.

kntime = 600 The maximum number of time steps, 600 in this case, used in the flow field solution.

kntlin = 6 The maximum number of iterations, 6 in this case, for each time step in the flow field solution.

kntrst = 10 The number of iterations before a complete restart file is written by the flow code, this is used if the computer solving the problem becomes unstable so the solution can be restarted from an intermediate solution.

lpac = t Sets the Physical Advection Correction to true for all transport equations except those for k and e, and is important for improving the accuracy of solutions with strong streamwise gradients and where total pressure is important.

poff = 101326. The pressure level shift for the solution.

pref = 101326. The reference pressure level for the solution.

rso_level = 0 The data written to the output file includes all restart and post-processing information.

rhofld = .3524 The density of the incompressible fluid (air).

sutherland = t Sets Sutherland's law to true for the calculation of thermal conductivity and molecular viscosity as given below;

$$CONDFL = \left(2.502x10^{-3}\right)T^{1.5}/(T+194.4)$$

$$VISCFL = \left(1.458x10^{-6}\right)T^{1.5}/(T+110.4)$$

trnw = t The control volume is transient and W velocity field is written to the restart file.

trnt = t The control volume is transient and the temperature field is written to the restart file.

transient_files = f Prevents transient information from being written at the end of each iteration because this has already been specified to occur every 30 time steps as a means of reducing file size in execution.

viscfl = 4.152e-5 The viscosity of the fluid (air).
dtime = 1 The size of each time step, one second in this case.
equation_of_state = t Uses the ideal gas law in the *propr.f* file.
density_insulation1 = 130. The density of the first layer of insulation.
density_insulation2 = 130. The density of the second layer of insulation.
density_steel = 7800. The density of steel.
cond_insulation1 = .2 The thermal conductivity of the first layer of insulation.
cond_insulation2 = .2 The thermal conductivity of the second layer of insulation.
cond_steel = 35. The thermal conductivity of the steel layer.
c_insulation1 = 880. The specific heat of the first insulation layer.
c_insulation2 = 880. The specific heat of the second layer of insulation.
c_steel = 530. The specific heat of the steel layer.
pref@[5,5,5] The node at which the reference pressure is set in the flow field.
write_properties = t Includes thermal property information in the output file.
mp1@[5,5,5] The location of monitor points used in the flow field of the transient solution.
mp2@[10,5,5]
mp6@[34,5,5]
mp7@[42,5,5]
!%tasctool_memory = -nr7m -ni7m -nc1m Comments on default memory configuration of the
!%tascbob3d_memory = -s1 various TASCflow utilities.
!%tascflow3d_memory = -ni2m -nr8m

FORTRAN Subroutines Used

Three FORTRAN subroutines were used in the examination of the bulkhead heat transfer calculation and the files *propt.f, propr.f,* and *bcdtrn.f* can be found in full text form in Appendix A. Each routine is summarized in the sections below.

Propt.f

Propt.f is a user-specified routine for calculating thermal properties. By default Sutherland's law is used, but for the thermal properties of the bulkhead materials used, data for various temperature ranges were specified according to Paul Spinn's MS thesis at Worcester Polytechnic Institute entitled "Semi-Empirical Heat Transfer Design Technique for Fiberous Insulation", 1996. The thermal properties calculated in this routine are the specific heat and thermal conductivity for the steel and insulation layers of the bulkhead within specified temperature values.

Propr.f

Propr.f is a routine that calculates the density of fluid and solid objects. The density of the solid objects remains the same in this case and the fluid density changes with temperature according to the Ideal Gas Law.

Bcdtrn.f

Bcdtrn.f is a routine that calculates user-specified boundary conditions, specifically the inlet temperature condition according to ISO 834 for this problem. This equation is shown in the Boundary Conditions section of this report.

Conclusions

A description of the Computational Fluid Dynamics modeling of a three-layer bulkhead subjected to a time-dependent temperature source has been given. The grid development,

boundary conditions, parameter file, and FORTRAN subroutines used in this process using the TASCflow general purpose fluid modeling package have been summarized and the full text of each associated file is included in Appendix A. The necessary information has been provided for modeling this problem using other flow codes, although it should be noted that differences may exist between TASCflow and other codes, so solutions to this problem may differ.

Appendix B -- TASCflow Files

Grid Development Files

- *bulkhead_9.gdf*
- *bulkhead_9.cdf*
- *bulkhead_9.sdf*
- *bulkhead_9.idf*

Boundary Condition File

- *bulkhead_9.bcf*

Parameter File

- *bulkhead_9.prm*

FORTRAN Subroutines

- *propt.f*
- *propr.f*
- *bcdtrn.f*

Bulkhead_9.gdf

VARIABLE DEFINITIONS

```
fluid_x = 0.750          !x dimension of fluid domain (length)
fluid_y = 0.600          !y dimension of fluid domain (width)
fluid_z = 0.600          !z dimension of fluid domain (height)
ins_x = 0.1              !thickness of insulation (total)
ins_y = 0.600            !width of modeled insulation section
ins_z = 0.600            !height of modeled insulation section
st_x = 0.033             !thickness of steel and insulation(total)
st_y = 0.600             !width of modeled steel/ins se ction
st_z = 0.600             !height of modeled steel /ins section

fluid_wsb_x = 0. !coordinates of west south bottom
fluid_wsb_y = 0. !corner of the fluid domain
fluid_wsb_z = 0.
ins_wsb_x = 0.75 !coordinates of west south bottom
ins_wsb_y = 0.           !corner of the insulation
ins_wsb_z = 0.
st_wsb_x = 0.85          !coordinates of west south bottom
st_wsb_y = 0.            !corner of the steel
st_wsb_z = 0.
```

POINT

```
fluid_wsb (fluid_wsb_x,fluid_wsb_y,fluid_wsb_z)
fluid_esb (fluid_wsb_x+fluid_x,fluid_wsb_y,fluid_wsb_z)
fluid_wst (fluid_wsb_x,fluid_wsb_y,fluid_wsb_z+fluid_z)
fluid_est (fluid_wsb_x+fluid_x,fluid_wsb_y,fluid_wsb_z+fluid_z)
fluid_wnb (fluid_wsb_x,fluid_wsb_y+fluid_y,fluid_wsb_z)
fluid_enb (fluid_wsb_x+fluid_x,fluid_wsb_y+fluid_y,fluid_wsb_z)
fluid_wnt (fluid_wsb_x,fluid_wsb_y+fluid_y,fluid_wsb_z+fluid_z)
fluid_ent (fluid_wsb_x+fluid_x,fluid_wsb_y+fluid_y,fluid_wsb_z+fluid_z)

ins_esb (ins_wsb_x+ins_x,ins_wsb_y,ins_wsb_z)
ins_est (ins_wsb_x+ins_x,ins_wsb_y,ins_wsb_z+ins_z)
ins_enb (ins_wsb_x+ins_x,ins_wsb_y+ins_y,ins_wsb_z)
ins_ent (ins_wsb_x+ins_x,ins_wsb_y+ins_y,ins_wsb_z+ins_z)

st_esb (st_wsb_x+st_x,st_wsb_y,st_wsb_z)
st_est (st_wsb_x+st_x,st_wsb_y,st_wsb_z+st_z)
st_enb (st_wsb_x+st_x,st_wsb_y+st_y,st_wsb_z)
st_ent (st_wsb_x+st_x,st_wsb_y+st_y,st_wsb_z+st_z)

Curve cv_sb Linear
fluid_wsb; fluid_esb; ins_esb; st_esb

Curve cv_nb Linear
fluid_wnb; fluid_enb; ins_enb; st_enb

Curve cv_st Linear
fluid_wst; fluid_est; ins_est; st_est

Curve cv_nt Linear
fluid_wnt; fluid_ent; ins_ent; st_ent
```

```
Curve fluid_wb Linear
fluid_wsb; fluid_wnb

Curve fluid_eb Linear
fluid_esb; fluid_enb

Curve fluid_wt Linear
fluid_wst; fluid_wnt

Curve fluid_et Linear
fluid_est; fluid_ent

Curve fluid_ws Linear
fluid_wsb; fluid_wst

Curve fluid_es Linear
fluid_esb; fluid_est

Curve fluid_wn Linear
fluid_wnb; fluid_wnt

Curve fluid_en Linear
fluid_enb; fluid_ent

Curve ins_eb Linear
ins_esb; ins_enb

Curve ins_et Linear
ins_est; ins_ent

Curve ins_es Linear
ins_esb; ins_est

Curve ins_en Linear
ins_enb; ins_ent

Curve st_eb Linear
st_esb; st_enb

Curve st_et Linear
st_est; st_ent

Curve st_es Linear
st_esb; st_est

Curve st_en Linear
st_enb; st_ent

! South surface of CV
Surface cv_S By Curves Bilinear
cv_sb; st_es; -cv_st; -fluid_ws

! North surface of CV
Surface cv_N By Curves Bilinear
cv_nb; st_en; -cv_nt; -fluid_wn
```

```
! Bottom surface of CV
Surface cv_B By Curves Bilinear
cv_sb; st_eb; -cv_nb; -fluid_wb

! Top surface of CV
Surface cv_T By Curves Bilinear
cv_st; st_et; -cv_nt; -fluid_wt

! West surface of CV
Surface cv_W By Curves Bilinear
fluid_wb; fluid_wn; -fluid_wt; -fluid_ws

! East surface of CV
Surface cv_E By Curves Bilinear
st_eb; st_en; -st_et; -st_es
```

Bulkhead_9.cdf

```
Grid Dimensions
ID= 47
JD= 9
KD= 9
---------------------------------------------------------------------------
Variable Definitions
---------------------------------------------------------------------------
Vertex Attachments
! vertex  ( I, J, K)
fluid_wsb      (1,1,1)   ! Vertex # 1    cv_sb@p#1     fluid_wb@p#1
                         ! fluid_ws@p#1                cv_s@st=(0,0)
                         ! cv_b@st=(0,0)               cv_w@st=(0,0)
fluid_esb      (15,1,1)  ! Vertex # 2    cv_sb@p#2     fluid_eb@p#1
                         ! fluid_es@p#1
ins_esb        (32,1,1)  ! Vertex # 3    cv_sb@p#3     ins_eb@p#1
                         ! ins_es@p#1
st_esb         (ID,1,1)  ! Vertex # 4    cv_sb@p#4     st_eb@p#1
                         ! st_es@p#1     cv_s@st=(1,0)
                         ! cv_b@st=(1,0)               cv_e@st=(0,0)
fluid_wnb      (1,JD,1)  ! Vertex # 5    cv_nb@p#1     fluid_wb@p#2
                         ! fluid_wn@p#1                cv_n@st=(0,0)
                         ! cv_b@st=(0,1)               cv_w@st=(1,0)
fluid_enb      (15,JD,1) ! Vertex # 6    cv_nb@p#2     fluid_eb@p#2
                         ! fluid_en@p#1
ins_enb        (32,JD,1) ! Vertex # 7    cv_nb@p#3     ins_eb@p#2
                         ! ins_en@p#1
st_enb         (ID,JD,1) ! Vertex # 8    cv_nb@p#4     st_eb@p#2
                         ! st_en@p#1     cv_n@st=(1,0)
                         ! cv_b@st=(1,1)               cv_e@st=(1,0)
fluid_wst      (1,1,KD)  ! Vertex # 9    cv_st@p#1     fluid_wt@p#1
                         ! fluid_ws@p#2                cv_s@st=(0,1)
                         ! cv_t@st=(0,0)               cv_w@st=(0,1)
fluid_est      (15,1,KD) ! Vertex # 10   cv_st@p#2     fluid_et@p#1
                         ! fluid_es@p#2
ins_est        (32,1,KD) ! Vertex # 11   cv_st@p#3     ins_et@p#1
                         ! ins_es@p#2
st_est         (ID,1,KD) ! Vertex # 12   cv_st@p#4     st_et@p#1
                         ! st_es@p#2     cv_s@st=(1,1)
                         ! cv_t@st=(1,0)               cv_e@st=(0,1)
fluid_wnt      (1,JD,KD) ! Vertex # 13   cv_nt@p#1     fluid_wt@p#2
                         ! fluid_wn@p#2                cv_n@st=(0,1)
                         ! cv_t@st=(0,1)               cv_w@st=(1,1)
fluid_ent      (15,JD,KD) ! Vertex # 14  cv_nt@p#2     fluid_et@p#2
                         ! fluid_en@p#2
ins_ent        (32,JD,KD) ! Vertex # 15  cv_nt@p#3     ins_et@p#2
                         ! ins_en@p#2
st_ent         (ID,JD,KD) ! Vertex # 16  cv_nt@p#4     st_et@p#2
                         ! st_en@p#2     cv_n@st=(1,1)
                         ! cv_t@st=(1,1)               cv_e@st=(1,1)
---------------------------------------------------------------------------
Node Distributions
Default=1
! start-vertex  end-vertex  expansion-factors  ! curve label
```

```
fluid_wsb     fluid_esb     100 @ r .1  ! cv_sb
fluid_esb     ins_esb       100 @ 1     ! cv_sb
ins_esb       st_esb        100 @ 1     ! cv_sb
fluid_wnb     fluid_enb     100 @ r .1  ! cv_nb
fluid_enb     ins_enb       100 @ 1     ! cv_nb
ins_enb       st_enb        100 @ 1     ! cv_nb
fluid_wst     fluid_est     100 @ r .1  ! cv_st
fluid_est     ins_est       100 @ 1     ! cv_st
ins_est       st_est        100 @ 1     ! cv_st
fluid_wnt     fluid_ent     100 @ r .1  ! cv_nt
fluid_ent     ins_ent       100 @ 1     ! cv_nt
ins_ent       st_ent        100 @ 1     ! cv_nt
fluid_wsb     fluid_wnb     100 @ 1     ! fluid_wb
fluid_esb     fluid_enb     100 @ 1     ! fluid_eb
fluid_wst     fluid_wnt     100 @ 1     ! fluid_wt
fluid_est     fluid_ent     100 @ 1     ! fluid_et
fluid_wsb     fluid_wst     100 @ 1     ! fluid_ws
fluid_esb     fluid_est     100 @ 1     ! fluid_es
fluid_wnb     fluid_wnt     100 @ 1     ! fluid_wn
fluid_enb     fluid_ent     100 @ 1     ! fluid_en
ins_esb       ins_enb       100 @ 1     ! ins_eb
ins_est       ins_ent       100 @ 1     ! ins_et
ins_esb       ins_est       100 @ 1     ! ins_es
ins_enb       ins_ent       100 @ 1     ! ins_en
st_esb        st_enb        100 @ 1     ! st_eb
st_est        st_ent        100 @ 1     ! st_et
st_esb        st_est        100 @ 1     ! st_es
st_enb        st_ent        100 @ 1     ! st_en
```

Bulkhead_9.sdf

Region cv_s

Region cv_n

Region cv_b

Region cv_t

Region cv_w

Region cv_e

Bulkhead_9.idf

```
!
! bulkhead problem #4: N.B. Wittasek
! IDF file
!
! General Motors

Region bulk elliptic
errxyz=4e-7
itmax=320
fluid_wsb, st_ent
```

Bulkhead_9.bcf

```
BOB3D_BCF
1
Embedding/attaching, block-off and b.c.'s from version 2.6-2 of TASCbob3D.
$$$GLS

 The computational domain consists of the following grid(s):
  1) [1:47,1:9,1:9]:MAIN
$$$GLE
$$$FLS
=-=-=-=-=-=-=-=-=-=-=-=-=-=-=-=-=-=-=-=-=-=-=-=-=-=-=-=-=-=-=-=-=-=-=-=-=-=-=-=-
 CONJUGATE HEAT TRANSFER SOLID object: "INSULATION1"

 Object includes regions:
  [16:32,1:9,1:9]

 These regions currently include the following block segments:
  [16:32,1:9,1:9]
=-=-=-=-=-=-=-=-=-=-=-=-=-=-=-=-=-=-=-=-=-=-=-=-=-=-=-=-=-=-=-=-=-=-=-=-=-=-=-=-
=-=-=-=-=-=-=-=-=-=-=-=-=-=-=-=-=-=-=-=-=-=-=-=-=-=-=-=-=-=-=-=-=-=-=-=-=-=-=-=-
 CONJUGATE HEAT TRANSFER SOLID object: "STEEL"

 Object includes regions:
  [32:35,1:9,1:9]

 These regions currently include the following block segments:
  [32:35,1:9,1:9]
=-=-=-=-=-=-=-=-=-=-=-=-=-=-=-=-=-=-=-=-=-=-=-=-=-=-=-=-=-=-=-=-=-=-=-=-=-=-=-=-
=-=-=-=-=-=-=-=-=-=-=-=-=-=-=-=-=-=-=-=-=-=-=-=-=-=-=-=-=-=-=-=-=-=-=-=-=-=-=-=-
 CONJUGATE HEAT TRANSFER SOLID object: "INSULATION2"

 Object includes regions:
  [35:47,1:9,1:9]

 These regions currently include the following block segments:
  [35:47,1:9,1:9]
=-=-=-=-=-=-=-=-=-=-=-=-=-=-=-=-=-=-=-=-=-=-=-=-=-=-=-=-=-=-=-=-=-=-=-=-=-=-=-=-
$$$FLE
$$$ATS

 The following grid/flow attributes have been specified:
   Flow field solution required.
   Flow requires energy equation solution.
   Flow is turbulent.
   All turbulent walls use the SAME wall treatment.
   Turbulent wall treatment: log-law.
   Flow is non-reacting.
   Flow does not include other scalar transport eqn's
   Non-participating thermal radiation not active.
   Diffusion model for radiation active.
   Moving walls exist.
   Overlap boundary condition attachment permitted.
   Do not read in profile boundary file (PRO).
   Transient boundary conditions required.
```

```
   Internal objects exist.
   Conjugate heat transfer objects present.
   Conduction heat transfer surfaces present.
$$$ATE
$$$PRM
fluids = t  ! Solve hydrodynamics
tmptre = t  ! Solve energy eqn
turbmd = t  ! Turbulence model on
trnbcs = t  ! Transient BCs
difrad = t  ! Diffusion model for radiation
$$$PRE
$$$BLS

Total number of specified boundary conditions =     5

=-=-=-=-=-=-=-=-=-=-=-=-=-=-=-=-=-=-=-=-=-=-=-=-=-=-=-=-=-=-=-=-=-=-=-=-
Boundary condition # 1 : WALL BOUNDARY.
FLUIDS     : Stationary wall
KINETIC E. : Wall
DISSIP.    : Wall
THERMAL    : Adiabatic wall

        Note: A Conjugate Heat Transfer interface condition will be
        applied to any face(s) referenced by this b.c. that are on
        the surface of a CHT solid object.

TR4-EQ     : Specified emissivity = 8.00000E-01
WALL MODEL : Log-law, smooth wall.

Attached to regions:
Default boundary condition
=-=-=-=-=-=-=-=-=-=-=-=-=-=-=-=-=-=-=-=-=-=-=-=-=-=-=-=-=-=-=-=-=-=-=-=-


=-=-=-=-=-=-=-=-=-=-=-=-=-=-=-=-=-=-=-=-=-=-=-=-=-=-=-=-=-=-=-=-=-=-=-=-
Boundary condition # 2 : CHT EXTERIOR BOUNDARY.
THERMAL    : Adiabatic wall

Attached to regions:
Default boundary condition
=-=-=-=-=-=-=-=-=-=-=-=-=-=-=-=-=-=-=-=-=-=-=-=-=-=-=-=-=-=-=-=-=-=-=-=-


=-=-=-=-=-=-=-=-=-=-=-=-=-=-=-=-=-=-=-=-=-=-=-=-=-=-=-=-=-=-=-=-=-=-=-=-
Boundary condition # 3 : CHT EXTERIOR BOUNDARY.
THERMAL    : Heat flux = Alfa * (T_wall - T_ref).
          Alfa=  7.80000D+00, T_ref=  2.98000D+02

Attached to regions:
 [47,1:9,1:9]

These regions currently include the following faces:
 [47,1:9,1:9]
=-=-=-=-=-=-=-=-=-=-=-=-=-=-=-=-=-=-=-=-=-=-=-=-=-=-=-=-=-=-=-=-=-=-=-=-
```

```
Boundary condition # 4 : INFLOW BOUNDARY.
FLUIDS    : U,V,W specified  U= 0.00000E+00 V= 0.00000E+00 W= 5.00000E+00
KINETIC E. : Inlet, TKE = 3/2(Tu*V)^2, turbulence intensity Tu= 7.0000E-02.
DISSIP.   : Inlet, EPS = (TKE^1.5)/L, eddy length scale L= 3.0000E-02.
THERMAL   : Transient inlet, user supplied.
        Scalar T=transient, "KEY"= 100
        User is supplying time function information
        via routine "BCDTRN". The value of "KEY" for this B.C.
        has been set by the user.
TR4-EQ    : Specified emissivity = 8.00000E-01

Attached to regions:
 [1:15,1:9,1]

These regions currently include the following faces:
 [1:15,1:9,1]
```

```
Boundary condition # 5 : OUTFLOW BOUNDARY.
FLUIDS    : Static pressure set, constant over the outlet, P= 1.013250E+05.
KINETIC E. : Outlet.
DISSIP.   : Outlet.
THERMAL   : Outlet.
TR4-EQ    : Specified emissivity = 5.00000E-01

Attached to regions:
 [1:15,1:9,9]

These regions currently include the following faces:
 [1:15,1:9,9]
```

```
$$$BLE
$$$BRS
$$$BOY
  3
INSULATION1                    2
 0.0000000E+00  1.0000000E+00  0.0000000E+00  0.0000000E+00  0.0000000E+00
      1
[16:32,1:9,1:9]
STEEL                     2
 0.0000000E+00  1.0000000E+00  0.0000000E+00  0.0000000E+00  0.0000000E+00
      1
[32:35,1:9,1:9]
INSULATION2                    2
 0.0000000E+00  1.0000000E+00  0.0000000E+00  0.0000000E+00  0.0000000E+00
      1
[35:47,1:9,1:9]
$$$CGR
  1
MAIN
$$$BCY
 30
```

```
T T T T F F T F T F F T F F T T T F F F F T F F F F F F F
  5
 Boundary condition #   1
   1       T
 Equation #   1
  3  11   7
 1  0  0
0.0000000E+00 0.0000000E+00 0.0000000E+00 0.0000000E+00
0.0000000E+00 0.0000000E+00 0.0000000E+00 0.0000000E+00
0.0000000E+00 0.0000000E+00 0.0000000E+00
 Equation #   2
  2   0   3
 0  2
 Equation #   3
  0   0   5
 Equation #   4
  0   0   5
 Equation #   5
  0   1   7
0.0000000E+00
 Equation #   6
  3   2   1
 3  1  1
4.1000000E-01  5.1999998E+00
 Equation #   7
  1   1   15
 1
8.0000001E-01
 Object/strip info
  0
  0
 Boundary condition #   2
   7       T
 Equation #   1
  0   0   0
 Equation #   2
  0   0   0
 Equation #   3
  0   0   0
 Equation #   4
  0   0   0
 Equation #   5
  0   1   7
0.0000000E+00
 Equation #   6
  0   0   0
 Equation #   7
  0   0   0
 Object/strip info
  0
  0
 Boundary condition #   3
   7       F
 Equation #   1
  0   0   0
Equation #   2
```

```
  0   0   0
 Equation #   3
  0   0   0
 Equation #   4
  0   0   0
 Equation #   5
  0   2  11
 7.8000002E+00  2.9800000E+02
 Equation #   6
  0   0   0
 Equation #   7
  0   0   0
 Object/strip info
  0
  1
 [47,1:9,1:9]
 Boundary condition #   4
   2       F
 Equation #   1
  1   3   1
 1
 0.0000000E+00  0.0000000E+00  5.0000000E+00
 Equation #   2
  2   0   2
 0  2
 Equation #   3
  1   1   8
 2
 7.0000008E-02
 Equation #   4
  1   1   8
 2
 2.9999999E-02
 Equation #   5
  2   1  13
 2 100
 0.0000000E+00
 Equation #   6
  0   0   0
 Equation #   7
  1   1  15
 1
 8.0000001E-01
 Object/strip info
  0
  1
 [1:15,1:9,1]
 Boundary condition #   5
  3       F
 Equation #   1
 11  10  14
 1  2  0  0  0
 0  0  0  0  0
 0
 1.0132500E+05  0.0000000E+00  0.0000000E+00  0.0000000E+00
 0.0000000E+00  0.0000000E+00  0.0000000E+00  0.0000000E+00
```

```
 0.0000000E+00 0.0000000E+00
 Equation #   2
   2   0   2
  0  2
 Equation #   3
   5   0   3
  1  4  0  0  0
 Equation #   4
   5   0   3
  1  4  0  0  0
 Equation #   5
   0   0  12
 Equation #   6
   0   0   0
 Equation #   7
   1   1  15
  1
 5.0000000E-01
 Object/strip info
   0
   1
 [1:15,1:9,9]
0892 : Profile boundary condition usage information
  60
   1 F F F F F F F F F F F F F  F F F F F F F F F F F F F F F F F
 F F F F F F F F  F F F F F F F F F F F F F F F  F F F F F F F

   2 F F F F F F F F F F F F F  F F F F F F F F F F F F F F F F F
 F F F F F F F F  F F F F F F F F F F F F F F F  F F F F F F F

   3 F F F F F F F F F F F F F  F F F F F F F F F F F F F F F F F
 F F F F F F F F  F F F F F F F F F F F F F F F  F F F F F F F

   4 F F F F F F F F F F F F F  F F F F F F F F F F F F F F F F F
 F F F F F F F F  F F F F F F F F F F F F F F F  F F F F F F F

   5 F F F F F F F F F F F F F  F F F F F F F F F F F F F F F F F
 F F F F F F F F  F F F F F F F F F F F F F F F  F F F F F F F

   0
$$$BRE
$$$OBJ
   3  21
INSULATION1                    2   1   1
  16   1   1  31   8   8   0.000   1.000   0.000   0.000   0.000
STEEL                        2   8   1
  32   1   1  34   8   8   0.000   1.000   0.000   0.000   0.000
INSULATION2                    2  15   1
  35   1   1  46   8   8   0.000   1.000   0.000   0.000   0.000
```

Bulkhead_9.prm

```
absorption = 0.7
bcinfo = t
cvfld = 735.
cpfld = 1141.7
condfl = .06752
ertime = .001
iskew = 2
knttrn = 30
kntime = 600
kntlin = 6
kntrst = 10
lpac = t
poff = 101326.
pref = 101326.
rso_level = 0
rhofld = .3524
sutherland = t
trnw = t
trnt = t
transient_files = f
viscfl = 4.152e-5
dtime = 1
equation_of_state = t
density_insulation1 = 130.
density_insulation2 = 130.
density_steel = 7800.
cond_insulation1 = .2
cond_insulation2 = .2
cond_steel = 35.
c_insulation1 = 880.
c_insulation2 = 880.
c_steel = 530.
pref@[5,5,5]
write_properties = t
mp1@[5,5,5]
mp2@[10,5,5]
mp6@[34,5,5]
mp7@[42,5,5]
!%tasctool_memory = -nr7m  -ni7m -nc1m
!%tascbob3d_memory = -s1
!%tascflow3d_memory = -ni2m -nr8m
```

Propt.f

```
C
C
C
C=======================================================================
C
      SUBROUTINE PROPT(CONDL,CPHEAT,CVHEAT,
     &                 U,V,W,P,T,PHI,NPHI,XYZ,
     &                 ILABEL,LABEL,I,J,K,ID,JD,KD)
C
CSCDT Calculates thermal properties of the fluid/solid.
C
CSCDB
C  PROPT is a user specified routine that calculates thermal
C  properties of the fluid/solid.
C
C  Input:
C
C    ILABEL = 0  fluid
C           > 0  MCF component index
C           < 0  solid CHT object with label given by 'LABEL'
C     LABEL : character string identifying equation solved
C     U,V,W : Cartesian velocity components
C         P : static pressure
C         T : static temperature
C       PHI : additional scalars
C      NPHI : number of additional scalars
C       XYZ : Cartesian coordinates of grid nodes
C     I,J,K : topological grid coordinates
C  ID,JD,KD : topological grid dimensions
C
C  Output:
C
C     CONDL : local thermal conductivity
C    CPHEAT : specific heat at constant pressure
C    CVHEAT : specific heat at constant volume
C
C  Local:
C
C    MAXMCF : work space parameter for multi-component fluids
C      POFF : pressure offset (level shift)
C      TOFF : temperature offset (level shift)
C     CONDFL : fluid conductivity
C     CONDSL : solid conductivity
C      CPFLD : fluid specific heat at constant pressure
C      CVFLD : fluid specific heat at constant volume
C      CCSOL : solid specific heat
C     SUTHER : logical variable indicating whether or not to use
C              Sutherland's law
C
C  Common Blocks:
C
C  /CONTRL/ is declared so that information can be added as needed
C          for desired equation of state.
```

```
C
C    IONUM  : integer, unit numbers in CONTRL common block.
C    IARR   : integer, integer switches in CONTRL common block.
C    RARR   : real, real constants in CONTRL common block.
C    CONST  : real, property constants in CONTRL common block.
C    LARR   : logical, logical switches in CONTRL common block.
C
C /MULTIF/ contains information for multicomponent fluids.
C
C    DENSQ  : real, component density.
C    ZMOLQ  : real, component molecular weight.
C    CONDQ  : real, component conductivity.
C    CPHTQ  : real, component specific heat at constant pressure.
C    CVHTQ  : real, component specific heat at constant volume.
C    LMCFQ  : logical, multi-component fluid.
C    EQSTQ  : logical, equation of state.
C    NMCF   : integer, number of components.
C    NMCFNA : integer, maximum scalar which is a multi-component fluid.
C
C  NOTE: The true levels of pressure (P) and temperature (T) are
C        assumed to be
C          P_true = P + POFF
C          T_true = T + TOFF
C        where POFF and TOFF are level shifts in the actual dependent
C        values of P and T that are solved for.
CSCDE
C
C=======================================================================
C
C-----------------------------
C Subroutine Arguments
C-----------------------------
C
      INTEGER NPHI,I,J,K,ID,JD,KD,ILABEL
C
      REAL U(ID,JD,KD),V(ID,JD,KD),W(ID,JD,KD),P(ID,JD,KD),T(ID,JD,KD),
     &     PHI(ID,JD,KD,*),XYZ(ID,JD,KD,3),CONDL,CPHEAT,CVHEAT
C
      CHARACTER*(*) LABEL
C
C-----------------------------
C Local Variables
C-----------------------------
C
      INTEGER MAXMCF
      PARAMETER (MAXMCF = 100)
C
      REAL CONDFL,CPFLD,CVFLD,CONDSL,CCSOL,POFF,TOFF,XVAL
C
      LOGICAL SUTHER
C
C-----------------------------
C Common Blocks
C-----------------------------
C
      COMMON/CONTRL/ IONUM(100),IARR(200),RARR(100),CONST(100),LARR(200)
```

```
      INTEGER IONUM,IARR
      REAL RARR,CONST
      LOGICAL LARR
C
      EQUIVALENCE (CONST(3),CONDFL),(CONST(11),CPFLD),(CONST(12),CVFLD),
     &          (CONST(29),CONDSL),(CONST(30),CCSOL),
     &          (CONST(13),POFF),(CONST(14),TOFF),(LARR(83),SUTHER)
C
      COMMON /MULTIF/ DENSQ(MAXMCF),ZMOLQ(MAXMCF),
     &             CONDQ(MAXMCF),CPHTQ(MAXMCF),CVHTQ(MAXMCF),
     &             LMCFQ(MAXMCF),EQSTQ(MAXMCF),NMCF,NMCFNA
      INTEGER NMCF,NMCFNA
      REAL DENSQ,ZMOLQ,CONDQ,CPHTQ,CVHTQ
      LOGICAL LMCFQ,EQSTQ
C
C --- Property data block
C
      PARAMETER (RGAS=8.3143)
C
      REAL CPCH4(5,2), CPO2(5,2), CPH2O(5,2), CPCO2(5,2), CPCH2O(5,2),
     &    CPN2(5,2), tmpcp1, tmpcp2, tmpcv1, tmpcv2,
     &    tmpk1, tmpk2
C
C-------------------------------
C Executable Statements
C-------------------------------
      TT = T(I,J,K) + TOFF
      XVAL = XYZ(I,J,K,1)
C
C     WRITE(6,*) 'check equation',i,j,k,xval,ilabel
C
C------ SINGLE-COMPONENT FLUID

      IF (ILABEL.EQ.0) THEN

C------ USE SUTHERLAND'S LAW FOR THERMAL CONDUCTIVITY -----
C

          IF (SUTHER) THEN
           CONDL  = 2.502E-3*(TT)**1.5/(TT+194.4)
          ELSE
          CONDL = CONDFL
          ENDIF
C
          CPHEAT = CPFLD
          CVHEAT = CVFLD
C
C------ MULTI-COMPONENT FLUID COMPONENT
C
          ELSE IF (ILABEL.GT.0) THEN
C       WRITE(6,*) 'ilabel > 0'
C       CPHEAT = RGAS / WM(ILABEL)
C
C       Units on CPHEAT are j/kg K
C
C---- USE SOLID DEFAULT THERMAL PROPERTIES
```

```
C
      ELSE IF (ILABEL.LT.0) THEN
C     WRITE(6,*) 'CHT (ilabel < 0)'
C
C     This is the CHT solid
C
                  IF((XVAL.GE. .75).AND.(XVAL.LT. .85)) THEN
C
C     WRITE(6,*) 'HERE WE ARE',XVAL
C The following information for thermal properties was taken from
C Paul Spinn's Thesis.  It represents the TASEF-2 values.
C
C-------------------------------------------------------
C---- TABULAR DATA FOR INSULATION THERMAL CONDUCTIVITY ----
C-------------------------------------------------------
         H2HEAT = CCSOL
C     WRITE (6,*)'Insulation k at ',XVAL,' at temp ',TT,' is ',CONDL
                  IF((TT.GE.273.).AND.(TT.LT.373.)) THEN
                   CONDL = .13
                  ELSEIF((TT.GE.373.).AND.(TT.LT.473.))THEN
                   CONDL = .15
                  ELSEIF((TT.GE.473.).AND.(TT.LT.573.))THEN
                   CONDL = .19
                  ELSEIF((TT.GE.573.).AND.(TT.LT.673.))THEN
                   CONDL = .22
                  ELSEIF((TT.GE.673.).AND.(TT.LT.773.))THEN
                   CONDL = .27
                  ELSEIF((TT.GE.773.).AND.(TT.LT.873.))THEN
                   CONDL = .33
                  ELSEIF((TT.GE.873.).AND.(TT.LT.973.))THEN
                   CONDL = .5
                  ELSEIF((TT.GE.973.).AND.(TT.LT.1073.))THEN
                   CONDL = .7
                  ELSEIF((TT.GE.1073.).AND.(TT.LT.1173.))THEN
                   CONDL = .86
                  ELSEIF((TT.GE.1173.).AND.(TT.LT.1273.))THEN
                   CONDL = 1.02
                  ELSEIF(TT.GE.1273.)THEN
                   CONDL = 1.05
                  ENDIF
C-------------------------------------------------------
C---- TABULAR DATA FOR INSULATION SPECIFIC HEAT ----------
C-------------------------------------------------------
C        WRITE(6,*)'Insulation Cp at ',XVAL,' at temp ',TT,' is ', CVHEAT
          IF((TT.GE.273.).AND.(TT.LT.100.)) THEN
                   CVHEAT  = 700.
                  ELSEIF((TT.GE.373.).AND.(TT.LT.473.))THEN
                   CVHEAT = 770.
                  ELSEIF((TT.GE.473.).AND.(TT.LT.573.))THEN
                   CVHEAT = 780.
                  ELSEIF((TT.GE.573.).AND.(TT.LT.673.))THEN
                   CVHEAT = 780.
                  ELSEIF((TT.GE.673.).AND.(TT.LT.773.))THEN
                   CVHEAT = 780.
                  ELSEIF((TT.GE.773.).AND.(TT.LT.873.))THEN
                   CVHEAT = 810.
```

```
                ELSEIF((TT.GE.873.).AND.(TT.LT.973.))THEN
                 CVHEAT = 880.
                ELSEIF((TT.GE.973.).AND.(TT.LT.1073.))THEN
                 CVHEAT = 900.
                ELSEIF((TT.GE.1073.).AND.(TT.LT.1173.))THEN
                 CVHEAT = 910.
                ELSEIF((TT.GE.1173.).AND.(TT.LT.1273.))THEN
                 CVHEAT = 1090.
                ELSEIF(TT.GE.1273.)THEN
                 CVHEAT = 1350.
                ENDIF
C
        ELSE IF ((XVAL.GE. .85).AND.(XVAL.LT. .856)) THEN
C
C-------------------------------------------------------
C---- TABULAR DATA FOR STEEL THERMAL CONDUCTIVITY ----
C-------------------------------------------------------
C       WRITE (6,*)'Steel k at ',XVAL,' at temp ',TT,' is ',CONDL
      H2HEAT = CCSOL
                IF((TT.GE.273.).AND.(TT.LT.373.)) THEN
                 CONDL  = 60.
                ELSEIF((TT.GE.373.).AND.(TT.LT.473.))THEN
                 CONDL = 57.
                ELSEIF((TT.GE.473.).AND.(TT.LT.573.))THEN
                 CONDL = 53.
                ELSEIF((TT.GE.573.).AND.(TT.LT.673.))THEN
                 CONDL = 48.
                ELSEIF((TT.GE.673.).AND.(TT.LT.773.))THEN
                 CONDL = 44.
                ELSEIF((TT.GE.773.).AND.(TT.LT.873.))THEN
                 CONDL = 39.
                ELSEIF((TT.GE.873.).AND.(TT.LT.973.))THEN
                 CONDL = 35.
                ELSEIF((TT.GE.973.).AND.(TT.LT.1073.))THEN
                 CONDL = 30.
                ELSEIF((TT.GE.1073.).AND.(TT.LT.1173.))THEN
                 CONDL = 28.
                ELSEIF((TT.GE.1173.).AND.(TT.LT.1273.))THEN
                 CONDL = 27.
                ELSEIF(TT.GE.1273.)THEN
                 CONDL = 27.
                ENDIF
C-------------------------------------------------------
C---- TABULAR DATA FOR STEEL SPECIFIC HEAT -----------
C-------------------------------------------------------
C       WRITE(6,*)'Steel Cp at ',XVAL,' at temp ',TT,' is ',CVHEAT
         IF((TT.GE.273.).AND.(TT.LT.373.)) THEN
                 CVHEAT  = 380.
                ELSEIF((TT.GE.373.).AND.(TT.LT.473.))THEN
                 CVHEAT = 380.
                ELSEIF((TT.GE.473.).AND.(TT.LT.573.))THEN
                 CVHEAT = 385.
                ELSEIF((TT.GE.573.).AND.(TT.LT.673.))THEN
                 CVHEAT = 460.
                ELSEIF((TT.GE.673.).AND.(TT.LT.773.))THEN
                 CVHEAT = 470.
```

```
                ELSEIF((TT.GE.773.).AND.(TT.LT.873.))THEN
                 CVHEAT = 505.
                ELSEIF((TT.GE.873.).AND.(TT.LT.973.))THEN
                 CVHEAT = 530.
                ELSEIF((TT.GE.973.).AND.(TT.LT.1073.))THEN
                 CVHEAT = 585.
                ELSEIF((TT.GE.1073.).AND.(TT.LT.1173.))THEN
                 CVHEAT = 675.
                ELSEIF((TT.GE.1173.).AND.(TT.LT.1273.))THEN
                 CVHEAT = 670.
                ELSEIF(TT.GE.1273.)THEN
                 CVHEAT = 670.
                ENDIF
C
        ELSE IF ((XVAL.GE. .856).AND.(XVAL.LE. .886)) THEN
C-------------------------------------------------------
C---- TABULAR DATA FOR INSULATION THERMAL CONDUCTIVITY ----
C-------------------------------------------------------
         H2HEAT = CCSOL
C       WRITE (6,*)'Insulation k at ',XVAL,' at temp ',TT,' is ',CONDL
                IF((TT.GE.273.).AND.(TT.LT.373.)) THEN
                 CONDL = .13
                ELSEIF((TT.GE.373.).AND.(TT.LT.473.))THEN
                 CONDL = .15
                ELSEIF((TT.GE.473.).AND.(TT.LT.573.))THEN
                 CONDL = .19
                ELSEIF((TT.GE.573.).AND.(TT.LT.673.))THEN
                 CONDL = .22
                ELSEIF((TT.GE.673.).AND.(TT.LT.773.))THEN
                 CONDL = .27
                ELSEIF((TT.GE.773.).AND.(TT.LT.873.))THEN
                 CONDL = .33
                ELSEIF((TT.GE.873.).AND.(TT.LT.973.))THEN
                 CONDL = .5
                ELSEIF((TT.GE.973.).AND.(TT.LT.1073.))THEN
                 CONDL = .7
                ELSEIF((TT.GE.1073.).AND.(TT.LT.1173.))THEN
                 CONDL = .86
                ELSEIF((TT.GE.1173.).AND.(TT.LT.1273.))THEN
                 CONDL = 1.02
                ELSEIF(TT.GE.1273.)THEN
                 CONDL = 1.05
                ENDIF
C-------------------------------------------------------
C---- TABULAR DATA FOR INSULATION SPECIFIC HEAT ----------
C-------------------------------------------------------
C         WRITE(6,*)'Insulation Cp at ',XVAL,' at temp ',TT,' is ', CVHEAT
          IF((TT.GE.273.).AND.(TT.LT.100.)) THEN
                 CVHEAT  = 700.
                ELSEIF((TT.GE.373.).AND.(TT.LT.473.))THEN
                 CVHEAT = 770.
                ELSEIF((TT.GE.473.).AND.(TT.LT.573.))THEN
                 CVHEAT = 780.
                ELSEIF((TT.GE.573.).AND.(TT.LT.673.))THEN
                 CVHEAT = 780.
                ELSEIF((TT.GE.673.).AND.(TT.LT.773.))THEN
```

```
                CVHEAT = 780.
               ELSEIF((TT.GE.773.).AND.(TT.LT.873.))THEN
                CVHEAT = 810.
               ELSEIF((TT.GE.873.).AND.(TT.LT.973.))THEN
                CVHEAT = 880.
               ELSEIF((TT.GE.973.).AND.(TT.LT.1073.))THEN
                CVHEAT = 900.
               ELSEIF((TT.GE.1073.).AND.(TT.LT.1173.))THEN
                CVHEAT = 910.
               ELSEIF((TT.GE.1173.).AND.(TT.LT.1273.))THEN
                CVHEAT = 1090.
               ELSEIF(TT.GE.1273.)THEN
                CVHEAT = 1350.
               ENDIF
C
C        WRITE(6,*) 'values',XVAL,ilabel,cvheat,condl
C
      ENDIF
   ENDIF
C
   RETURN
   END
```

Propr.f

```
C
C
C
C=======================================================================
C
      SUBROUTINE PROPR(RHO,ARP,ARB,EQST,
     &                 U,V,W,P,T,PHI,NPHI,XYZ,
     &                 ILABEL,LABEL,I,J,K,ID,JD,KD)
C
CSCDT Evaluates density of fluid or solid at node I,J,K
C
CSCDB
C  PROPR is a user specified routine that evaluates the density
C  of a fluid or solid at node I,J,K.
C
C  Input:
C
C    ILABEL = 0  single component fluid
C           > 0  MCF component index
C           < 0  solid CHT object with label given by 'LABEL'
C     LABEL : character string identifying equation solved
C     U,V,W : Cartesian velocity components
C         P : static pressure
C         T : static temperature
C       PHI : additional scalars
C      NPHI : number of additional scalars
C       XYZ : Cartesian coordinates of grid nodes
C    ARP,ARB : coefficients in linearized equation of state
C      EQST : logical variable indicating whether or not to use the
C             equation of state
C     I,J,K : topological grid coordinates
C  ID,JD,KD : topological grid dimensions
C
C  Output:
C
C       RHO : control volume density
C
C  Local:
C
C    MAXMCF : work space parameter for multi-component fluids
C      POFF : pressure offset (level shift)
C      TOFF : temperature offset (level shift)
C        SN : small number
C     CONDL : local thermal conductivity
C        CP : specific heat at constant pressure
C        CV : specific heat at constant volume
C    RIDEAL : ideal gas constant for fluid
C    RHOSOL : solid density
C    RHOFLD : fluid density
C
C  Common Blocks:
C
C  /CONTRL/ is declared so that information can be added as needed
```

```
C       for desired equation of state.
C
C   IONUM  : integer, unit numbers in CONTRL common block.
C   IARR   : integer, integer switches in CONTRL common block.
C   RARR   : real, real constants in CONTRL common block.
C   CONST  : real, property constants in CONTRL common block.
C   LARR   : logical, logical switches in CONTRL common block.
C
C /MULTIF/ contains information for multicomponent fluids.
C
C   DENSQ  : real, component density.
C   ZMOLQ  : real, component molecular weight.
C   CONDQ  : real, component conductivity.
C   CPHTQ  : real, component specific heat at constant pressure.
C   CVHTQ  : real, component specific heat at constant volume.
C   LMCFQ  : logical, multi-component fluid.
C   EQSTQ  : logical, equation of state.
C   NMCF   : integer, number of components.
C   NMCFNA : integer, maximum scalar which is a multi-component fluid.
C
C NOTE: The true levels of pressure (P) and temperature (T) are
C     assumed to be
C       P_true = P + POFF
C       T_true = T + TOFF
C     where POFF and TOFF are level shifts in the actual dependent
C     values of P and T that are solved for.
CSCDE
C=======================================================================
C
C-------------------------
C Subroutine Arguments
C-------------------------
C
      INTEGER NPHI,ILABEL,I,J,K,ID,JD,KD
C
      REAL U(ID,JD,KD),V(ID,JD,KD),W(ID,JD,KD),P(ID,JD,KD),T(ID,JD,KD),
     &     PHI(ID,JD,KD,*),XYZ(ID,JD,KD,3),RHO,ARP,ARB
C
      LOGICAL EQST
C
      CHARACTER*(*) LABEL
C
C-------------------------
C Local Variables
C-------------------------
C
      INTEGER MAXMCF
      PARAMETER (MAXMCF = 100)
C
      REAL POFF,TOFF,RHOSOL,RHOFLD,SN,CONDL,CP,CV,RIDEAL
      PARAMETER (SN = 1.E-20)
C
C-------------------------
C Common Blocks
C-------------------------
C
```

```
      COMMON/CONTRL/ IONUM(100),IARR(200),RARR(100),CONST(100),LARR(200)
      INTEGER IONUM,IARR
      REAL RARR,CONST
      LOGICAL LARR
C
      EQUIVALENCE (CONST(13),POFF),(CONST(14),TOFF),
     &          (CONST(1),RHOFLD),(CONST(28),RHOSOL)
C
      COMMON /MULTIF/ DENSQ(MAXMCF),ZMOLQ(MAXMCF),
     &          CONDQ(MAXMCF),CPHTQ(MAXMCF),CVHTQ(MAXMCF),
     &          LMCFQ(MAXMCF),EQSTQ(MAXMCF),NMCF,NMCFNA
      INTEGER NMCF,NMCFNA
      REAL DENSQ,ZMOLQ,CONDQ,CPHTQ,CVHTQ
      LOGICAL LMCFQ,EQSTQ
C
C-----------------------------
C Executable Statements
C-----------------------------
C
C============= SINGLE-COMPONENT FLUID ==================
C
      IF (ILABEL.EQ.0) THEN
C
C------ Constant density ------
C     Set through PRM file parameter RHOFLD if EQUATION_OF_STATE=T
C
       IF (.NOT.EQST) THEN
        RHO = RHOFLD
C
C------ Equation of state ------
C
       ELSE
C
C Get thermal properties of single fluid
         CALL PROPT (CONDL,CP,CV,
     &          U,V,W,P,T,PHI,NPHI,XYZ,
     &          ILABEL,LABEL,I,J,K,ID,JD,KD)
C
C Calculate coefficients of the linearized equation of state
C for density, such that
C       RHO = ARP*P + ARB = (P+POFF)/(RIDEAL*(T+TOFF))
C Apply ideal gas law
C
        RIDEAL = CP - CV
        ARP = 1.0/(RIDEAL*(T(I,J,K)+TOFF+SN))
        ARB = POFF*ARP
        RHO = ARP * P(I,J,K) + ARB
       ENDIF
C
C
C============= MULTI-COMPONENT FLUID SPECIES ============
C
      ELSE IF (ILABEL.GT.0) THEN
C
C------ Constant density for species ------
C     Set though PRM file parameter DENSITYn if EQSTn=T
```

```
C
      IF (.NOT.EQSTQ(ILABEL)) THEN
       RHO = DENSQ(ILABEL)
       ARP = 0.0
       ARB = 0.0
C
C------ Equation of state for species ------
C
      ELSE
C
C  Get thermal properties of component and apply ideal gas law
        CALL PROPT (CONDL,CP,CV,
     &            U,V,W,P,T,PHI,NPHI,XYZ,
     &            ILABEL,LABEL,I,J,K,ID,JD,KD)
        RIDEAL = CP - CV
        ARP = 1.0/(RIDEAL*(T(I,J,K)+TOFF+SN))
        ARB = POFF*ARP
        RHO = ARP * P(I,J,K) + ARB
      ENDIF
C
C
C============== SOLID (CHT) DENSITY ==============
C
     ELSE
      RHO = RHOSOL
     ENDIF
C
     RETURN
     END
```

Bcdtrn.f

```
C
C
C
C=======================================================================
C
      SUBROUTINE BCDTRN(LABEL,VAL,STIME,KEY)
C
CSCDT User specified transient boundary condition value.
C
CSCDB
C     BCDTRN is a user supplied routine for spatially uniform
C     temporally varying boundary conditions. This subroutine is ONLY
C     called for each boundary condition set that was designated as a
C     specified function of time in the boundary condition
C     pre-processor.
C
C     Based on the variable name, LABEL, (valid names give below) an
C     the user entered KEY value (entered in TASCbob3D), the variable
C     value, VAL, must be assigned a value based on the simulation time,
C     STIME.
C
C
C     Input:
C       LABEL  : character, the name of variable that needs a value.
C
C            The ONLY valid strings that LABEL can assume are:
C
C              i) 'U', 'V', 'W' : Cartesian coordinate velocity
C                 components, at an inlet boundary condition.
C                 In a rotating frame of reference, these values
C                 represent the relative frame velocity
C                 components.
C
C             ii) 'P': static pressure at an outlet or inlet.
C
C            iii) 'P_TOTAL': total pressure at an inlet. In
C                 rotating frames of reference this value
C                 represents the absolute frame total pressure.
C
C             iv) 'TOTAL_MASS_FLOW': the total mass flow through
C                 ALL faces assigned to a transient mass flow
C                 boundary condition (inlet or outlet).
C
C              v) 'T': static temperature at an inlet.
C
C       KEY    : integer, the integer that was entered in the boundary
C              condition pre-processor that can be used to identify
C              transient boundary condition specifications (when more
C              than one transient b.c. has been specified).
C       STIME  : real, the current simulation time (units of time)
C
C     Output:
C       VAL    : real, the assigned value of the variable named
```

```
C             LABEL, at simulation time STIME, for the boundary
C             condition set assigned the number KEY in TASCbob3D.
C
CSCDE
C
C=======================================================================
C
C-------------------------
C Subroutine Arguments
C-------------------------
C
      REAL VAL,STIME
C
      INTEGER KEY
C
      CHARACTER*(*) LABEL
C
C-------------------------
C Executable Statements
C-------------------------
C
      IF    (LABEL.EQ.'U') THEN
C-------- U velocity component at an inlet.
       VAL = 0.0
      ELSEIF (LABEL.EQ.'V') THEN
C-------- V velocity component at an inlet.
       VAL = 0.0
      ELSEIF (LABEL.EQ.'W') THEN
C-------- W velocity component at an inlet.
       VAL = 0.0
      ELSEIF (LABEL.EQ.'P') THEN
C-------- Static pressure at an outlet or inlet.
       VAL = 0.0
      ELSEIF (LABEL.EQ.'P_TOTAL') THEN
C-------- Total pressure at an inlet.
       VAL = 0.0
      ELSEIF (LABEL.EQ.'TOTAL_MASS_FLOW') THEN
C-------- Total mass flow though ALL faces assigned a transient mass b.c
       VAL = 0.0
      ELSEIF (LABEL.EQ.'T') THEN
C-------- Static temperature at an inlet.
C
       VAL = 0.0
C
C-----------------------------------------------------------------
C-------This is a transient temperature spec following IMO 834------
C-----------------------------------------------------------------
C
C      Assumes that STIME is in seconds:
       IF (KEY.EQ.100 .AND. LABEL.EQ.'T') THEN

        VAL = (750. * (1. - EXP(-3.79553 * (STIME/3600.)** 0.5))
     &    + 170.41 * (STIME/3600.) ** 0.5 +298.)
       ENDIF
C
C    Test of output to error file
```

```
      WRITE (6,*) "IN NATE'S BCTRN.F",STIME,VAL
    ENDIF
C
    RETURN
    END
```